R-00-34

Maqarin natural analogue project: Phase IV

Reconnaissance mission report (April 28th to May 7th, 1999)

John A T Smellie (Editor)
Conterra AB

August 2000

Svensk Kärnbränslehantering AB
Swedish Nuclear Fuel
and Waste Management Co
Box 5864
SE-102 40 Stockholm Sweden
Tel 08-459 84 00
+46 8 459 84 00
Fax 08-661 57 19
+46 8 661 57 19

ISSN 1402-3091
SKB Rapport R-00-34

Maqarin natural analogue project: Phase IV

Reconnaissance mission report (April 28th to May 7th, 1999)

John A T Smellie (Editor)
Conterra AB

April 2000

Summary

Final planning of the Technical Proposal for Phase IV of the Maqarin Natural Analogue Project was preceeded by a ten day Reconnaissance Mission to the Jordan sites from April 28th to May 7th, 1999. The main objective of this mission was to: i) allow new organisations within the project to become familiar with the geological context of the Maqarin and Central Jordan sites and also to appreciate the prevailing technical and logistical limitations, ii) carry out limited field investigations, and (iii) based on the experience from these two points, provide the opportunity to finalise the Maqarin Phase IV Technical Proposal.

This report details the results of the mission.

Sammanfattning

För att planera fortsättningen av projektet ”Maqarin Natural Analogue” har ett antal lämpliga platser i Jordanien rekognoserats. Detta tog tio dagar, från 28 april till 7 maj 1999. Resans främsta mål var att: i) låta de nya organisationerna i projektet bekanta sig med de geologiska förhållandena på undersökningsplatserna i Maqarin och centrala Jordanien – inte minst för att på ort och ställe se vad som går att göra, ii) utföra begränsade fältundersökningar, och iii) med erfarenhet från de två föregående punkterna skriva färdigt planen för fas IV av Maqarinprojektet (Maqarin Phase IV Technical Proposal).

Den här rapporten presenterar resultatet av resan.

Contents

1 Background

As a result of the meeting at BGS on January 25th, 1999, convened to discuss the content and organisation of the Maqarin Phase IV programme, it was agreed that the Phase IV Technical Proposal should be preceeded by a Reconnaissance Mission to Jordan. This would: i) allow project newcomers to familiarise themselves with the geology and also to appreciate the technical and logistical limitations at both the Maqarin and Central Jordan sites, ii) carry out limited field investigations, and (iii) based on the experience from these two points, provide the opportunity to finalise the Maqarin Phase IV Technical Proposal.

Consequently, a 10 day reconnaissance mission was planned from April 28th to May 7th; the details of the mission are reproduced in **Appendix 1**. The following main tasks were to be accomplished:

Eastern Springs, Maqarin

- *TASK 1: Background Information* (e.g. maps; number of existing boreholes/drill cores and their condition; availability of specialised equipment; logistic back-up etc.).
- *TASK 2: Structural Evaluation* (e.g. site-scale structural geometry; evaluation of fracture filling phases for potential age-dating etc.).
- *TASK 3: Geomorphological Evaluation* (e.g. evaluation of tectonics/geomorphology to further constrain geological events in the area – combustion/cement zone; high pH evolution/reactivation events etc.).
- *TASK 4: Geophysical Measurements* (e.g. surface resistivity data as input to litho-structural interpretation of the site – potential locations for future drilling etc.).
- *TASK 5: Adit A-6 Activities* (e.g. assessment of drilling; preliminary core drilling; mapping and sampling etc.).

Central Jordan

- *TASK 6: Fossil Hyperalkaline Reaction Zones* (e.g. to assess the full potential of the fossilised high pH reaction zones – late-stage high pH plume evolution; long-term hydration studies; clay stability in the presence of high pH waters etc.).

Generally these tasks were successfully accomplished and a considerable amount of regional and site-specific field data was collected for interpretation. In addition, many rock samples were selected for archivation and some were distributed for immediate scoping analysis. Drilling in the Adit A-6 was successful, adding an important extra dimension to earlier studies. The results of these tasks are reported in detail below.

Good fortune during the mission also brought added difficulties. Because of the success of the Adit A-6 activities, it is necessary now to protect the completed boreholes and other equipment from theft and vandalism. This has necessitated the installation of a gate across the adit entrance and the construction of a boom at the turn-off from the main road which leads up to the adit; the road to the adit has also been improved. These

improvements greatly facilitated later activities inside Adit A-6 (e.g. mapping, drilling, groundwater sampling etc.), carried out in October/November, 1999, as part of the Phase IV programme.

2 Results from activities carried out at Maqarin

Studies at Maqarin have involved a wide range of geological and geomorphological observations. Integration of geostructural information has been facilitated by the use of field measurements, aerial photographs, satellite imagery and supporting photographic material. **Appendix 2** presents a collage of photographs viewing the topography of the Eastern Springs area from the east.

2.1 Fracture analysis and structural overview [1]

Much background work on the regional and local structural history of the Maqarin site has already been described in the previous Phase I, II and III reports. The objective of the Phase IV structural surveys will be to: (i) investigate whether further information is available from satellite imagery and aerial photographs, in order to place the Adit A-6 and other local data into a wider site context, (ii) undertake detailed fracture mapping in order to develop fracture network models that would be suitable for incorporating into flow simulation models (together with hydraulic test data), (iii) re-visit the published literature for northern Jordan, Israel and southern Syria to see if structural insights from other areas can be applied to the Maqarin area, and (iv) examine whether there is a relationship between the observed fracture patterns and the spatial distribution of metamorphic zones in the Bituminous Marl Formation and Chalky Limestone Formation. The detailed fracture mapping and associated analysis is to be closely integrated with mineralogical studies of vein-fill material.

2.1.1 Regional setting

Maqarin is located in an area of relatively complex structural deformation, although apart from pervasive fracturing the site itself is surprisingly unaffected by intense structuration. The regional tectonics are dominated by the sinistral movement of the Arabian plate relative to North Africa. The Dead Sea Rift Valley, from the Gulf of Elat in the south, north to the Sea of Galilee and beyond, is the surface expression of this plate boundary. Superimposed on the transverse plate movement, active extension is evident all along the margin, resulting in an asymmetric graben structure (the eastern footwall side is topographically higher than the western footwall side and this asymmetry is reflected by offsets in a regional Eocene stratigraphic marker horizon). A major question that is still unanswered is ‘is the rifting due to concurrent transtension along the strike slip margin, or is the extensional strain an expression of east-west tensional stresses that are superimposed on the strike slip movement’? Some authors prefer the

[1] Paul Degnan, Tony Milodowski, Alistair Pitty and Colm Jordan.

former explanation and interpret the Dead Sea and other basins as transtensional pull-aparts, however, pure tensional stresses superimposed on the relative lateral plate movements, resulting from far-field Red Sea rifting, cannot be discounted.

In Israel, Jordan and Syria a series of en echelon fold structures trending NE-SW exist. These folds may be an example of classical compressional deformation associated with transpressional stresses along strike-slip zones, or they may pre-date the transverse movement. Work on the Negev antiforms (e.g. Arkin, 1989) suggests that the folds are cut by later horst and graben structures.

The orientation of the Yarmouk valley is broadly coincident with the southern limit to a line of volcanoes in southern Syria. Low topographic relief volcanoes are numerous in southern Syria and the line of volcanoes may reflect a lineament of crustal weakness. A map of earthquake epicentres in the region for the past decades also shows an apparent east-west orientation of seismic activity at depth that coincides with an extension eastwards of the course of the Yarmouk valley. Although there does not appear to be a fault control along the course of the river itself, at least as expressed by surface displacements, there may be an underlying east-west structural influence.

The above brief review of the tectonics of the region indicates that there are possibly four major and discrete phases of deformation since the deposition of the Late Cretaceous to Lower Tertiary rocks of Maqarin. In chronological order, from oldest to youngest, these are postulated to be:

- NE-SW oriented folds (age unknown, but likely to be Oligocene/Eocene).
- E-W extension related to Red Sea rifting and/or partially coeval.
- Transverse fault movement due to the more rapid movement of the Arabian plate northwards, relative to the African plate. Possible transtension at fault jogs. Age less than 20 Ma.
- The east-west zone expressed by volcanism and earthquake epicentres indicates local extension (or oblique/strike slip movement; the earthquake data need to be studied). It is likely that the zone may be a reflection of the transfer of strain off the Dead Sea Rift valley.

Each of the above phases of deformation is likely to have left a fracture record in the Maqarin area.

2.1.2 Structure of the Maqarin area

The presentation of data and preliminary assessment of the structure of the Maqarin area is being reported here and its organisation can be considered in four sections, (i) insights from the satellite imagery, (ii) interpretation of aerial photographs, (iii) detailed outcrop mapping, and (iv) detailed mapping in Adit A-6.

Satellite imagery

On behalf of the Maqarin consortium, BGS purchased Landsat and SPOT images of the Maqarin area **(Appendix 3)**. Landsat images have a 30 m per pixel resolution and are panchromatic (7 bands; 3 visible spectrum, 3 infra-red and 1 thermal). Three bands can be displayed at any one time. The SPOT imagery is monochromatic, but has a higher

spatial resolution, 10m per pixel. The two datasets were combined, giving a high resolution multichromatic image. BGS undertook a preliminary interpretation prior to the field trip and the results were studied in the field, although not in detail. Some of the features identified on the satellite image are discussed here.

- A significant lineament trending ENE on the Syrian plateau was identified on the satellite image, and this was verified as a scarp-feature that could be extrapolated for a distance of several kilometres.
- A region of enclosed depressions was identified on the image and this corresponds to an area previously ascribed as sink-holes (Khoury et al., 1998), which has a genetic connotation. They are further described in the next sub-section (aerial photographs).
- At least three areas of major land-slipping were postulated along the southern margin of the Yarmouk River. Overlapping relationships suggested a chronology for the land slips.
- Gently eastward dipping strata in Wadi Shallala were ascribed to the eastern limb of a gentle antiform. This conforms to a NE plunging fold as interpreted by Khoury et al. (1998).
- Numerous NE-SW lineaments were postulated and appear to be clustered in three domains.

Apart from the enclosed domains and the major lineament in southern Syria, none of the other features have actually been confirmed in the field. See below for discussion on the land slips.

Aerial photographs

Stereoscopes with x3 magnification have been used to analyse the aerial photographs; these are available as TIFF images and can be downloaded from the Maqarin server at the University of Bern (U. Mäder, written comm. 1999). The lineament on the plateau on the Syrian side of the Yarmouk River is identified, but other lineaments postulated from the satellite imagery cannot be defined as definite structural features. The gentle antiform plunging NE is identified in the Yarmouk River valley, but its hinge-line cannot be defined on the plateaus.

The landslips on the southern side of the Yarmouk River have been looked at in some detail. The bedding within the arcuate areas is totally undisturbed and the sectors appear to represent simple gradual back-cutting erosion. There is no mass wastage apparent from the air photos, but in the field there are some obvious debris flow deposits at the bottom of the slopes, with up to decimetre scale intact blocks within a disorganised matrix of smaller material. The apparent overlap of ‘landslide’ areas appears to be where one erosion front is cutting into another.

A provisional interpretation, for discussion and ground-truthing, is that the features represent the cumulative expression of minor slope movement (resulting in scree falls and cohesionless debris flows). The aerial photographs do not suggest large scale and catastrophic individual events. An accurate interpretation is essential, given the significance of catastrophic land slippage as a facilitator of oxygen ingress to depth and possibly as a combustion mechanism.

Another area of interest is the region of enclosed depressions. The depressions are clearly seen as circular to elliptic features that are several to a few tens of metres in depth. Why is this domain so different from everywhere else? What is the process that formed them. Unfortunately, to date no new insights have resulted from the analysis of the aerial photographs. More work will be undertaken on the aerial photographs in the near future.

Fracture mapping – outcrop

Four main areas were studied in detail for fracture characteristics. These are: (i) Wadi Shallala road cut, (ii) the road cutting a few hundred metres to the west of Maqarin Station, (iii) the bench above the Yarmouk River bridge, running east of the sentry post, and (iv) a small alluvial terrace above the Bituminous Marls a few hundred metres east of the bridge and off the road. Several other localities were spot checked for dominant fracture orientations.

Some of the results of the fracture mapping (orientation, vein fill, density) are provided on the attached spreadsheets **(Appendix 4)**. Detailed analysis and integration with larger scale structural orientations has not been started yet. **Figures 2-1 to 2-5** illustrate examples of structural deformation observed at Maqarin.

2.1.3 Data analysis

The information that has been provided on the spreadsheets are the uninterpreted field data (NB they need to be adjusted for 2°E magnetic declination in Jordan). Although it is obvious that different fracture trends dominate in a particular field location, the controls and the areal extent of the domains are not yet known. They will be studied in the context of the four regional tectonic events (see Regional Setting section) and in their own right. Despite the presence of fracture domains, there are consistent regional fracture patterns and a basic fracture chronology can be identified based on cross-cutting relationships. This, however needs to be verified by a larger dataset. At this stage what can be stated is that: (i) the fractures represent multiple deformation events reflecting different stress orienations, (ii) many of the fractures have been reactivated, as evidenced by multi-generation crack seal vein fills, (iii) the sub-horizontal lithostratigraphic layering has been overprinted by high angle fracture sets that have in places resulted in vertical zones of more intense fracturing and less intense fracturing, often with regular separation distances at any one locality, (iv) there are no large scale faults present, nor any mesoscale folds (including parasitic folds related to the large antiform plunging NE), and (v) kinematic indicators suggest that much of the small scale slip that is observed has been of a high angle strike slip nature.

Figure 2-1. *Bituminous Marl overlain by alluvial deposits. Some of the fractures in the bituminous-rich marl have been reactivated and cut through the lowermost part of the more poorly consolidated alluvial deposits (to right of hammer). Location, approx. 200 m east of bridge.*

Figure 2-2. *Zone of closely spaced fractures in thick bedded sub-horizontal limestone. Wadi Shallala.*

Figure 2-3. *En echelon pinnate joints with vein fill, on a fracture face. Suggests sinistral strike slip movement on fracture (fault?) face. Road cutting west of Maqarin station.*

Figure 2-4. *Zone of intense fracturing delineated from less fractured rock to the right by a thick calcite filled crack-seal vein.*

Figure 2-5. *Calcite slickenfibres indicating latest movement on the plane was dextral.*

Over the coming few months the following data analysis will be carried out:

1. Well locations (from Appendix B of the Phase III report) have been entered into the Rockworks99 database.
2. The topographic contours over a 6 km^2 area on the 1:50,000 map are to be digitilised and entered onto Rockworks99.
3. Fracture data and locations will be entered into Rockworks99.
4. 3D lithostratigraphic model will be created from borehole interpretations and outcrop maps (using the programme 'Slicer' in conjunction with the Rockworks99 database).
5. FRACMAN to be used to statistically analyse fracture patterns (outcrop and provisional satellite derived) and construct preliminary networks that would be suitable for use in flow simulators. This is preliminary work only as far more information is required on fracture orientations and density.

2.1.4 Future fieldwork requirements

Further mapping of the area is required to provide detailed fracture coverage, both in terms of the orientation/density and also the mineral fills. Most mapping will be along the road cuts and wadis and, hopefully at a later date, from the river banks and possibly on the Syrian side.

NB Fracture mapping of the core would be beneficial. Although the core is presumably unoriented, the fracture density, vein fill and cross cutting relationships could be derived. This information is particularly required to overcome the bias induced by having long horizontal outcrop sections, relative to vertical.

Several 'pods' of metamorphosed limestone have been recognised at outcrop. On the road from the main sentry post down to the Yarmouk River, it appears that the zone is delineated by intense vertical fracturing to either side. This may also be the case with an outcrop seen from a distance in Wadi Sijin. Do the fractures represent an original control on the extent of combustion, or do they represent a response to the combustion? Detailed examination should resolve this.

2.2 Notes and data on some ground-surface features with geomorphological interpretations[2]

Ground-surface characteristics in the Maqarin area were addressed at a wide range of scales; these ranged from the atomic scale of natural background gamma radiation, to the origin and dating of large-scale landforms like the Wadi al Habis chasm, 2 km west of the Western Springs.

[2] Alistair Pitty.

The topics are presented in the following order:

- Gravel and slope deposits.
- Ground-surface roughness indices.
- Background gamma radiation.
- Some larger-scale landforms.
- Conclusions.

2.2.1 Gravel and slope deposits

Location of gravel samples

There is much scope for more detailed study of the instructive fluvial gravels in the Maqarin area. This conclusion is suggested by the limited, exploratory data, summarised in **Table 2-1**. The location of the 8 sampling points is mapped in **Figure 2-6**.

Table 2-1. Exploratory data for 8 gravel locations in the Maqarin area.

Location	Altitude (m asl)	Age (Ma)	Median L-axis	Wear (mm)	Chert	Lime-stone	Basalt	N
1 Dhunayba (upper)	405	>3–5	56	7.6	23	77	–	30
2 Dhunayba (lower)	400	>3–5	67	6.3	32	68	–	22
3 Aqraba (higher)	370	c.3	47	7.5	28	72	–	29
4 Aqraba (lower)	360	c.3	52	5.1	40	60	–	25
5 Maqarin (high)	170	0.7	61	11.4	20	–	76	25
6 Maqarin (middle)	140	0.2	58	12.1	80	7	13	15
7 Maqarin (low)	90	c. 50 ka	67*	6.4	13	27	60	15
8 Al Arqub (terrace)	40	c. 50 ka	68*	11.9	13	37	47	–

* See text.

1. Sampling points 1 and 2 are close to Dhunayba village, at the edge of the plateau on the east side of Wadi Shallala, 4 km southeast of Maqarin Station.
2. Sampling points 3 and 4 are just below the ridge crest, on the S side of the Yarmouk Valley, 0.5 and 1.5 km east of Aqraba village.
3. Sampling points 5 and 6 are located on the south side of the Yarmouk Valley, at points above Adit A-6.
4. Sampling point 7 is close to the metalled road, to the west of the track leading up to Adit A-6.
5. Sampling point 8 is further down the Yarmouk Valley, 3.5 km west of Maqarin Station, upslope from the next station, to the west of Maqarin Station.

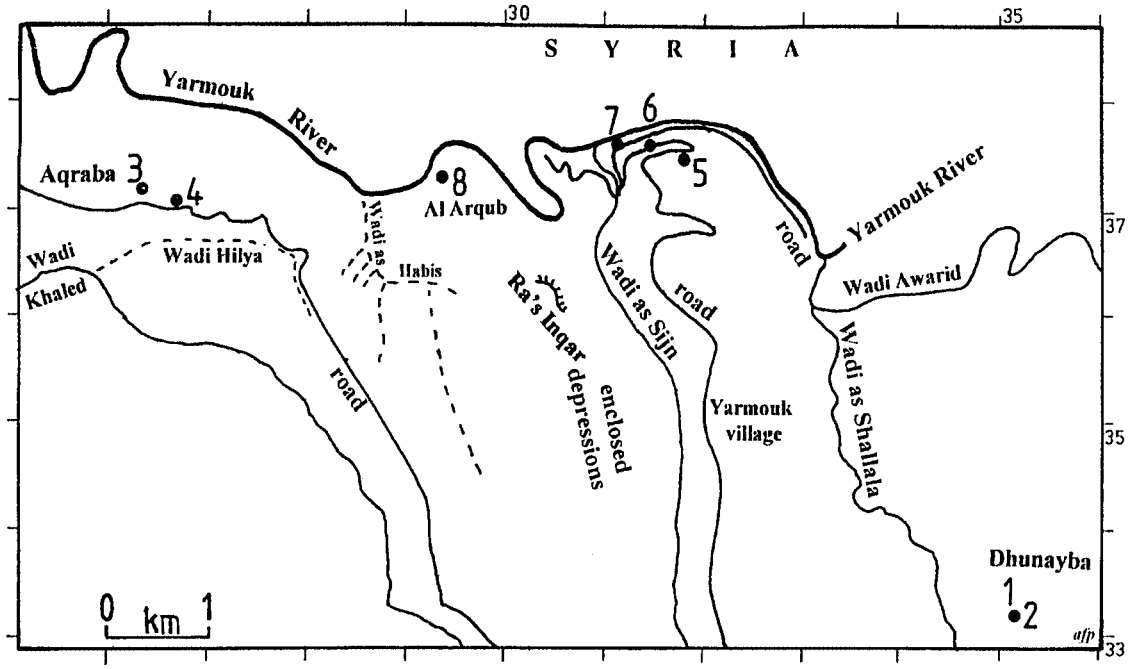

Figure 2-6. *Location of gravel sampling points and other selected features. Dashed lines indicate wadis that are dry, or where there is only occasional flow; the others are spring-fed.*

Description of gravel locations

The sampling points are tabled in order of decreasing altitude above sealevel, as estimated by interpolation from the spacing of the 10 m contour intervals on the 1:25,000 map **(Table 2-1**, column 2). Remarkably, there is independent evidence to suggest an approximate age for all samples.

1. Points 1 and 2 lie immediately underneath the thin extension of the Cover Basalt (53 Ma), which reached as far south as Dhunayba.
2. Points 3 and 4 may represent gravels from the streams which then subsequently began to erode through the Cover Basalt. The possibility that they too, like the Dhunayba gravels, extend stratigraphically **beneath** the Cover Basalt, could not be proved from the brief inspections in the Aqraba area.
3. Points 5 and 6 are most instructive. Here, the gravels occupy two 'gulls' in the valleyside, fissures probably opened up by mechanical relaxation of the valleyside after incision by the main river. The gravels may be backwater deposits, in recesses along the former river bank, when the opened fissures were at the former level of the river.

   (The possible presence of such fissures had been predicted in an earlier report).
4. Point 7 is a former river terrace which lies beneath a tufa dam, at the confluence of the Wadi Sijin with the Yarmouk. Point 8 is also a partly buried terrace but, in this case, the gravels of the former Yarmouk have been overridden by extensive land-slide debris.

Ages of gravel samples

In column 3 of **Table 2-1**, the bases for the estimates of age of the various gravels differ. The Dhunayba gravels clearly underlie the Cover Basalt, dated at 5-3 Ma. The possible age of the Aqraba gravels will be discussed after the data and pebble lithology and morphometry has been discussed. Sampling point 5 is a critical location, being only about 20 m below the base of the Yarmouk Basalt. Above Adit A-6, the Yarmouk Basalt appears to occupy the southern half of a former channel, and is locally about 70 m thick. The age of the gravels at point 5, therefore, is therefore estimated as being shortly after the deposition of the Yarmouk Basalt ceased.

The lithology of the gravel at Sampling point 5 is approx. 75% basalt, but most pebbles are deeply, if not entirely, weathered. In one sample, a weathering rind was 17 mm thick. (Proposed literature search and review will facilitate further comment on this feature). Lower down the hillslope above Adit A-6, the percentage of basalt in the gravel sample is reduced, and pebbles are less weathered. Here, one pebble had a weathering rind, 5 mm thick. Approximately, therefore, these gravels are about one-third the age of those at the higher level.

A nominal age of about 50 ka is suggested for the two Sampling points, 7 and 8, which are about 40 above the present river level. Evidence from nearby locations suggests that this was a period of significantly increased fluvial activity in the Levant. Also, massive tufa deposits at Bet Shean Valley across the Jordan Valley from the Yarmouk outlet, may also have regional significance for the palaeoenvironment and dating of similar deposits, like those at the outlet of the Wadi Sijin. The massive and extensive Bet Shean travertine was deposited from 41 to 22 ka BP. and attributed to wetter conditions during that period (Kronfeld et al., 1988).

Pebble morphometry

Three main axes. The basic method of measuring the three main orthogonal axes of each pebble was employed – length (L), breadth (B), and depth (D). Only the median value of length (L) is reported, in the third column of Table 2-1. No conscience bias was exercised in selecting pebbles for samples 1–6. Therefore, some simple conclusions can be drawn from the median values reported, such as the gravels of the lower unit at Dhunayba (2) being somewhat larger than those in the upper unit. (The two units are separated by the pink, marl horizon, perhaps reflecting a lacustrine episode between the two fluvial phases).

Both asterisked values for sites 7 and 8 (**Table 2-1**) greatly underestimate an ‘average’ size, as there are large boulders present. Here, only pebbles about 100 mm in length or less were measured. Basalt boulders, up to 40 cm long are evident at point 7 and those at point 8 may exceed 70 cm in length. Clearly, large floods were a feature of the Yarmouk River by the time it had cut down to within 40 m of present level.

Callieux ‘index of wear’. This method compares the rounding of corners of a pebble with a chart of concentric circles, and ‘wear’ is reported as the radius of the ideal shape to which the pebble corner corresponds most closely. Although only an approximate, if not semi-quantitative approach, the means reported in the 4th column of **Table 2-1** reveal both instructive similarities and contrasts in the degree of ‘wear’ exhibited by the 8 samples. For instance, the ‘wear’ on both the upper unit at Dhunayba and the higher sample at Aqraba is very similar. Equally noteworthy is that the gravels in the latter half

of the samples (locations 5–8) are more worn than those at locations 1–4. This includes the low-level location at Maqarin (7), since the mean value is distorted by shards of clasts, particularly limestone, which appear to have been crushed after deposition. The mean value for 'wear' on basalt pebbles only is 10.4 mm.

Pebble lithology

Although not justified by the small sample sizes, lithologies are reported in percentages, to facilitate exploratory comparisons. Most obviously, basalts are absent from locations 1–4. However, the similarity between the upper unit at Dhunanyba (location 1) and the higher sample at Aqraba (loaction 3) is striking. Limestones are absent from the deeply weathered gravels at location 5, whilst chert is strikingly dominant in the gravels in the lower 'gull' (location 6). The two samples, both approximately 40 m above the present river level (locations 7 and 8) may be members of the same terrace feature.

Slope deposits

A major characteristic of the Tabaqat Nasra, the local name for the valleyside slope near Adit A-6, is the extent of slope deposits, their thickness, and their variety. Unlike the gravel deposits, the clasts are angular and unweathered. Due to their extent and thickness, there are few outcrops of *in situ* bedrock on the Tabaqat Nasra.

Three main types of slope deposit can be readily identified:

1. Basalt fragments form aprons of debris, up to 5 m or more in thickness, on lower slopes. Block glide of monoliths of individual blocks of basalt is a conspicuous feature of the upper slopes.
2. Limestone scree, made up of loose, angular fragments is commonly developed between the basalt aprons. The clasts are well-sorted but, in cross-section, bedding in discrete layers is evident, with contrasted mean particle sizes between layers. Such sharp contrasts in bedded slope deposits may reflect significant environmental changes, such as deforestation and over-grazing.
3. Diamicton, a deposit which incorporates a wide range of particle sizes, typical coarse clasts in a clayey matrix. Such deposits are developed on the lower slopes of the Tabaqat Nasra, and are up to 3 m thick. They probably represent lower slope accumulations of debris which has undergone a long period of weathering during transport downslope. This would explain the clayey matrix and the persistence of chert, to make up the coarse fraction.

2.2.2 Ground-surface roughness indices

Background

Measurements of ground-surface roughness were made, for three main reasons:

1. A major feature of the Maqarin area, which is typical of closely similar climatic areas in the Levant, is the calcareous duricrust which covers tracts of hillslope. Locally, this is known as 'nari'. In the field, its two main characteristics are is relatively smoothly continuous surface expression, and its inclination, parallel to the ground surface. In both cases, it should be distinguishable from bedrock, which has stepped outcrops and sub-horizontal bedding. However, previous workers are not always made this distinction clear, and misleading conclusions about local structural features in the Maqarin area. It was postualted that measurements of ground-surface roughness could make this distinction clearer.

2. A major hydrometerological consideration in the Maqarin geochemical studies is the modes of infiltration of precipitation into the ground. As an expression of surface detention, which would favour infiltration rather than runoff, surface roughness – at several scales – could be a useful index of field conditions. This suggestion applies particularly for the entire valleyside above Adit A-6. As inspection of the mirror-image, Syrian valleyside shows, the entire length of these valleysides is largely mantled by aprons of scree debris, of both basaltic and limestone clasts. Lower down, presumably derived from weathering of basalt, clasts are embedded in a clayey matrix. Here, ground surfaces are smoother.

3. An index of ground-surface roughness does not give a number unique to a given lithology or geomorphological situation. However, it may be an underestimated parameter for routine characterisation, in an exploratory study to describe an area of special scientific interest.

Method

The basic data is a sequence of consecutive measurements of slope angle, of unit length. In the present case, a unit length of 1 m was employed. From this data, a 'roughness index' (R.I.) is calculated as the mean - regardless of sign – of the consecutive differences between such measurements. Visually, 'roughness' is evident from line graphs, in which consecutive angles are plotted in sequence (**Figure 2-7**).

Data

General. Due to time constraints, only a nominal number of terrain types were surveyed (**Figure 2-8**) and, in 4 of the 6 cases, only short traverses were appropriate. **Table 2-2** illustrates some of the more obvious types of ground surface in the Maqarin area, and underlines the possibilities of more extensive sampling. The importance of extensive basalt surfaces is a self-evident feature of the Yarmouk area, although limited locally to outcrops on the north margin of the Adh Dhlla bench (traverse 1). Both 'nari' traverses (2 and 3) were on the hillslopes to the south of the Adh Dhlla bench, immediately to the south of the access road.

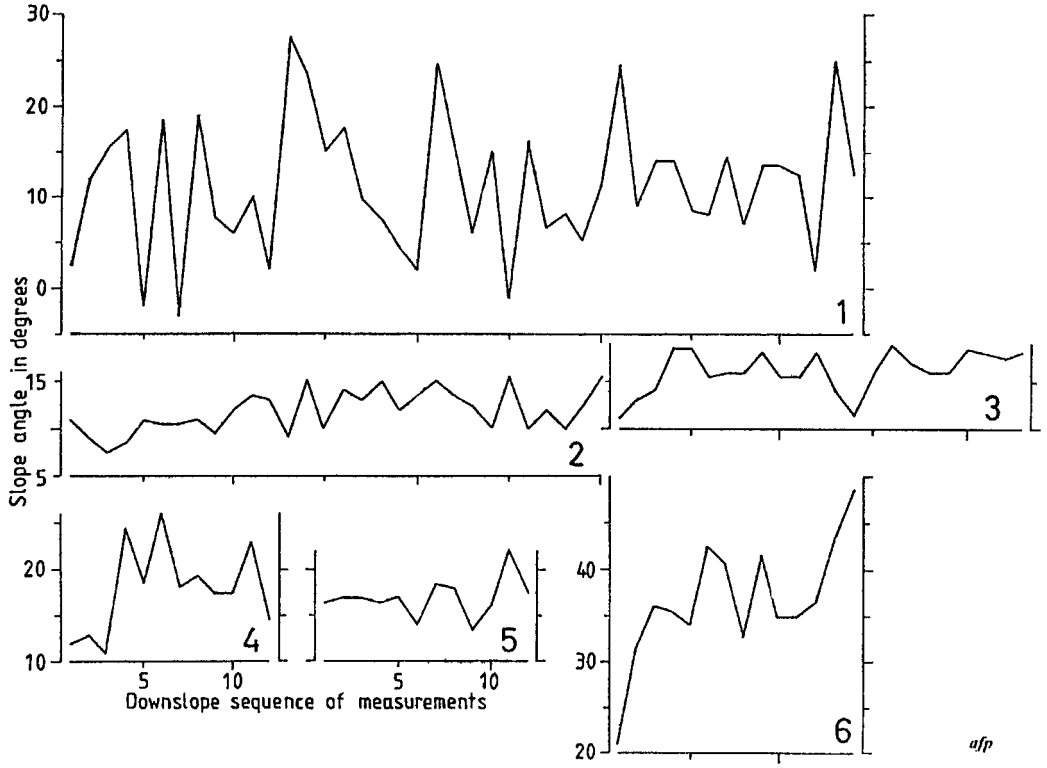

Figure 2-7. *Line graphs illustrating 'roughness' on differing ground-surface types. The traverses are basalt (1), 'nari' (2 and 3), cemented rock debris (4 and 5), and sheeptracks on Bituminous Marl (6). The location of the traverses, tl–t6, is shown on* ***Figure 2-8****.*

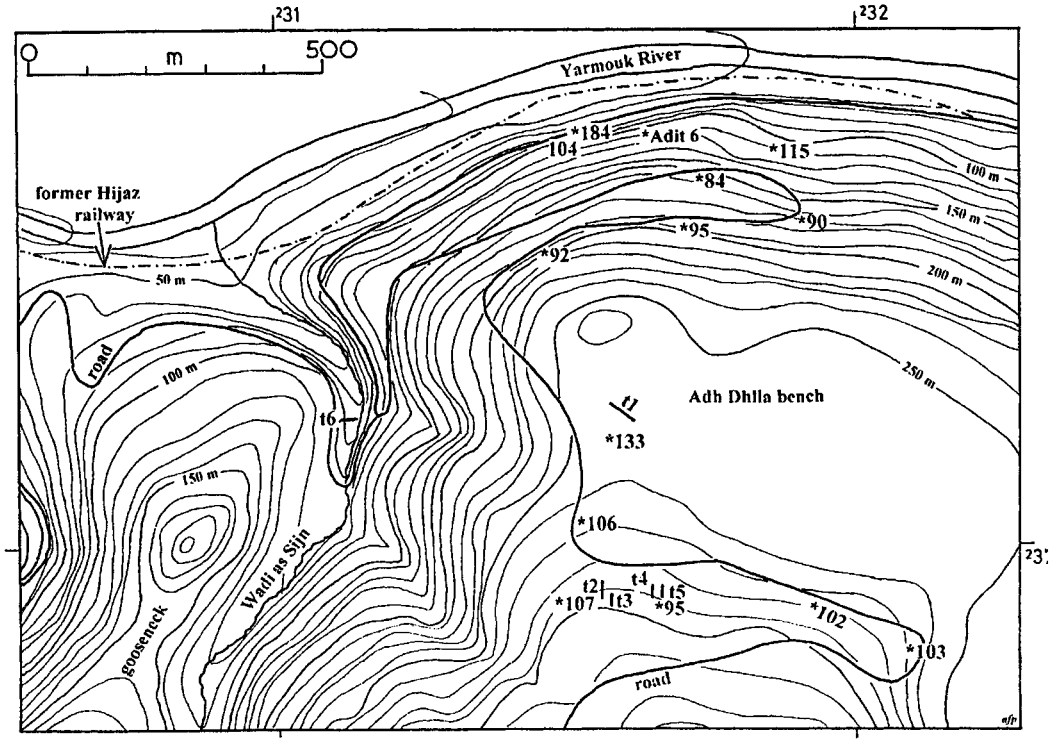

Figure 2-8. *Map of the Maqarin area in the vicinity of Adit A-6, showing location (*) of natural background gamma counts.*

The values are counts per minute (cpm) or nGy hr^{-1} (i.e. 5/6 of the counts), the median value of 40, one minute counts. The location of 'roughness' traverses, t1–t6, is also shown.

Table 2-2. Examples of ground-surface roughness indices.

Code	Description	N	R.I.
1.	Basalt	44	9.05
2.	Nari 1	30	2.33
3.	Nari 2	23	1.77
4.	Ancient debris flow 1	12	5.05
5.	Ancient debris flow 2	12	2.45
6.	Terracettes, BMF	14	4.96

Larger-scale irregularities

The main tract of irregular ground in the Maqarin area is found on the upper slope of the west side of the Wadi Sijin. Here, enclosed depressions and irregular, intervening ridges extend over an area of 150 ha. Unusually, there is no local name for an area of such a size. The limestone bedrock is exposed as scattered blocks, and persistent stratification is not well-developed. The depressions may be up to 100 m in length.

The irregularity of the ground surface in this area, which presumably accelerates infiltration rates, may be a significant influence on the groundwaters which emerge at the Western Springs, 1.5–3.5 km to the NNW. Three tentative explanations might explain the origin of the enclosed depressions.

First, as is evident from the sharply inverted cone shapes on stereoscopic images of air photos, a similarity with ‘sinkholes’ or ‘dolines’ of karst terrain is suggested. However, a ‘sinkhole’, by definition, is linked to a surface stream which disappears at that point. (The graphic Yorkshire term, in the Ingleborough area, is ‘swallet’). One possibility is that a former surface stream came from the Syrian side of the Yarmouk, when the Cover Basalt was continuous over the Maqarin area and, at a point along the southern margin of the Cover Basalt, sank into the limestone. However, a common feature of ‘sinkholes’ is that they form a line along such contacts between limestone and overlying, less permeable strata. A difficulty in describing the Wadi Sijin depressions by the genetic term, ‘sinkhole’, therefore, is that there are no other similar tracts of enclosed depressions in the Maqarin area.

Secondly, ‘dolines’ develop as inverted-cone forms within a thick soil cover, overlying limestone, and are widespread in the Dinaric Karst. The depressions are formed in that cover by eluviation of fines into the jointed, subjacent bedrock. Certainly, in the Wadi Sijin enclosed depressions, there is clearly downslope movement of soil towards the centre of each hollow. Again, the difficulty of explaining these features as typical ‘dolines’ is their highly localised occurrence. Typically, ‘dolines’ develop as extensive fields.

A third explanation for the origin of the area of irregular topography in Wadi Sijin is that of mass movement, with foundering of the caprock rim of the western valleyside, followed by downslope block glide of the disjointed rafts of bedrock. In such locations, enclosed depressions commonly develop to the rear of such rafts, and typically may contain lakes. Such features are known in the landslipped areas of the eastern bank of the lower Yarmouk Valley.

2.2.3 Natural background gamma radiation

Three reasons prompted the collection of this data, as an exploratory exercise. The main reason relates to the difficulty, in the field, of distinguishing between 'nari', the widely developed, calcareous duricrust and outcrops of limestone bedrock. As the first contains a percentage of wind-blown dust, it was supposed that this might give a slightly different gamma signal. A second reason relates to the presence of bedrocks with radioactive materials present, notably the Bituminous Marl. Possibly, a 'natural analogue' study, within the context of radioactive waste disposal, could justifiably map natural background variability. For instance, would a 'nari' veneer have any discernible influence in containing activity from a subjacent 'source'? Thirdly, experience repeatedly suggests that many geomorphological observations are made incidentally, only because the field worker has been anchored to a specific spot, for some other purpose.

As the locations for the gamma counts in **Figure 2-8** confirm, their downslope sequence offered a range of altitudes and aspects, from which general observations could be made. These observations were also sustained, as experience suggests that a 40-minute counting period is needed, to even out the pulses and lulls which characterise mean values for gamma signals.

Proceeding downhill, along the access road, the first measurements (103 cpm) was on a 'nari' surface, with 102 cpm for a cemented rock debris outcrop. The lower 95 cpm was recorded for another outcrop of the cemented rock slide debris, possibly because it contains large blocks of chert. The 107 cpm location is again 'nari', high on the hillside, overlooking Wadi Sijin; nearby, 106 cpm was recorded for a chalky limestone outcrop. The higher value of 133 cpm was made on weathered basalt, but the contrasted value of 92 cpm was also on basalt, from a fresh, artifical exposure near the base of the unit. 95 cpm was also recorded from a basalt outcrop, at a point where a fossil soil was present at the junction between successive lava flows. The values of 90 and 84 cpm were both made on limestone exposures. Lower down, 104 cpm was recorded for the diamicton, largely chert clasts in a clayey matrix, with 184 cpm for a Bituminous Marl outcrop. Finally, to the east of Adit A-6, a value of 115 cpm was recorded for chalky scree material.

All these values can be compared with results from central Jordan:

- Bituminous Marl, Khushaym Matruk, median value 225 cpm
- Cement zone, 3 m above top of the Bituminous Marl 188 cpm
- Metamorphosed Cement zone, El Hammam 450 cpm

These data are presented for descriptive purposes only. Probably, the sample size is too small to test the working hypotheses which had been posed. However, the contrast between the top and base of the basalt unit focused attention of the thickness of this unit, which is locally at least 70 m thick above Adit A-6.

2.2.4 Some larger-scale landforms

Basalt-filled palaeochannels

At Aqraba, inspection of the exposures of the Yarmouk Basalt, from vantage points at about 370 m asl, showed clearly the distinctive characteristics of these bodies. In particular, the palaeochannels, occupied by the basalt, are smoothly concave in cross-section. In other locations, valleyside remnants of dissected channel fills remain as

segments of the former saucer shapes. These appear to be ‘glued’ on to the limestone, where it forms the valley sides. Based on Late Quaternary and Holocene lavas in British Columbia (U. Mäder, per. comm., 1999), basalts may preserve inclined flow features where they probably served as feeder channels from wadis on the Syrian flank of the Yarmouk valley.

The concave base to palaeochannel fills must be emphasised, since their local thickness may be double that of average figures which are commonly quoted. The axis of such a palaeovalley must run directly over some point in Adit A-6, directly beneath.

Wadi al Habis chasm

The Wadi al Habis is a short, deeply incised valley. Strikingly, it descends more than 400 m within 2 km of the interfluve at its head. The possibility, mentioned in earlier reports, that river diversion has occurred in this locality, was examined more closely during the Reconnaissance Mission. This chasm-like incision is just to the west of the Western Springs area. The effect of its incision – probably abrupt – on changes in groundwater levels in this area, is clearly relevant to several aspects of the Maqarin Project enquiries.

In plan view (**Figure 2-6**), the headwater 0.5 km of the Wadi al Habis appears formerly to have continued due west, to link up with the Wadi Hilya and then on to the Wadi Khaled. About 0.5 km from its interfluve head, the Wadi al Habis turns sharply to the north, the ‘elbow of capture’ of classic geomorphological studies of drainage diversions. In cross-section, as shown in the longitudinal profiles of **Figure 2-8**, this is equally a point of sharply increased channel gradient (the ‘knickpoint’ of classic studies). The inferred gradient of the former palaeovalley can be linked with the altitude of the abandoned col (the ‘wind gap’ of classic studies). Support for this interpretation includes relict gravels and cobbles on the col floor.

Judging from commonly developed geomorphological features in the Maqarin area, the diversion of the Wadi al Habis may have been due to large-scale landslipping, in which the northern side of the palaeovalley foundered into the Yarmouk valley. Increased erosional undercutting at the base of this slope, by the shifting valley meanders of the Yarmouk, may have triggered this postulated failure.

There is also evidence concerning the origin of the drainage system, the possible timing of the diversion, and of subsequent modifications, too. Remarkably, the altitude of the interfluves at the head of both wadis is immediately below the level of the former Cover Basalt outcrop (**Figure 2-9**). Possibly, therefore, the valleys in this area first developed in an east-west direction along the southern margin of the Cover Basalt (i.e. ca. 3 Ma ago). The diversion occurred well after 3 Ma, since incision of 50-60 m had occurred below the plateau top.

On the other hand, the diversion of the Wadi al Habis clearly pre-dates Late Quaternary times. This is evident from the lowest reach of the longitudinal profile, where a regularised concavity had developed, before renewed downcutting of about 50 m occurred in the main Yarmouk valley, below a secondary knickpoint. Further up the Yarmouk valley, fluvial gravels and boulders , at about this altitude above the main river, may have been deposited about 50 ka ago.

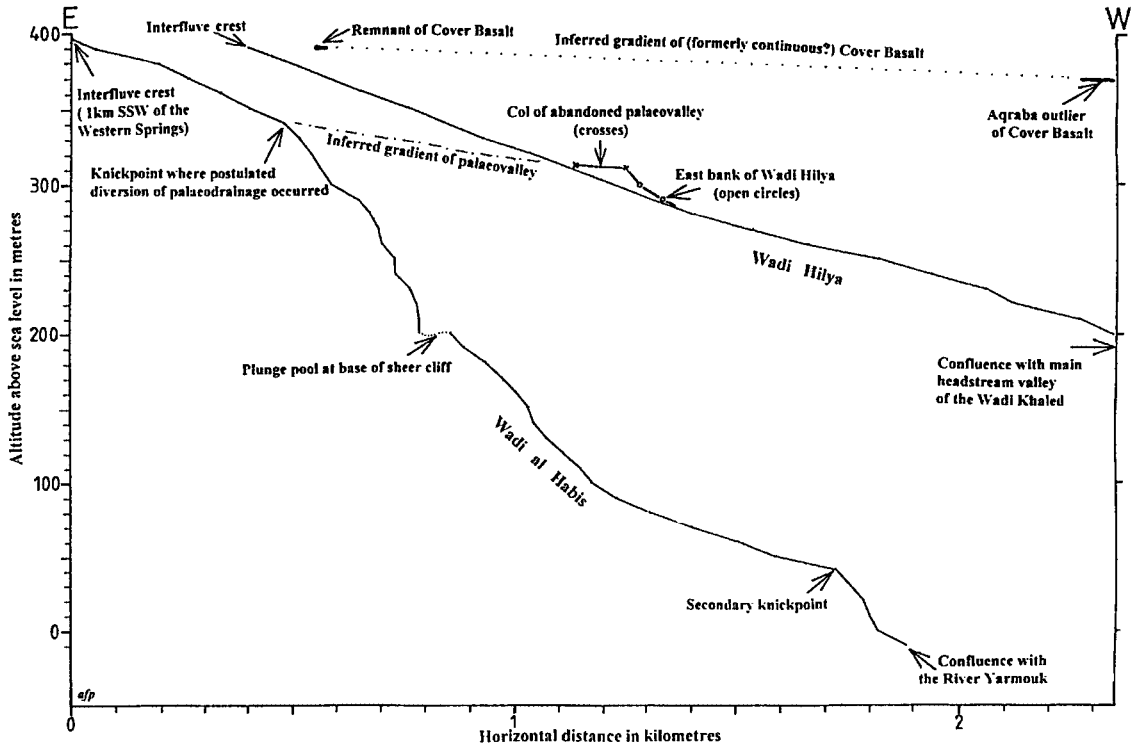

Figure 2-9. *Longitudinal profiles of the Wadi al Habis and the Wadi Hilya. Other selected features are shown. Note that both wadis start only a few metres below the inferred level of the former Cover Basalt outcrop. The location of the wadis is shown on* ***Figure 2-6.***

Tentatively, the Wadi al Habis chasm appears to post-date the deposition of the Yarmouk Basalt, ca. 0.8–0.7 Ma ago, but field survey in its lower reaches may clarify this point.

Wadi Sijin

Field survey along the channel floor of this wadi may be worthwhile. Significant features, noted in passing, include:

1. a classic gooseneck is shown in the south-west corner of **Figure 2-8**. Here, lateral undercutting by adjacent streams locally narrows the shared interfluve. This is a common feature on the Maqarin area, but the example, near the northern end of Wadi Sijin, is remarkable for its asymmetry in cross-section. The interfluve of the gooseneck is only some 30 m above the Wadi Sijin, whereas the drop down to the Yarmouk is more than 120 m. Therefore, sub-channel drainage from the Wadi Sijin, seeping through to the Yarmouk valley floor, may be a significant possibility;

2. cemented scree, apparently similar to the cemented rock debris on the southern margin of the Adh Dhlla bench, is present on the valley floor;

3. channel braiding is an unusual feature of the Wadi Sijin valley floor. An explanation for why **two** channels persist in parallel should be sought.

Ra's Inqar camber

To the SSW of the Wadi Sijin, the western end of the Ra's Inqar escarpment is a prominent skyline feature (**Figure 2-6**). At the western end, the caprock, near-horizontal in disposition, forms a sharp rim to the southern side of the Yarmouk valley. However, towards its SE end, the escarpment suddenly bends down, with the apparent dip becoming parallel to the inclination of the hillside. This appears to be a clear example of 'cambering' of a caprock. This type of mass movement has been mentioned in earlier reports, as being critical to an understanding of the geohistory of the Maqarin area.

2.2.5 Conclusions

Conclusions to the enquiries on a 'reconnaissance mission' might be most helpfully listed as simply as exercises for which more focused work might be attempted.

1. Prepare a field map of the slope deposits on the valleyside strip above Adit A-6.
2. Quick-set levelling, from a bench mark or spot height, to features on the Adit A-6 valleyside strip, or use of altimeter, if determination of exact heights is not justified.
3. Enlargement of sample sizes for which gravel data has been collected, ideally N = 100, and locate other sites.
4. Expedition to explore the channel floor of the Wadi Sijin, as far as Yarmouk village.
5. Expedition to explore the lower end of Wadi al Habis, with particular to possible lava flow relicts, and river terrace materials.
6. Field survey of features in the zone of 'enclosed depressions'.
7. Enlargement of number and surface types for which 'roughness' has been measured, perhaps to N=30.
8. Prepare a map of 'nari' surfaces.

- Extend natural gamma measurement sites, particularly where 'nari' appears to overlie the Bituminous Marl.
- Resume desk studies to scan current literature for relevant. new studies of geohistory and palaeoenvironment.
- Enlarge desk-study coverage to address new questions, posed by findings on the Reconnaissance Mission e.g.:
- – Identify general rules for how river drainage patterns are re-established after lava has filled the previous channel .
- Search for archaeological information about the cliff dwellings in Wadi al Habis.
- Continue and extend literature review:
  - In part in directions prompted by new evidence and interpretations and assertations (e.g. karst sinkhole literature, e.g. Kemmerly, 1982). Very recent publications (e.g. Wilcox, 1999)
  - Check on older and/or obscure references previously not considered (e.g. Stiller and Kaufman, 1985; Mouterde, 1953).

2.3 Geophysical survey[3]

2.3.1 General

Ground surface resistivity measurements (**Appendix 5**) were carried out at the Eastern Springs site to establish the lithostructural character of the upper 150 m of bedrock. These data were used to confirm the constructed geological profiles based on extrapolation of information from wells drilled in the 1950s and 1960s, thus providing the basis for locating suitable boreholes for future hydrological and hydrochemical investigations in the area.

A total of six profiles (3 in a N-S and 3 in an E-W direction) were measured. The spacing of the current electrodes was limited by the topography of the measured site, a relatively flat plateau of arable land (400x400 m) directly above the location of Adits A-6 and A-7 (**Figure 2-10**). Beyond this peneplain the topography slopes sharply 45° and more to the north, west and east. To the south it rises rapidly to another level. Extending the current electrodes beyond the peneplain to these steep slopes generally results in resistivities which can not be interpreted.

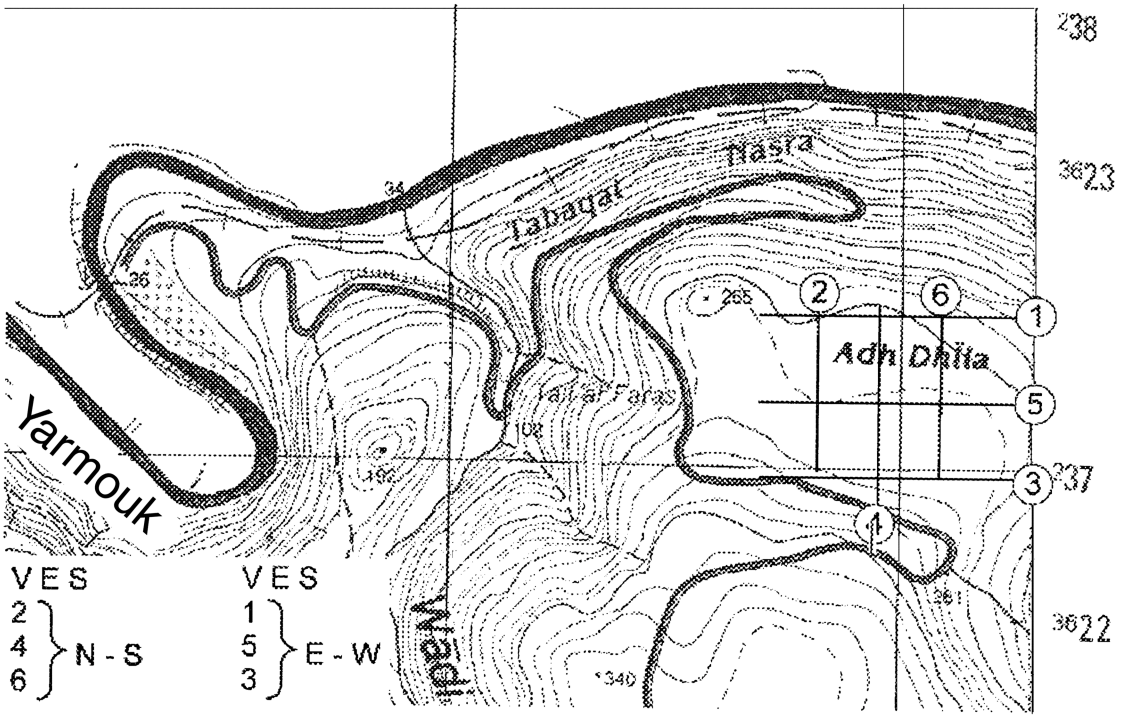

***Figure 2-10**. Location of ground resistivity traverses (1–6).*

[3] Elias Salameh.

2.3.2 Results

The coordinates of the traverses and the compilation of results and interpreted rock types are presented in **Tables 2-3 and 2-4**. For comparison, **Figures 2-11 to 2-16** show the geology along the traverses extrapolated from well logging data representing existing boreholes in the immediate area. Since the rock types in the area are well known from surface geology observations, together with investigation boreholes, pits and adits, the main lithological units chosen were restricted to basalts, bituminous marls, chalky marls, hillslope debris and soils. Interpretation was therefore limited to the clarity of these lithological units (i.e. stratification); information obtained from the boreholes drilled during the dam site investigations in the 1950s and 1960s were extremely useful in interpreting the results of resistivity measurements.

Table 2-3. GPS coordinates of geophysical profiles measured at the Eastern Springs.

Profile No.	GSP location			
1	N	32	43	948
	E	35	52	108
2	N	32	43	735
	E	35	52	033
3	N	32	43	607
	E	35	52	100
4 and 5	N	32	43	716
	E	35	52	125
6	N	32	43	720
	E	35	52	240

The resistivity data showed a good correlation with the geological sections (**Figures 2-10 to 2-16**) confirming the geology to 150 m depth.

Table 2-4. Results from the measured geophysical profiles 1–6.

Profile No.	Resistivity (Ω m)	Thickness (m)	Depth (m)	Lithology
1	20.6	0.5	0.5	Wet salty soil
	513.2	2.2	2.7	Dry basalt
	181.2	13.5	16.2	Basalt (+ wet clays)
	911.3	37.6	53.8	Basalts (wetted)
	171.5	>60	>100	Altered rock
2	18.7	0.7	0.7	Soil
	2.7	1.7	2.4	Soil
	476.6	8.8	11.2	Basalts (+ some clays)
	3639.1	>140	>150	Dry basalt
3	98.6	0.8	0.8	Dry soil
	38.4	7.5	8.4	Wet soil (+ rock debris)
	33.2	14.1	22.4	Wet soil (+ rock debris)
	302.2	21.7	44.1	Basalt + lateral altered rock
	2184	>100	>150	Dry altered rock
4	24.9	1.0	1.0	Wet salty soil
	3.8	1.0	2.0	Wet salty soil
	5.4	2.6	4.6	Wet salty soil
	33.8	2.6	7.2	Wet basalt (+ rock debris)
	208.4	11.4	18.6	Wet basalt (+ clays)
	869.9	140	150	Wet basalt (+ lateral contact with altered rock)
5	27.6	0.9	0.9	Wet, partly salty soil
	3.1	1.2	2.1	Wet, partly salty soil
	8.7	2.5	4.6	Wet, partly salty soil
	56.0	4.1	8.8	Basalt (+ high moisture clay)
	132.0	23.1	31.8	Wet basalt
	652.3	>130	>150	Wet basalt (+ altered soil/palaeosoil)
6	23.1	1.3	1.3	Wet soil (+ rock debris)
	72.1	1.3	2.6	Wet soil (+ rock debris)
	176.4	4.3	6.9	Baked palaeosoil
	165.8	8.0	14.9	Wet basalt (+ clay in joints)
	158.6	8.2	23.1	Wet basalt (+ clay in joints)
	241.4	8.0	23.1	Wet basalt (+ clay in joints)
	579.7	>120	>150	Basalt (+ lateral contact with altered rock)

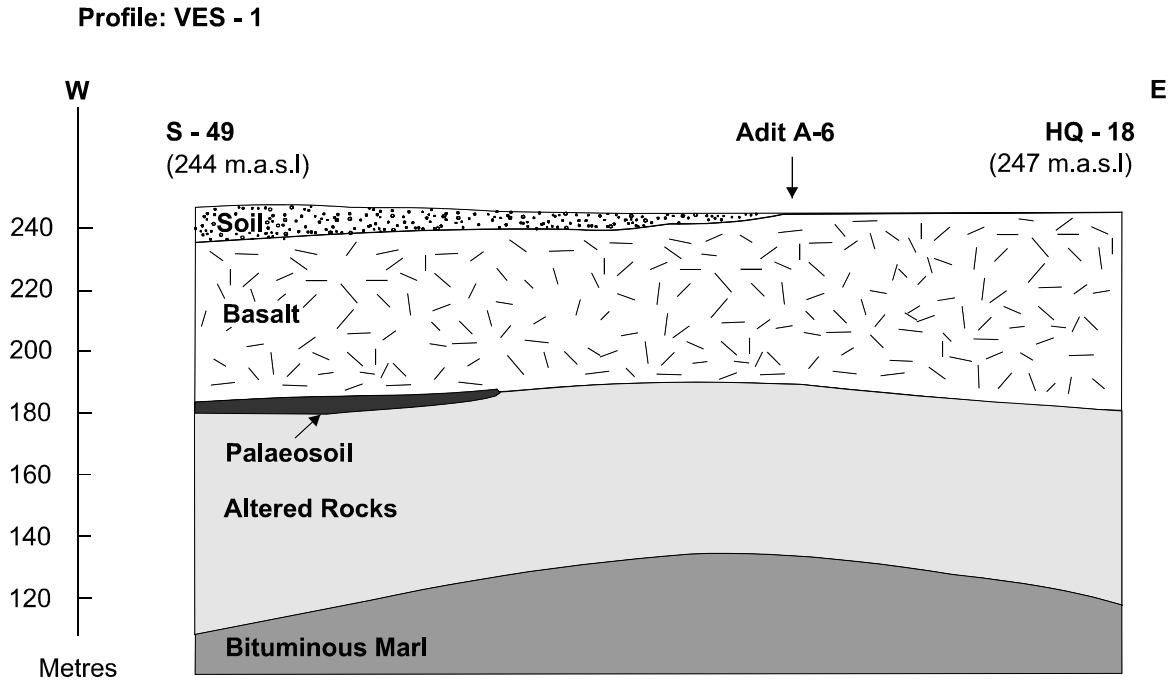

Figure 2-11. *Geological profile along E-W ground resistivity traverse 1 (Profile 1; VES-1).*

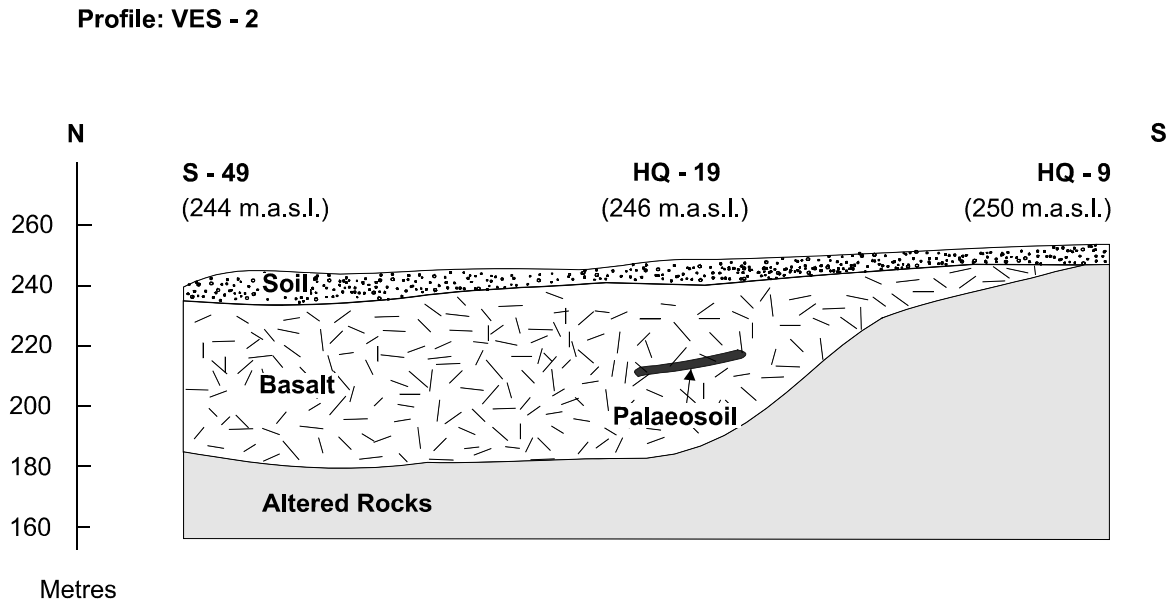

Figure 2-12. *Geological profile along N-S ground resistivity traverse 2 (Profile 2; VES-2).*

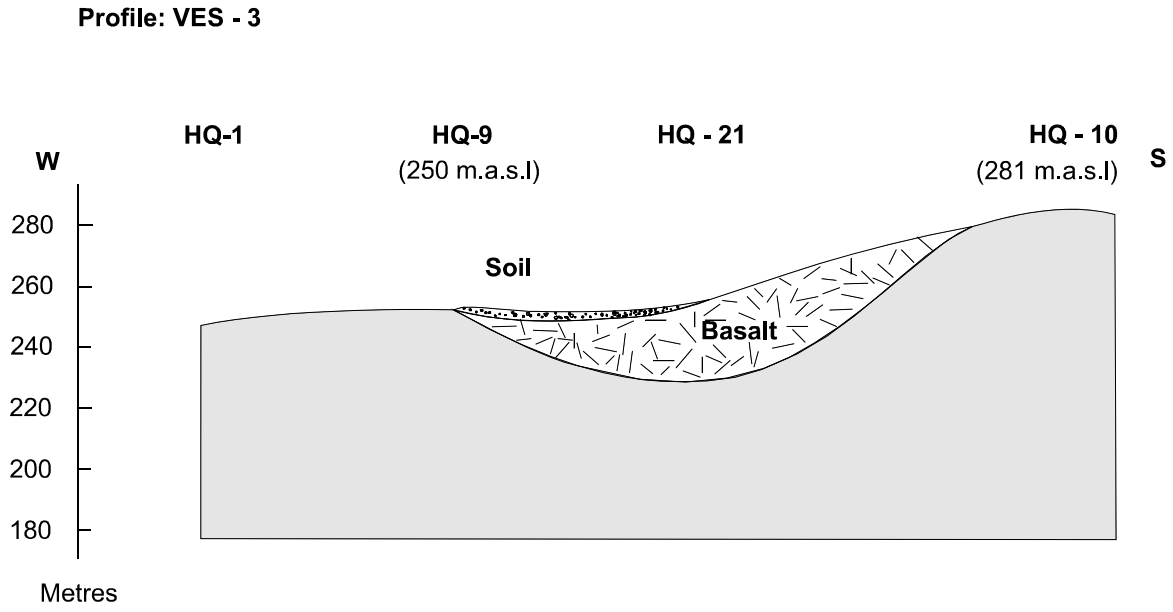

Figure 2-13. *Geological profile along E-W ground resistivity traverse 3 (Profile 3; VES-3).*

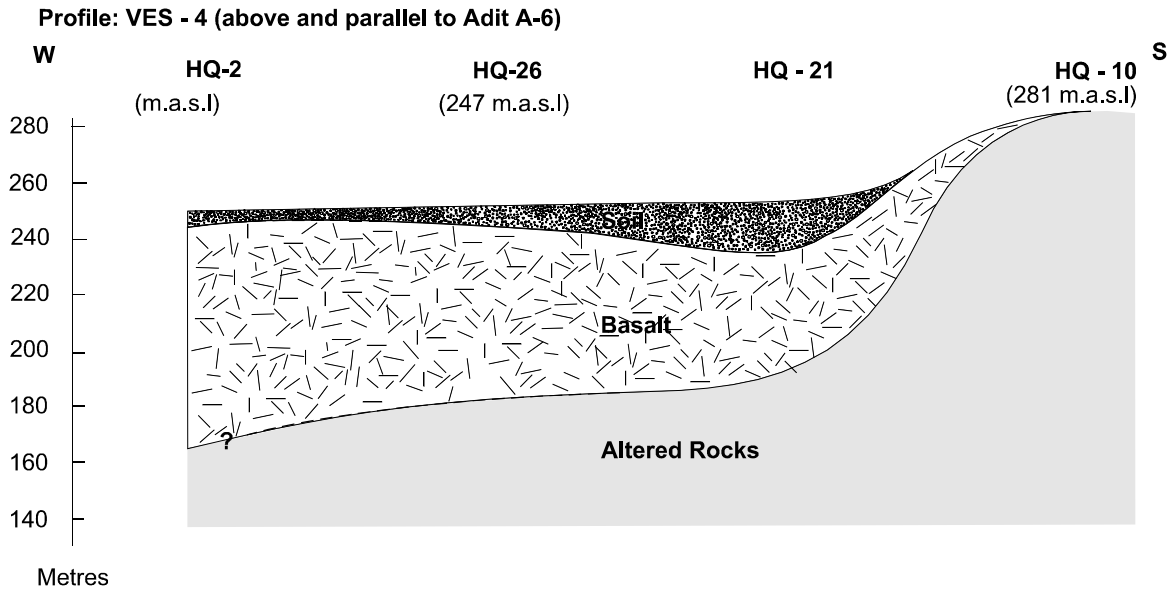

Figure 2-14. *Geological profile along N-S ground resistivity traverse 4 (Profile 4; VES-4).*

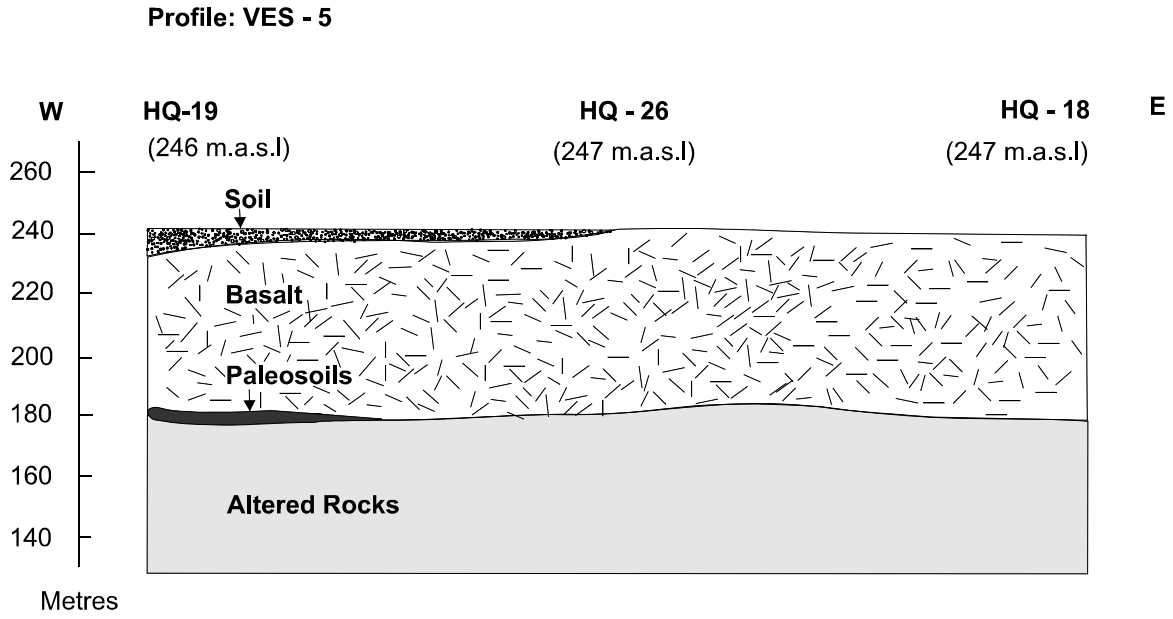

Figure 2-15. *Geological profile along E-W ground resistivity traverse 5 (Profile 5; VES-5).*

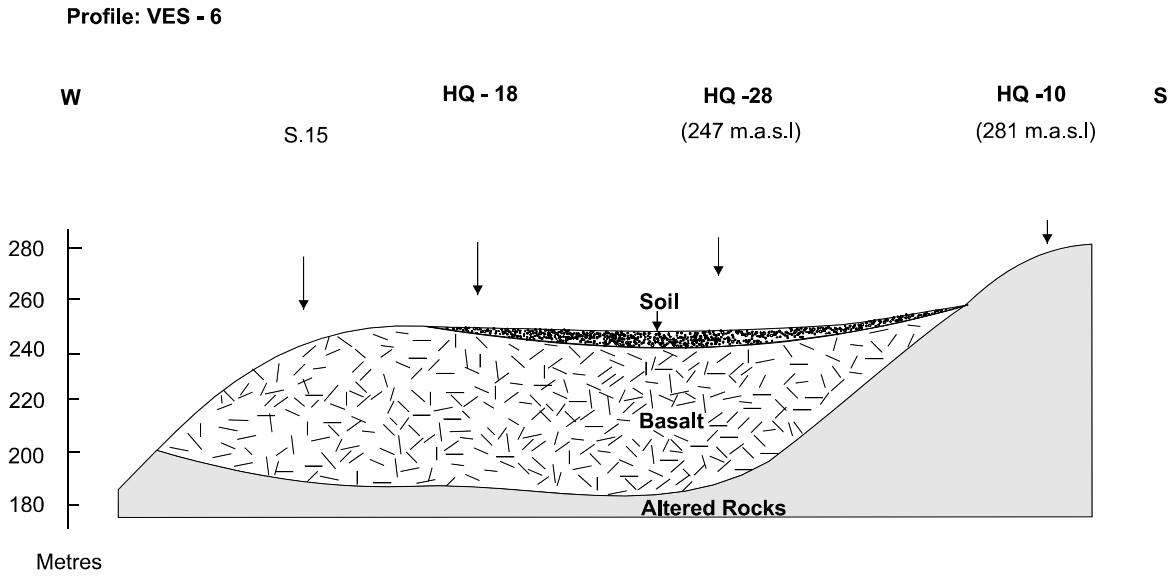

Figure 2-16. *Geological profile along N-S ground resistivity traverse 6 (Profile 6; VES-6.*

2.4 Rock sampling

Outcrop samples were collected from the near-vicinity of the Adit A-6 entrance and at specific locations during reconnaissance traverses across the Eastern Springs area. Details of these samples are documented in the Sample Archive List (**Appendix 8**).

3 Results from activities carried out in Adit A-6

One of the main objectives of the mission was to assess the potential for drilling within Adit A-6 using the Hilti drill which had been used unsuccessfully during Phase II. Drilling directly from the adit is of interest: (i) to collect rock samples along specific profiles (e.g. unaltered marl/cement zone and cement zone/transition zone/unaltered marl), and (ii) to sample high pH groundwaters from hydraulically active fractures in the different rock-types under reducing conditions, more representative of a repository environment. Furthermore, this approach should allow the role of colloids and microbes in high pH waters to be studied more realistically and thoroughly.

Prior to drilling, the physical condition of the adit had to be evaluated for safety reasons. Surprisingly most sections of the adit were found to be reasonably stable. Consequently, the drilling locations were protected only with thin sheets of corrugated iron secured on a wooden framework to prevent loose fragments from becoming dislodged during drilling.

3.1 Drilling[4]

The main objective of demonstrating the ability to drill and recover core in Adit A-6 was achieved: two holes **(Tables 3-1; 3-2)** were successfully drilled, one in unaltered bituminous biomicrite ("Bituminous Marl") and one in the pyrometamorphic zone ("cement zone"). An improved base plate design and a better anchoring system for the drill rig was used compared to previous futile attempts.

A somewhat limited budget and relatively short preparatory time necessitated a simple approach: drilling with a small Hilti core drill apparatus with extension barrels of 60 mm O.D. and a drill bit for cement with a relatively wide cutting edge (64 mm O.D., 54 mm I.D.). The cement bit turned out to be neither optimal for unmetamorphosed rock nor for the metamorphic zone, but nevertheless it allowed to complete two holes, albeit at slow speed. Both holes were packed off with hydraulic packer systems, either to monitor pressure build up (unmetamorphosed rock), or to prepare for sampling high-pH fluid (metamorphic zone). Details of the equipment and installations are provided in **Appendix 6**.

[4] Urs Mäder.

Table 3-1. Diamond drill hole at sampling location D1 (previously M2).

Location:	Adit A-6, tunnel metre 44.6 m, E-side
Orientation:	Drilling direction 135°, inclined 19° upwards
Depth:	Drilled: 4.5 m, core recovered to 4.25 m
Packed-off interval:	Approx. 3.1–4.5 m (1.4 m length)
Core recovery:	100% of oriented core
Core storage:	BGS
Core log:	No lithological/structural log; depth marked on core segments
Remarks:	Opposite of crest line is marked as continuous line on core
Main features:	No (alkaline) water conducting features; few calcite-filled veins

Preparatory work for drilling was commenced on April 30, 1999. Drilling started on May 1 and finished on May 3. The packer system was emplaced on May 4, 1999, and had to be reset once the same day. Apparently the packer was disturbed by some unwanted visitor after the reconnaissance mission later in May or June.

Drilling proceeded in the unaltered bituminous micrite **(Table 3-1**) without major problems. There was substantial eccentricity over the first drilled metre resulting in a reduced diameter of the core and an increased and irregular diameter of the drill hole. At larger depth the problem of eccentricity largely diminished resulting in core of good quality and a good drill hole condition for setting packers. Fresh alkaline drip water was used as drilling fluid in order not to contaminate any feature that might conduct alkaline water, at the expense of some contamination of the bituminous biomicrite.

A single packer of 1 m packer length was set with a single extension tube of 2 m length to seal the bore hole at approximately 3.1 m depth. The packed-off interval is accessed by a sampling/testing line (red) at about 20 cm above the packer, and a vent/bleed line (yellow) extending to the end of the cored hole held in place by a wire guide. The sampling line (red) is furnished with a pressure gauge and shut off by a valve with a snap-on connection (to fit the hand pump). The central extension rod is also open to the interval, and is closed shut by a large valve attached to the lower end of the extension rod. The test interval was filled with fresh spring water and left shut for pressure recovery.

Table 3-2. Diamond drill hole at sampling location D2 (previously M1).

Location:	Adit A-6, tunnel metre ~141m, W-side
Orientation:	Drilling direction 290°, inclined 10° upwards
Depth:	Drilled: 2.2 m, core recovered to 2.1 m
Packed-off interval:	Last 0.9 m
Core recovery:	Approx. 80% of non-oriented core in relatively small pieces
Core storage:	BGS
Core log:	No lithological / structural log; depth marked on core or wrapper
Remarks:	None
Main features:	Breccia and matrix lithologies; distinct outflow of alkaline water

The drilling site was prepared May 3, 1999, and drilling continued from May 4 to 6. A single hydraulic packer was emplaced on May 6.

Drilling in the 'hard' part of the brecciated pyrometamorphic zone **(Table 3-2)** proved to be difficult and proceeded very slowly. Vibrations and eccentricity problems were substantial. Also, the power of the Hilti was limiting in applying pressure to the drill bit. Additionally, one of the cutting segments got knocked off the drill bit during the last phase of drilling. Drilling was halted at a depth of 2.4 m for practical reasons, after reaching a minimal depth of at least 2 m for setting a packer properly.

A single packer of 1 m packer length was set with an extension tube of 0.5 m length to seal an interval of 0.9 m length. The packer was inflated with fresh spring water. The packed-off interval is accessed by a sampling/testing line (red) ending at about 20 cm above the packer, and a bleed/vent line (yellow) extending to the end of the cored hole held in place by a wire guide. The sampling line (red) is shot off by a valve and furnished with a pressure gauge and snap-on connection. The central extension rod is also open to the interval, and is closed shut by a large valve attached to the lower end of the extension rod. The packer used is the lower packer of a double packer assembly. The feed-through lines for the non-existing upper interval are sealed just below the packer. The test interval was flushed with high-pH water before setting the packer. The bleed line (yellow) was left open in order to allow for continuous flushing of the in-situ high-pH fluid.

3.1.1 Activities planned during the summer of 1999

It was decided that drilling was to continue during the summer and autumn months with the following priorities:

1. Drilling two further boreholes (D3; D6) in the unmetamorphosed zone in order to intersect a high-pH fluid conducting feature, and to provide a well constrained and unaltered sample for rock-matrix-diffusion studies, and for fluid/solid sampling of the conducting features.

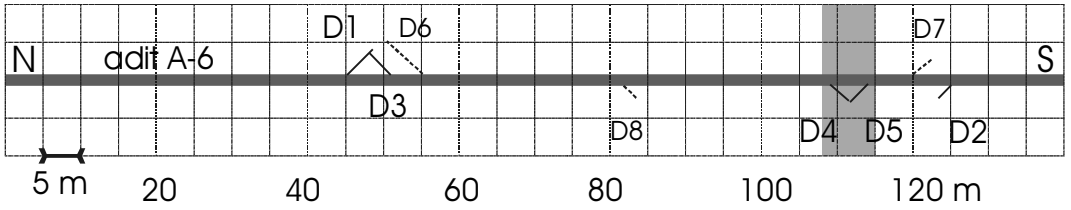

Figure 3-1: *Plan view of Adit A-6 with locations of diamond drill holes. The transition zone from the unaltered limestone (N) to the cement zone (S) is shaded. Drilling phases: spring 1999 (D1, D2), summer 1999 (D3-D5), autumn 1999 (D6-D8).*

2. Drilling 2 boreholes (DD4; D5) in the transition zone from unmetamorphosed to pyrometamorphic rocks in order to sample and characterise the transition zone in samples free of any alteration.

3. Drilling one additional borehole (D7) in the cement zone to complement D2.

The positions of the drilled boreholes are schematically illustrated in **Figure 3-1**.

3.1.2 Current status

A gate had been constructed in June 1999 in order to protect Adit A-6 from unwanted 'visitors'; road access to the adit had been restored for 4WD vehicles.

3.1.3 Future objectives

Future drilling activities will be decided on during the project meeting in September 1999 within the framework of finalising the proposal for Phase IV.

3.2 Structural mapping[5]

Detailed fracture characterisation was started but not completed; further mapping and a detailed interpretation is pending.

[5] Tony Milodowski and Paul Degnan.

3.3 Lithological mapping and sampling[6]

Installation of generator-powered lighting provided the opportunity for serious mapping and sampling within the adit.

3.3.1 M1 fracture zone

The thick coating of travertine which characterises the cement zone was first removed before selecting samples along the exposed M1 fracture zone located on the west wall of the adit, 130 m from the entrance. The sampled profile is about 2 metres from the adit floor. The samples were collected using a knife (or chisel) and are labelled from A to G (**Figure 3-2; Table 3-3**). The measured distances are from left to the right on the figure.

3.3.2 Transition zone

This profile was sampled along the west wall of the adit, the samples being taken at about 1.5 m from the floor of the adit (except sample TZ (-1) at about 2 m) (**Figure 3-2; Table 3-4**). The transition zone between the cement and the unaltered marl constitutes a diffuse, inclined interface located at about 113 m (**Figures 3-3 and 3-4**). Eleven samples have been collected, most of them being located along a 5 metre section between 109m and 114 m.

The objective of this sampling is:

2. to better understand the mineralogical evolution of the marl (clay content etc.) from combustion through to reaction with high pH groundwaters;
3. to make a parallel comparison with the Khushaym Matruk site in Central Jordan were a fossil interface between hyperalkaline reaction and unaltered marl is observed;
4. to sample fractures were alkaline waters have been circulating (data on matrix diffusion and alteration phases); and
5. to evaluate large scale diffusion processes in the marl and possibly derive a temperature profile.

[6] *Tony Milodowski, Laurent Trotignon, Hani Khoury and Lise Griffault.*

Table 3-3. Description of samples collected across the M1 fracture zone.

Sample	Sample size	Description
A	0–3 cm	Hydrated cement; beige; hard
B	3–7 cm	Altered cement; white; less hard than A
C	7–8 cm	Fracture with red filling; soft
D	8–13 cm	Highly altered cement; white; soft
E	13–17 cm	Complex zone with symmetrical rims E1: thin red rim E2: ocre filling E3: internal purple filling
F	17–22 cm	Highly altered cement; white; soft
G	22–27 cm	Altered cement; pale pink; hard

Table 3-4. Description of samples collected along the transition zone profile.

Sample field name	Catalogue reference number	Distance (m) to adit entrance	Description
TZ (-3) 504m	M99-1-33a to 33d	50–100	Bituminous Marl
TZ (-2) 1044m	M99-1-33a to 33d	104	Bituminous Marl; fungal growth
TZ (-1) 1094m	M99-1-33a to 33d	109	Slightly baked Bit. Marl; large N-S fracture in roof with white/grey filling and brown rim
TZ (+1) 110.54m	M99-1-33a to 33d	110.5	Dark grey baked Bit.Marl with veinlets
TZ (+2) 111.54m	M99-1-33a to 33d	111.5	Baked Bit.Marl; brownish/reddish in colour; green products; veinlets
TZ (+3a) 1134m	M99-1-33a to 33d	113	Strongly baked Bit.Marl; light brown to grey; soft (clay?)
TZ (+3b) 113.34m	M99-1-33a to 33d	113.3	Baked Bit. Marl; reddish; green products in fractures
TZ (+4a) 113.54m	M99-1-33a to 33d	113.5	Strongly altered cement; red and white alteration products
TZ (+4b) 1144m	M99-1-33a to 33d	114	Pristine cement nodule + alteration products; crack filled with products; diffusion profile at rim
TZ (+5) 115 m	M99-1-33a to 33d	115	Altered cement; white/beige; red cracks
TZ (+6) 118 m	M99-1-33a to 33d	118	Near M1 fracture zone; hydrated Cement + alteration products

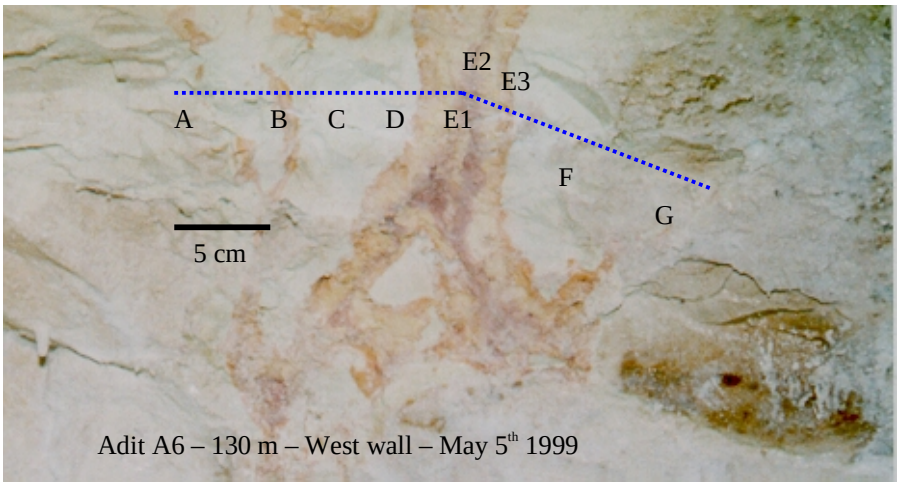

Figure 3-2. *Sampled profile (A-G) across the M1 fracture zone.*

Figure 3-3. *Transition zone profile: Sample location TZ(-1); adit roof fracture.*

Figure 3-4. *Transition zone profile; Sample location TZ (+3b). Transition between cement-like material (white and red, left) and strongly baked marl (brown to grey, right) is clearly visible.*

4 Results from activities carried out in Central Jordan[7]

In the quest to find clay-rich sedimentary horizons showing fossilised reactions with high pH waters, three areas were visited in Central Jordan: i) Sweileh, 16 km NW of Amman, ii) Daba, about 50 km south of Amman, and iii) Khushaym Matruk, about 80 km south-east of Amman. A preliminary visit to all three localities showed that Khushaym Matruk was the most promising and a small group returned later to the site to document the stratigraphy and collect samples for study.

4.1 The Sweileh locality

4.1.1 Geology

The Lower and Upper Cretaceous rocks crop out in the Sweileh area east of the metamorphosed (cement) zone. The Lower Cretaceous Sandstone unit is overlain by the Nodular Limestone Unit which in turn is overlain by the Echinoidal Limestone Unit; this is itself overlain by the Massive Limestone Unit (Wadi Sir Limestone). The Silicified Limestone Unit (Amman Silicified Formation), which crops out in the metamorphosed area, overlies the Echinoidal Limestone Unit and underlies the Phosphorite Unit (Al Hisa Phosphorite Formation). The Phosphorite Unit in the area is metamorphosed. The remnants of the Chalk Marl Unit (Muwaqqar Chalk Marl Formation) are also present in the area.

The main structure in the area is an anticline which is intersected by a flexture trending NNE-SSW.

4.1.2 The marble/cement zone

The marble/cement outcrops of the Sweileh area belong to the upper part of the Phosphorite Unit and the lower part of the Chalk Marl Unit. The rocks are varicoloured and similar to those in central Jordan (see below). The green, black and brown varieties are most common. Apatite schist is the most abundant unit and reflects the high pressure structural control during the recrystallisation process.

[7] University of Jordan, Amman; Commissariat à l'Énergie Atomique, Cadarche; SARL Etudes Recherches Matériaux, Poitiers.

4.2 The Central Jordan sites

These sites comprise Daba (Khan Ez-Zabib) and Siwaqa with an areal extent of about 662 and 660 sq. km respectively. Their northern boundaries are located 25 km and 50 km south of Amman.

4.2.1 General geology

The exposed rocks in the two areas range in age from Upper Cretaceous (Campanian) to Eocene; superficial deposits are of Pleistocene to Recent in age.

The Amman Silicified Limestone Formation (Campanian) is the oldest present in the area, with the uppermost exposed part consisting of thin to thick bedded chert inter-bedded with micritic limestone. This Formation is overlain by the Al Hisa Phosphorite Formation (Maestrichtian) which consists of silicified phosphorite, phosphorite-bearing oysters and phosphate layers. Above the phosphorite beds lies the Muwaqqar Chalk Marl Formation (Maestrichtian-Upper Paleocene). The upper Muwaqqar Formation (regional equivalent to the Bituminous Marl Formation in Maqarin) is composed of bituminous-rich marl which, in most of the outcropping parts, is metamorphosed to varicoloured marble/cement. The Umm Rijam Chert Limestone Formation overlies the bituminous-rich marl in the unmetamorphosed areas. Sand and gravel (Pleistocene), travertines (deposited from alkaline springs), and alluvial and Wadi sediments (Recent), overlie all younger rock-types.

Two fault sets dominate in the Daba area; an E-W extension of the Zarqa Main Fault and the NW-SE striking Wadi Al Hammam Fault set. The main E-W fault in the Siwaqa area is the Siwaqa Fault system.

4.2.2 The Daba marble/cement zone

These marbles typically occur as lenticular bodies in the south and southeastern parts of the Daba area. The marble occurs in the upper metres of the Muwaqqar Chalk Marl Formation and the greatest thickness is found at Tulul Al-Hammam, where it ranges up to ten metres. The Daba marble varies in colour from brown to green to black; fractures and fissures are filled with secondary mineral phases.

4.2.3 The Siwaqa marble/cement zone

These marbles/cements occur in the upper part of the Muwaqqar Chalk Marl Formation, overlying the bituminous-rich marl (30m), which crops out only in the Khushaym Matruk area. The marble is brown-black in colour and fractures are filled with secondary mineral phases.

Since the Siwaqa marbles of the Khushaym Matruk area is the only exposed site in central Jordan where both the bituminous-rich marl and the marble (i.e. cement zone) are in direct contact, and fossilised travertines of high pH water origin occur, this site was chosen for further study. In addition, previous scoping analyses of some selected samples had indicated higher clay contents than previously observed at Maqarin (H. Khoury, per. comm., 1999). Since clay stability in a hyperakaline groundwater environment was of particular interest for potential Phase IV studies, this site was sampled thoroughly.

4.3 Investigations at the Khushaym Matruk site

The Kushaym Matruk area (N 31°16 570 ; E 36° 14’ 775), belongs to the southern extension of the Daba Marble Zone (see Maqarin Phase II Report (1998), Linklater Ed., p 38). The site itself is located at the western end of a low range of hills, and the contact between the bituminous-rich marl and the metamorphosed or cement zone is clearly visible (**Figure 4-1**). The grey bituminous-rich marl (i.e. Muwaqqar Formation) crops out at the base of the hills, about 5 to 10 metres in vertical extension. Above the marls, and forming the upper parts of the hills (i.e. about a 50 m vertical extension), are marble and travertine formations. The travertine is commonly found at the hill summits (forming a resistant cap to erosion), on the slopes, and near the interface between the marl and the overlying cement zone.

At the present day, the groundwater table lies some 150–200 m deep and the site is therefore totally desaturated.

Figure 4-1. *View of the Khushaym Matruk site from the SW. The grey, slightly dipping layer is the Muwaqqar Formation (bituminous-rich marls). The white arrow shows the location of the sampled profile.*

4.3.1 Sampling

Initially some general samples were taken from the slopes and summits of the hills (**Figure 4-2**), e.g. cement samples showing fractures and diffusion rims were collected near the top of the hill. Efforts then focussed on the interface between the bituminous-rich marl and the cement/travertine sequence. This interface shows, on a vertical scale of about 5 m, the following sequence (from top to bottom):

1. strongly fractured cement/travertine (white/beige);
2. a green interface layer (chromium-rich) with a thickness of 0.3 to 1 m; this layer is soft and, at some places, forms two texturally different zones;
3. Bituminous-rich marl; zones of different colour and texture are found in the first metres of the marl (white, red, grey). In some of these sections the marl is very soft and is thought to contain significant concentrations of clay minerals.

Another important feature of this interface are vertical fractures intersecting both the cement zone and the underlying marl formation (**Figure 4-3**). These fractures are filled with secondary products (calcite and/or gypsum + other phases) and probably constituted percolation paths for fluids released from the cement zone. At one location, a very sharp interface can be seen in the marl, displaying a horizontal zonation between

Figure 4-2. *Khushaym Matruk site: Location of the profile sampled from the cement zone (on the right) to soft (shaley) bituminous-rich marl horizons. Seven samples were collected along this 30 m long profile.*

Figure 4-3. *Khushaym Matruk: Locality 4, showing large vertical fractures intersecting the travertine and marl.*

grey marl and what seems totally whitened marl (**Figure 4-4**). This sharp contrast is presently not understood but it could indicate a reaction front preserved in the marl.

The first sampling was carried out along a profile (**Figure 4-5**) traversing the marl/ cement interface at a location which had been sampled previously. This consists of soft, shaley marl horizons which were shown to be clay-rich (about 20% from preliminary analysis; H. Khoury written comm., 1999).

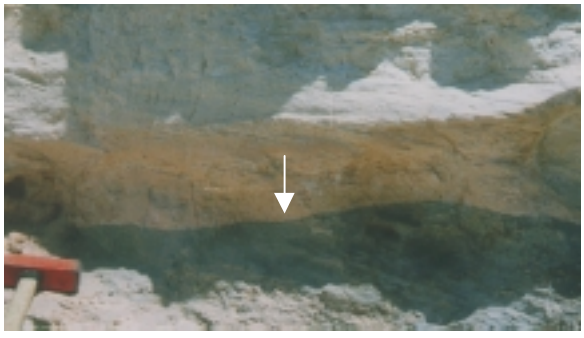

Figure 4-4. *Khushaym Matruk: Locality 5 showing the sharp interface between grey and whitened marl.*

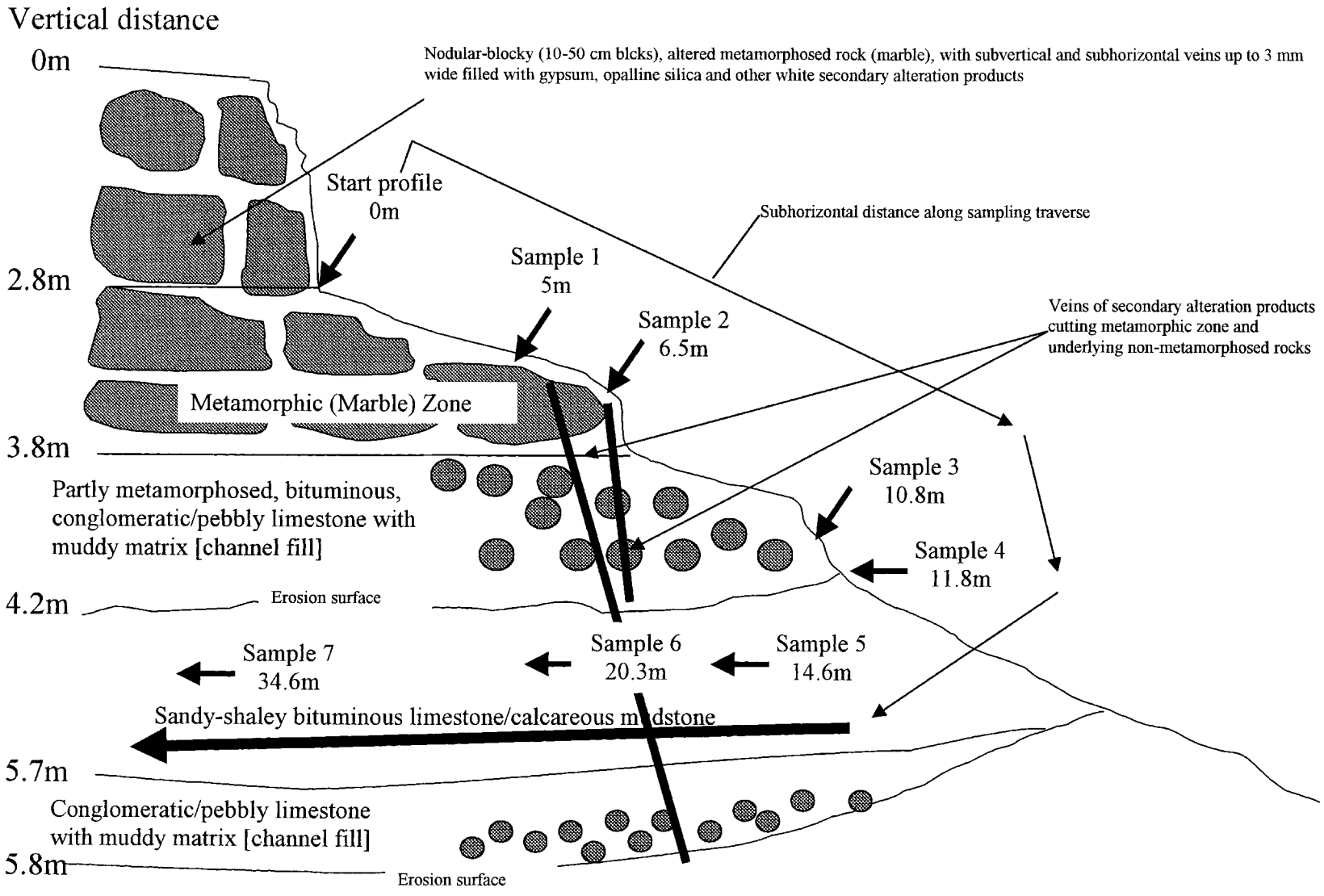

Figure 4-5. *Sketch of the sampled profile at the Khushay Matruk locality.*

During the second visit, sampling was planned to address the following objectives:

1. to further explore the contact between the marl and the cement at the southern edge of the Khushaym Matruk hill;
2. to identify and sample zones where vertical fractures have intersected the interface, and
3. to sample small scale profiles across the cement/marl profile.

Successive locations around the hill, roughly along an E-W direction, were sampled and described.

Location 1: (N 31°16'420 ; E 36°14'982): Bank of metamorphosed bituminous-rich marl, green to black in colour with some overlying travertine. No sample was taken at this spot.

Location 2: (N 31°16'500 ; E 36°14'933): Cement outcrop half way to the top of the hill. 1 sample réf. K99-1-15 collected (red cement with fractures).

Location 3: (N 31°16'367 ; E 36°14'897): Vertical fractures intersecting the marl; fracture fillings. 1 sample collected (réf. K99-1-16).

Location 4: (N 31°16'464 ; E 36°14'842): Slightly baked marl under travertine (**Figure 4-3**). Large subvertical fractures with calcite filling and green products. Sample bags K99-1-17 and K99-1-18.

Location 5: (N 31°16'488 ; E 36°14'777): Contact between travertine and marl (**Figure 4-4**); fractures and vertical veins cross-cutting the marl.

K99-1-19: veins cutting the marl.

K99-1-20: sharp contact between the grey and white marl.

K99-1-21: marl + fillings in a large horizontal fracture.

Location 6: (N 31°16'569 ; E 36°14'776): Interface between the travertine and marl. A small trench was excavated in the marl to sample soft (baked ?) samples. Samples collected at this spot are labelled K99-1-22 to 24.

Location 7: (located about 100 m south from Location 6): Same horizon as sample K99-1-24 (interface between the soft travertine layer and the marl). This sample was collected in order to check the spatial variability of this interface.

In addition to these individual locations. a profile was sampled in the vicinity of Locality 5 (**Figure 4-6**). This profile (**Figure 4-7**) extends from the bottom of the travertine layer, through the chromium-rich green layers, to the uppermost zones of the bituminous-rich marl.

Figure 4-6. *Khushaym Matruk: Locality 5.*

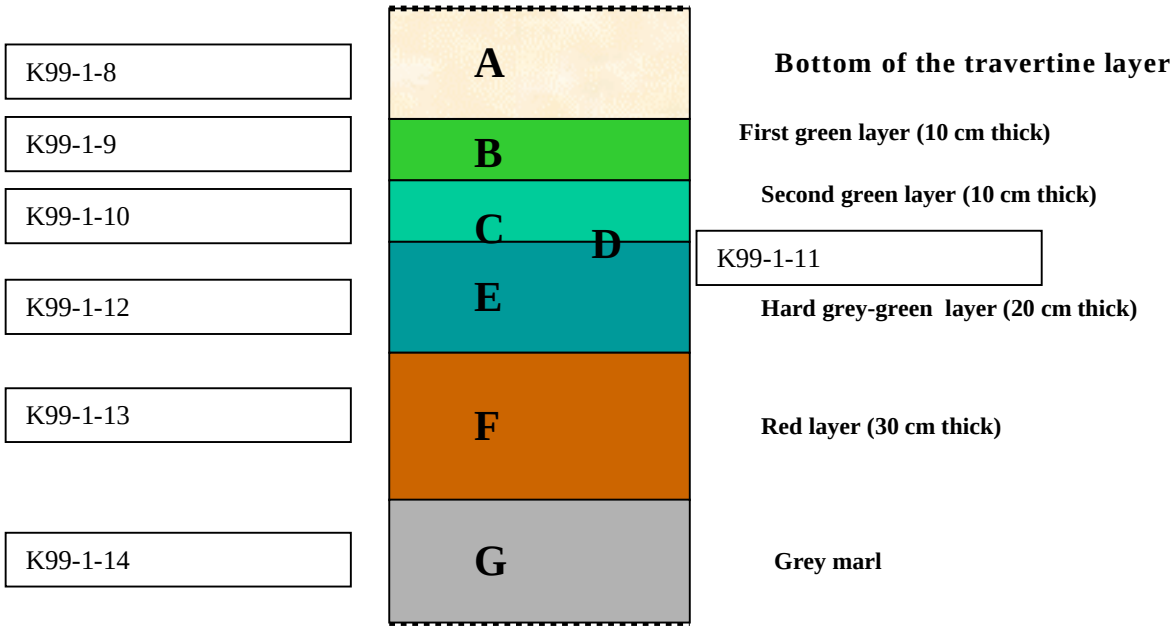

Figure 4-7. *Sketch of the profile sampled at Khushaym Matruk (Locality 5); cement zone/marl interface.*

4.3.2 Preliminary studies (University of Jordan[8])

A total of 17 samples were analysed by X-ray diffraction to identify the mineral content; the same samples were treated to separate the clay minerals. Preliminary results indicated the absence of any clay minerals (**Table 4-1**), despite the fact that a previously collected marl sample from the site indicated the presence of expansive clay (smectite). XRF analysis, however, indicated some high Al_2O_3 and SiO_2 contents (samples K99-1-4, K99-H4, K99-1-22) that might suggest the presence of clay material (**Table 4-2**). The presence of expansive smectite clay (>10%) was subsequently confirmed in several samples (**Table 4-3**).

Table 4-1. XRD Preliminary Results.

Sample No.	Calcite	Gypsum
K99-1-1	Xxx	xx
K99-1-2	Xxxx	x
K99-1-3	Xxxxx	–
K99-1-4	Xxxxx	
K99-1-5	Xxxxx	
K99-1-6	Xxxxx	
K99-1-7	Xxxxx	Tr
K99-1-8	Xxxxx	x
K99-1-9	Xxxxx	xxxx
K99-1-10	Xxxx	x
K99-1-11	–	xxxxx
K99-1-12	Xxxxx	Tr
K99-1-13	Xxxxx	Tr
K99-1-14	Xxxxx	–
K99-1-22	Xxxxx	–
K99-1-23	Xxxxx	–
K99-1-24	–	xxxxx

Tr = Trace

[8] Coordinated by Hani Khoury.

Table 4.2. XRF analysis of Kushaym Matruk samples.

Item	S.ID	Fe_2O_3 (%)	MnO (%)	TiO_2 (%)	CaO (%)	K_2O (%)	P_2O_5 (%)	SiO_2 (%)	Al_2O_3 (%)	MgO (%)	Na_2O (%)
1	K99/B 1–1	1.09	0.00	0.11	38.22	0.00	1.42	8.80	2.92	2.08	0.00
2	1–2	0.49	0.00	0.03	49.66	0.00	0.77	4.71	1.78	2.79	0.00
3	1–3	0.51	0.00	0.04	50.56	0.00	0.70	3.98	1.59	2.01	0.00
4	1–4	2.46	0.04	0.24	38.67	0.00	1.18	13.90	5.85	1.91	0.00
5	1–5	0.90	0.12	0.09	37.75	0.00	0.62	9.86	3.22	1.78	0.00
6	1–6	0.77	0.06	0.06	46.99	0.30	1.55	6.05	2.31	1.69	0.00
7	1–10	0.62	0.02	0.05	37.21	0.00	0.74	6.78	1.76	2.55	0.00
8	1–11	0.55	0.08	0.04	40.41	0.00	0.74	8.38	1.98	3.65	0.00
9	1–12	0.66	0.00	0.05	46.47	0.00	0.82	6.26	1.99	2.45	0.00
10	1–13	1.47	0.00	0.15	41.54	0.00	2.20	10.16	3.62	2.66	0.78
11	1–14	1.08	0.00	0.11	39.84	0.00	1.50	16.90	4.36	3.73	0.00
12	1–22	2.07	0.00	0.22	39.10	0.00	2.36	13.97	5.92	2.90	0.00
13	1–23	1.33	0.00	0.12	46.67	0.00	2.18	8.15	3.02	2.58	0.00
14	1–24	1.20	0.00	0.11	35.55	0.00	1.16	10.42	3.41	2.32	0.00

Table 4-3. X-Ray Diffraction results.

Sample No.	Calcite	Gypsum	Smectitic clay %
K99-1-1	Xxx	xx	5–10
K99-1-2	Xxxx	x	<5%
K99-1-3	Xxxxx	–	<5%
K99-1-4	Xxxxx		Al-silicate phases
K99-1-5	Xxxxx		<5
K99-1-6	Xxxxx		5–10
K99-1-7	Xxxxx	Tr	<5
K99-1-8	Xxxxx	x	5–10
K99-1-9	Xxxxx	xxxx	–
K99-1-10	Xxxx	x	<5
K99-1-11	–	xxxxx	5–10
K99-1-12	Xxxxx	Tr	<5
K99-1-13	Xxxxx	Tr	>10
K99-1-14	Xxxxx	–	5–10
K99-1-22	Xxxxx	–	>10
K99-1-23	Xxxxx	–	5–10
K99-1-24	–	xxxxx	5–10

Tr = Trace

4.3.3 Preliminary studies (Commissariat à l'Énergie Atomique (CEA, Cadarache[9])

Investigations have been made on two out of four profiles from the Khushaym Matruk site. The first profile has a vertical extension of about one metre and displays six main layers corresponding to samples K99-1-8 to K99-1-14 (**see Figures 4-6 and 4-7**). This profile extends from the bottom of the travertine layer (altered cement zone) down to the upper layers of the Bituminous Marl. Samples K99-1-11 to K99-1-14 were studied.

The second profile has a vertical extension of about 0.5 metre and consists of two samples of altered Bituminous Marl (K99-1-22 and K99-1-23), corresponding stratigraphically to layers under or at the bottom of the previous profile.

The aim of these investigations is: a) to determine the nature of the mineral phases, particularly of clay minerals, on these two profiles, and b) to evaluate if possible the concentration and chemical composition of the clay phases.

The analytical techniques used were: FTIR spectroscopy (Brüker and Nicollet), SEM with EDX (Philips XL30 + Oxford analyzer), XRD (Siemens D500 with Co cathode and Brüker with Cu cathode), Differential Thermal Analysis –Thermo Gravimetry-Evolved Gas Analysis (simultaneous thermobalance Netzsch STA409 coupled with a mass spectrometer Balzers Thermostar 300), chemical analyses (XRF, ICP-AES, ion-chromatography).

In the two following sections the results obtained by these techniques will be presented and commented for each profile.

Results

1. Profile 1 (samples K99-1-11 to K99-1-14).

   - K99-1-11 (raw material ground in a porcelain mortar).

     The IR spectrum (from 500 to 4000 cm^{-1}) reveals that the major phases of this sample are calcite and gypsum; the minor phases are apatite and clay phases (**Figures 4-8 and 4-9; Table 4-4**). The XRD confirms the presence of all these phases and shows that the clay phases are probably of smectitic type (**Figure 4-10**). This is in agreement with observations made at the University of Jordan (see Section 4.3.2).

     DTA + TG +EGA further characterises these clay-type phases. The evolved H_2O curves (**Figures 4-11 and 4-12**) indicate that they are composed of a mixture of three distinct minerals, each of which may be distinguished by temperatures at which water is evolved, i.e. around 500°C, 600°C and 820°C. The last peak is possibly attributed to a trioctaedral clay (saponite?). In addition, the calcite content of sample K99-1-11 is 46 wt% by EGA of CO_2 (**Figure 4-13**) and the gypsum content is the highest amongst the studied samples. Preliminary SEM-EDX investigations show the presence of Mg-Cr bearing aluminosilicates in sample K99-1-11C (green parts).

[9] Summary written by L Trotignon, J Raynal and F Mercier; investigations were carried out by F Audubert, A Dodi, B Donazzon, F Mercier, V Michaud, J Raynal, and L Trotignon.

Table 4-4. Identification and interpretation of major IR absorption bands on spectra from raw samples K99-1-11C to K99-1-14C and K99-1-22C (Figures 4-8 and 4-9).

	K-99-1-11c	K99-1-12C	K99-1-13C	K991-14C	K99-1-22C	
525	✓	✓	✓		✓	smectite volk
548	✓					smectite volk
573	✓	✓	✓	✓	✓	apatite
605	✓	✓	✓	✓	✓	gypsum + F-apatite
626	✓				✓	smectite volk? sap?
648	✓					smectite volk? sap? Smect tri (ATD 800°C)
669	✓	✓	✓	✓	✓	gypsum
690	✓					smectite sap? Smect tri (ATD 800°C)
713	✓	✓	✓	✓	✓	calcite
850	✓	✓	✓	✓	✓	calcite
875	✓	✓	✓	✓	✓	calcite
913					✓	smectite AlAlOH (OH deformation)
1003	✓					gypsum
1045	✓	✓	✓	✓	✓	smectite + F, apatite
1095		✓	✓	✓	✓	F. apatite
1115	✓	✓	✓	✓	✓	gypsum
1153	✓	✓	✓	✓	✓	gypsum
1434	✓	✓	✓	✓	✓	calcite
1620	✓	✓	✓			gypsum
1625					✓	smectite
1684	✓	✓	✓			gypsum
1797	✓	✓	✓	✓	✓	calcite
2517	✓	✓	✓	✓	✓	calcite
2593		✓	✓	✓	✓	calcite
2872	✓	✓	✓	✓	✓	calcite
2990	✓	✓		✓	✓	calcite
3255	✓	✓	✓			gypsum
3401	✓	✓	✓	✓		gypsum
3421					✓	smectite
3496	✓	✓	✓			gypsum
3548	✓	✓	✓			gypsum volk
3625					✓	smectite AlAlOH (OH stretching)

(volk = volkonskoïte; sap = saponite)

- K99-1-12 (raw material ground in a porcelain mortar).

  The IR spectrum indicates the presence of similar phases as described in sample K99-1-11, i.e. calcite, gypsum, apatite and clay phases (**Figures 4-8 and 4-9, Table 4-4**). The XRD shows, however, that the clay content is lower (**Figure 4-10**). DTA + TG displays the presence of only one marked peak of evolved water at about 500°C (beidellitic clay?) and a shoulder around 600°C (**Figures 4-11 and 4-12**). The calcite content deduced is 67 wt% (**Figure 4-13**) and the gypsum content is the lowest amongst the studied samples.

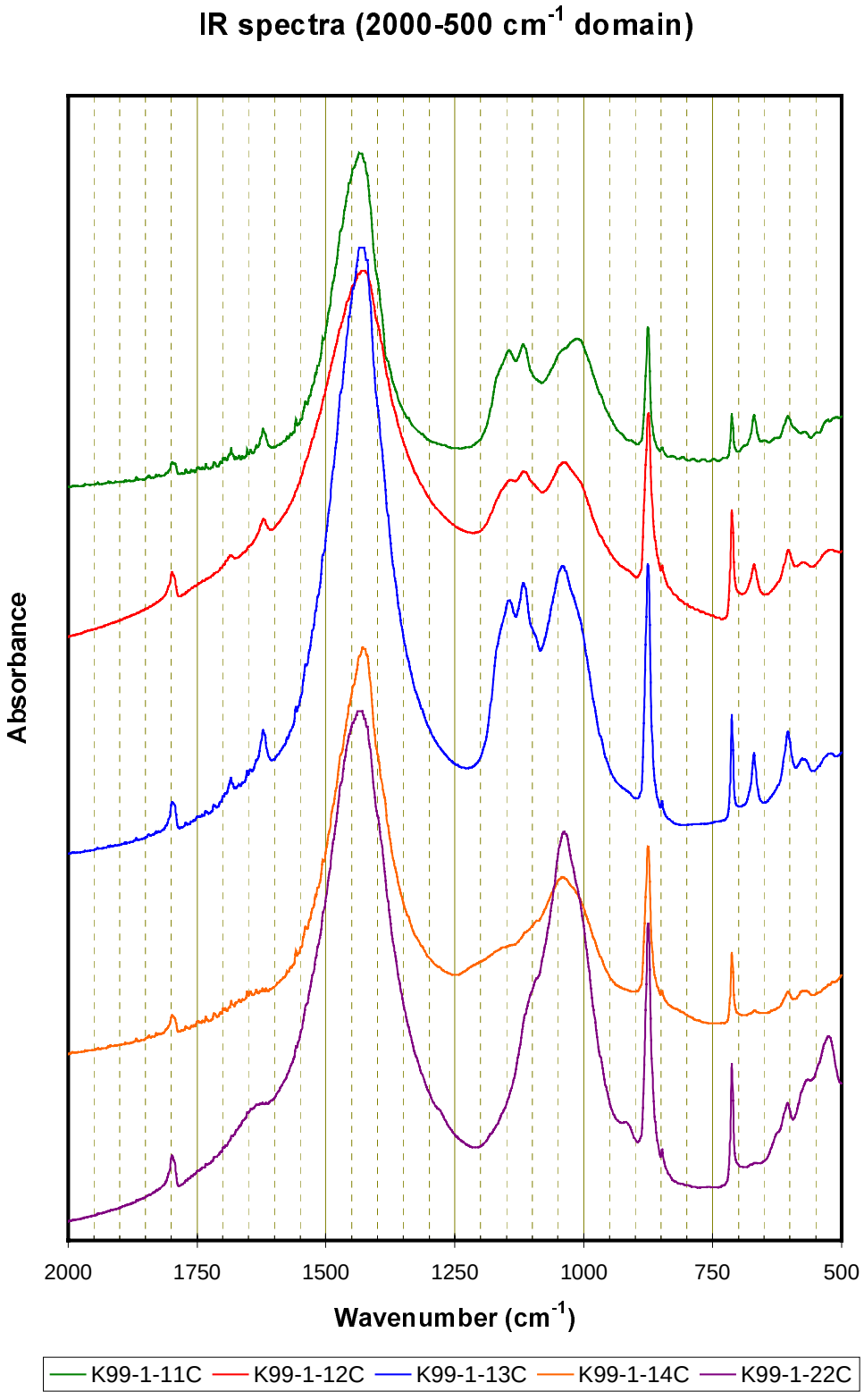

Figure 4-8. *IR spectra of samples K99-11-C to K99-1-14C and K99-1-22C in the spectral range 500 cm^{-1} to 2000 cm^{-1} (resolution is 2 cm^{-1}).*

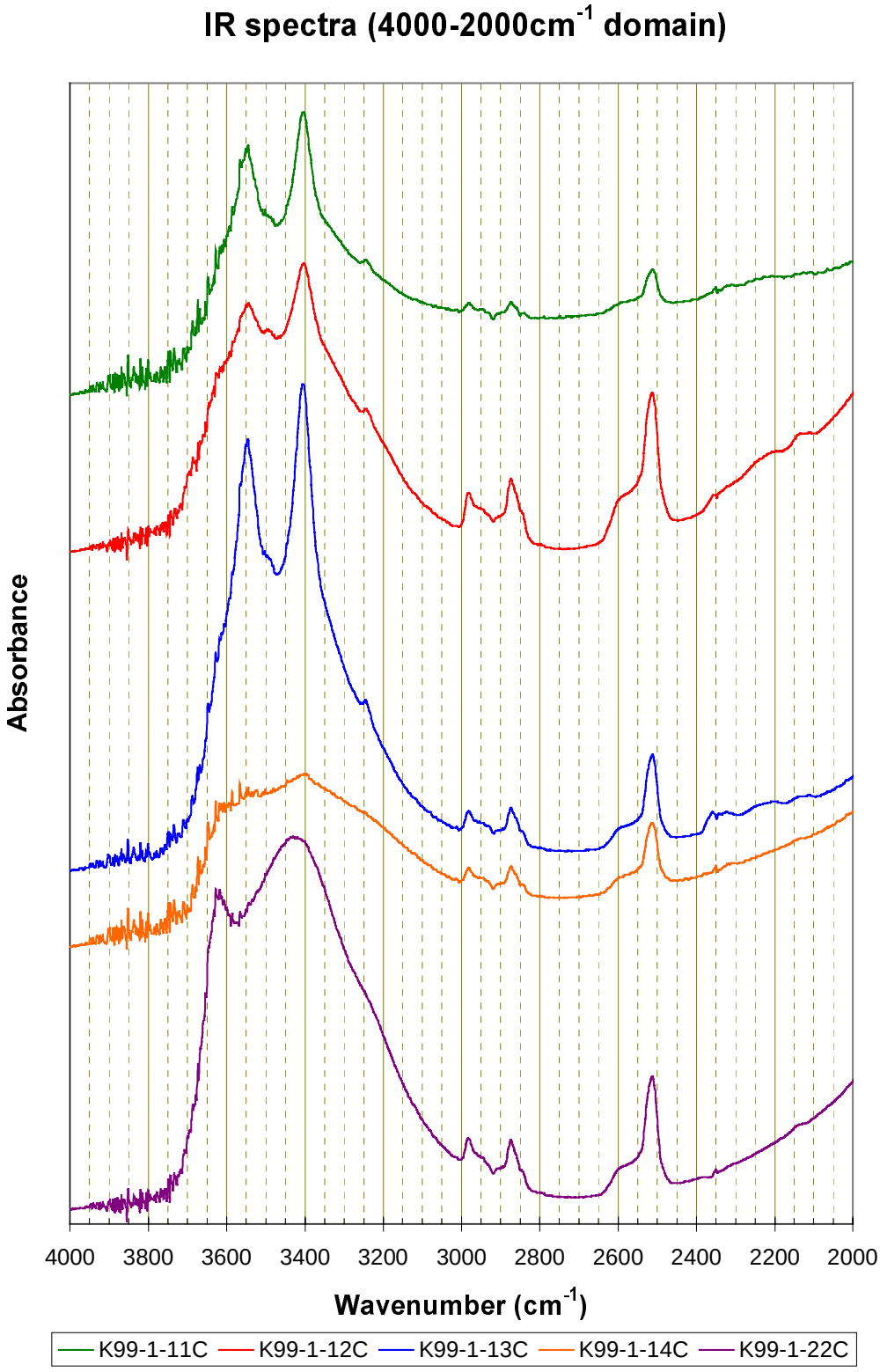

Figure 4-9. *IR spectra of samples K99-11-C to K99-1-14C and K99-1-22C in the spectral range 2000 cm^{-1} to 4000 cm^{-1} (resolution is 2 cm^{-1}).*

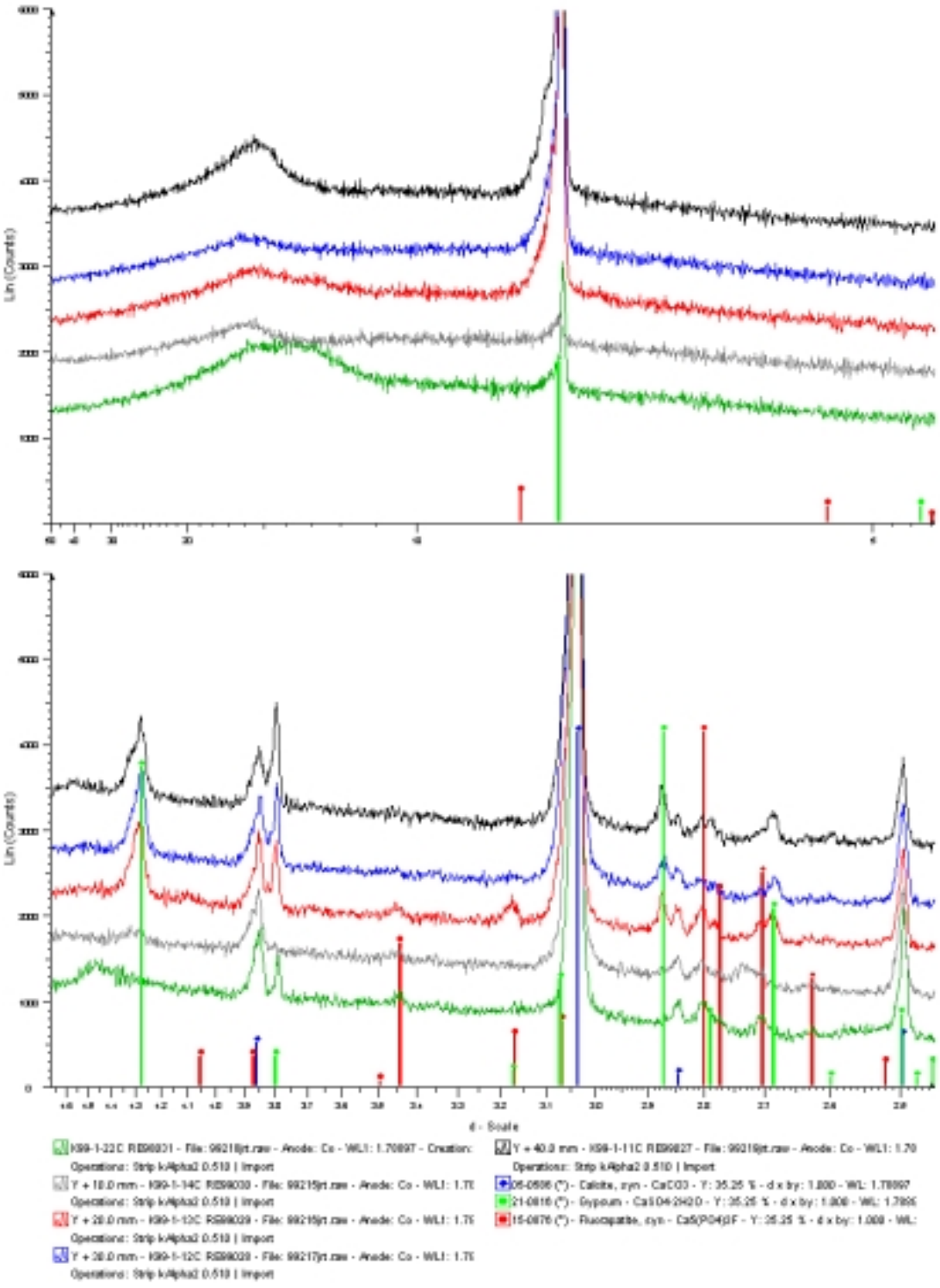

Figure 4-10. *XRD spectra for samples K99-1-22C (bottom green), K99-1-14C (grey), K99-1-13C (red), K99-1-12C (blue) and K99-1-11C (top, black).*

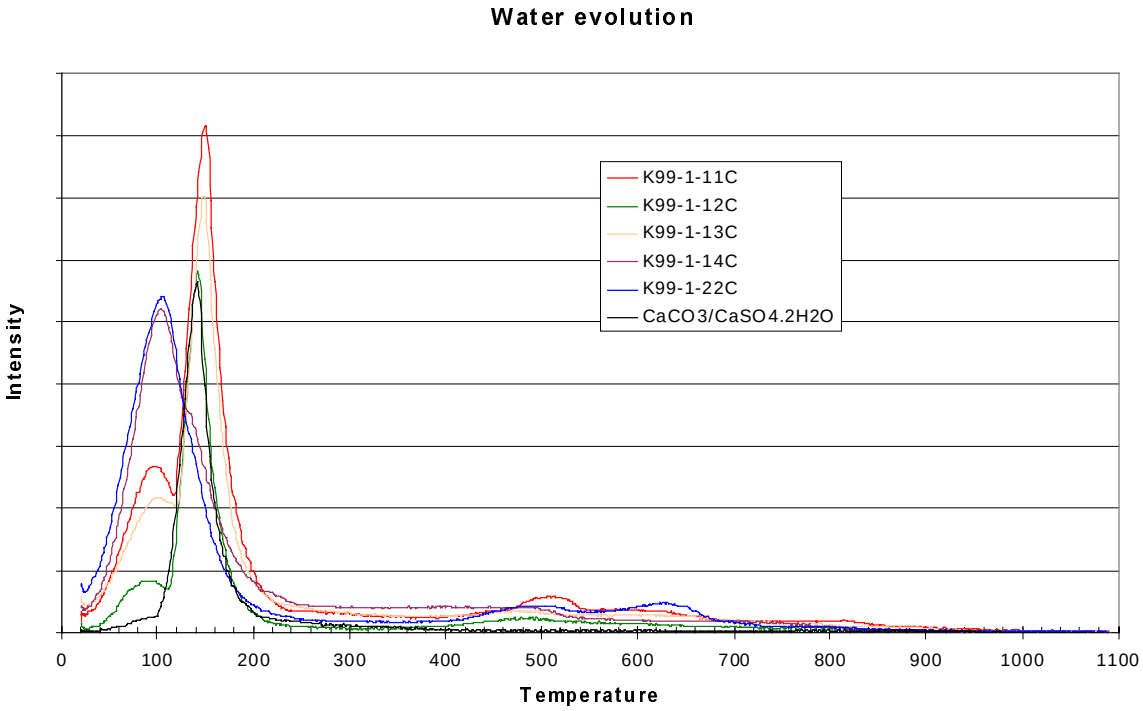

Figure 4-11. *Evolution of evolved water as a function of temperature for the studied samples and a calcite/gypsum mixture (intensity scale in arbitrary units).*

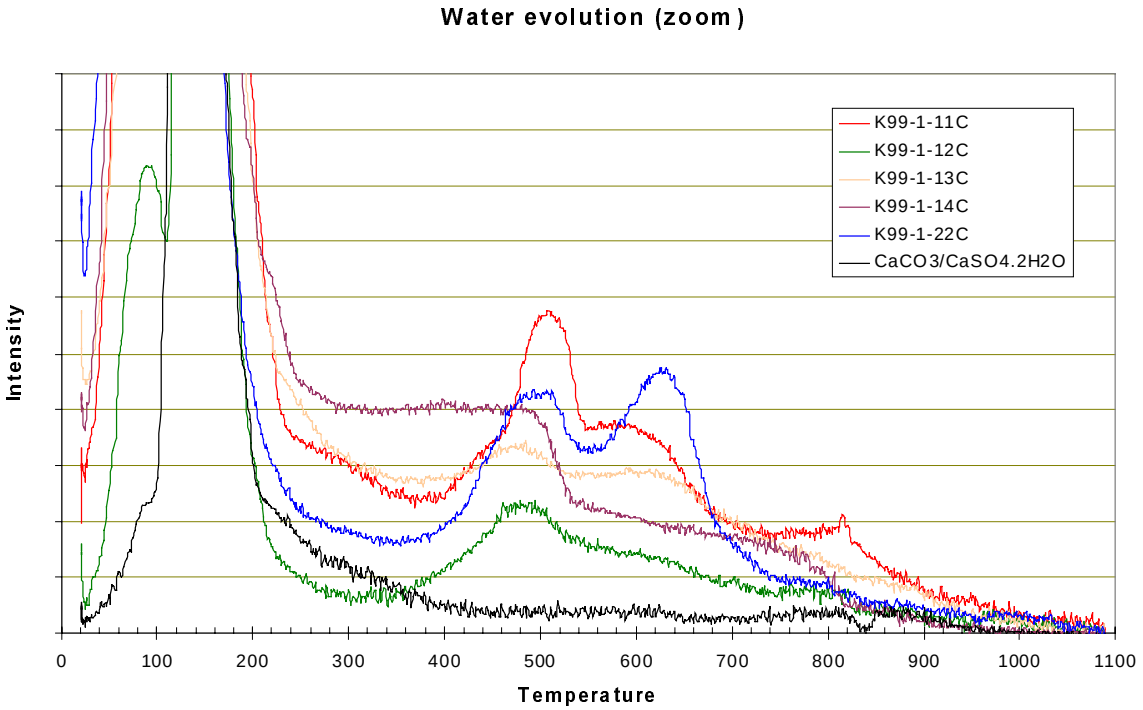

Figure 4-12. *Evolution of evolved water as a function of temperature for the studied samples and a calcite/gypsum mixture (blow-up of Figure 4-11) (intensity) scale in arbitrary units).*

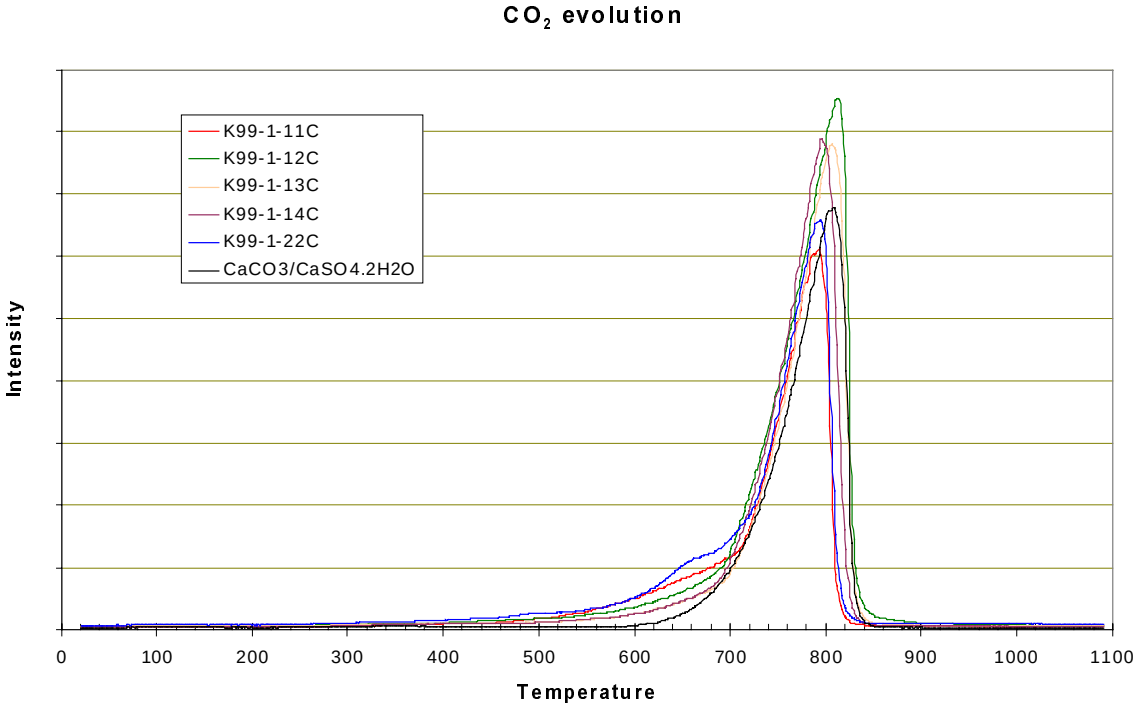

Figure 4-13. *Evolution of evolved CO_2 as a function of temperature for the studied samples and a calcite/gypsum mixture (intensity scale in arbitrary units).*

- K99-1-13 (raw material ground in a porcelain mortar + purified fraction with HCl 0.15 N).

  The IR spectrum of the raw material is comparable to those obtained from samples K99-1-11 and K99-1-12 (**Figures 4-8 and 4-9; Table 4-4**). The major absorption bands of the spectrum of the acid purified sample display a pattern that is very close to that of a smectitic clay; OH stretch band at 3620 cm^{-1}, and usual bands due to phyllosilicates, at 1026 cm^{-1}, 919 cm^{-1}, 524 cm^{-1}, 469 cm^{-1} and 461 cm^{-1}. The XRD spectrum of the raw material is comparable to that of K99-1-12 (**Figure 4-10**). DTA + TG shows the presence of two marked peaks of evolved water at around 500°C and 600°C (**Figures 4-11 and 4-12**). The calcite content is estimated at 56 wt% (**Figure 4-13**) although the calcite content deduced from mass loss after acid treatment of the sample is only 43 wt% (**Table 4-5**). This discrepancy may be due to the heterogeneity of the fractions. **Table 4-6** reports semi-quantitative chemical analyses of the purified fraction for sample K99-1-13C. It can be noted that this material is mainly composed of a combination of Si, Al, Mg, Fe and Ca. The idea that this residue is mainly composed of an aluminosilicate mineral (possibly a clay mineral) is thus clearly supported.

Table 4-5. Dissolution runs; results of gravimetric analysis.

Sample	Initial mass	Acid	Mass loss in CO_2 (% $CaCO_3$)	Dried residue (wt%)	Dissolved fraction (wt%)
K99-1-23 C	2.001 g	HCl	-0.47 g (53.4%)	0.3043 g (15.2 wt%)	31.4 wt%
K99-1-23 C	1.0005 g	Acetic	-0.22 g (50.0%)	< 0.195 g (< 19.5 wt%)	> 30.5 wt%
K99-1-22 C	1.0006 g	HCl	-0.20 g (45.5%)	0.210 g (21.0 wt%)	33.5 wt%
K99-1-13C	1.0007 g	HCl	-0.19 g (43.2%)	0.225 g (22.5 wt%)	34.3 wt%

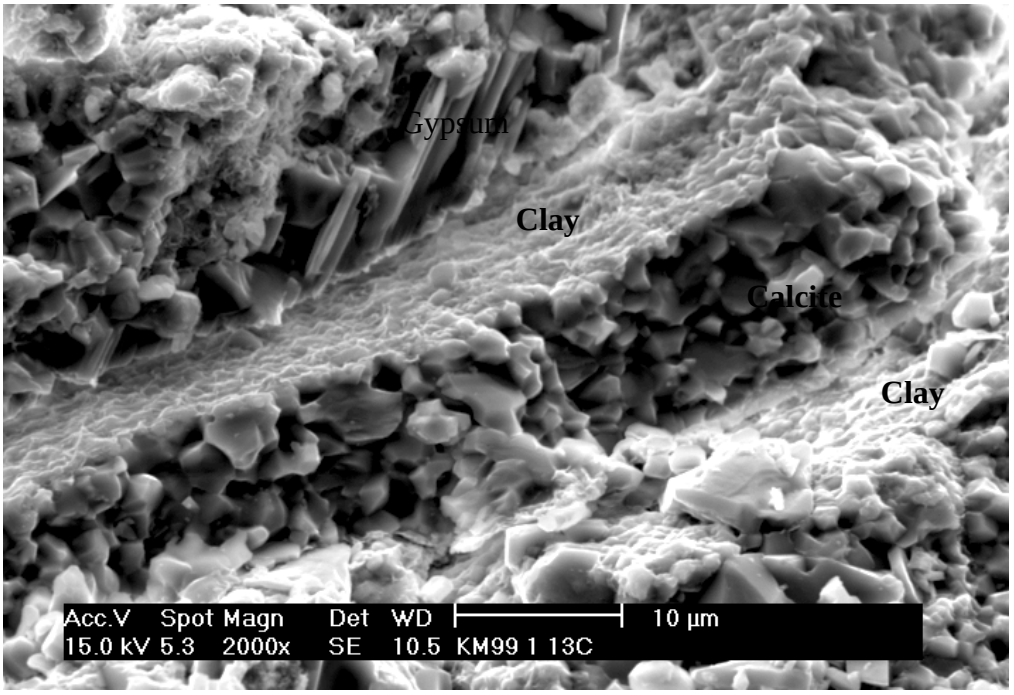

Figure 4-14. *SEM image taken on sample K99-1-13C. On this picture, a calcite layer is sandwiched between two double clay layers. Gypsum is also observed on the upper part of the picture.*

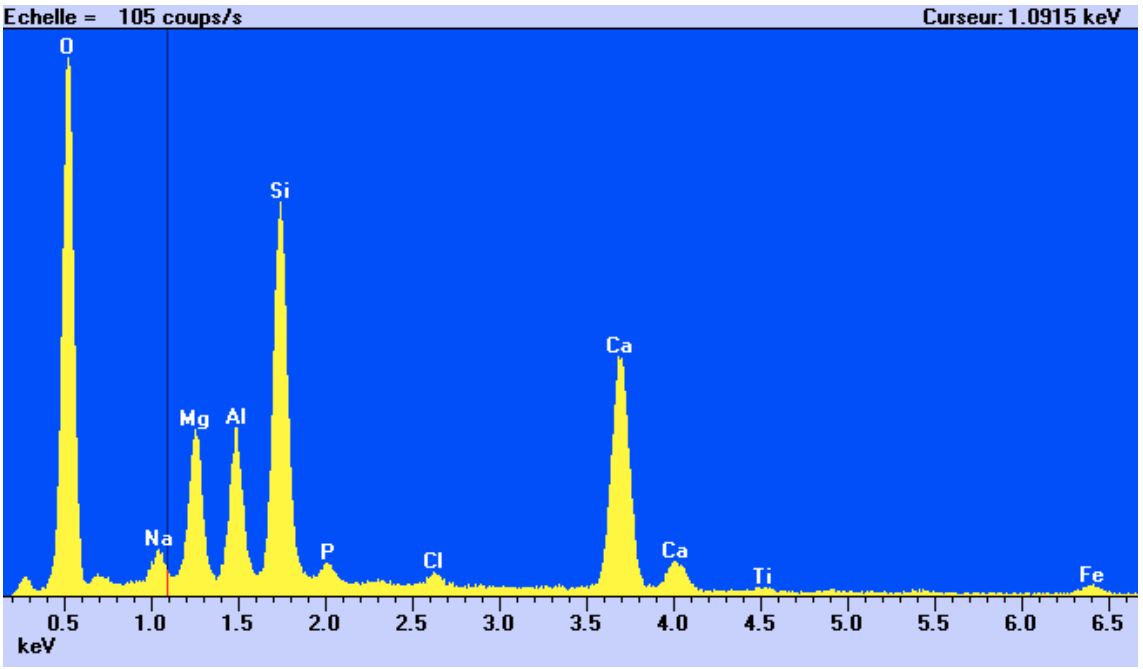

Figure 4-15. *EDX spectrum of the clayey material on sample K99-1-13C (15 kV).*

A fragment of sample K99-1-13 was examined under the SEM (**Figure 4-14**); calcite, gypsum and clayey phases are easily distinguished. Calcite has several habits: automorph crystals (about 10 µm size), remnants of fossils or tests and fracture fillings. Within the sample gypsum, calcite and the clayey fraction are texturally organised as fracture fillings (**Figure 4-14**). An EDX spectrum of the clay fraction (**Figure 4-1**5) confirms that this aluminosilicate contains Na, Mg, Ca and Fe.

- K99-1-14 (raw material ground in a porcelain mortar)

  IR spectroscopy (**Figures 4-8 and 4-9; Table 4-4**) shows the presence of calcite, gypsum and apatite and suggests a low clay content; XRD shows a weak peak around 16Å (**Figure 4-10**). These findings are in agreement with investigations performed at the University of Jordan (see Section 4.3.2). The evolved water curve (**Figure 4-11**) has an unusual shape that makes interpretation difficult and needs to be checked and perhaps run again. The calcite content is 56 wt%. Preliminary SEM-EDX investigations on the K99-1-14 sample reveal, in addition to calcite and gypsum, the presence of two different aluminosilicate phases: a Mg-Ca aluminosilicate which could correspond to a clay phase (although its morphology is not well defined) and a Na-Ca aluminosilicate which could correspond to a zeolitic phase (needle morphology). This zeolitic phases seems associated with large calcite crystals.

2. Profile 2 (samples K99-1-22 and K99-1-23).

   - K99-1-22 (raw material ground in a porcelain mortar + purified fraction with HCl 0.15 N).

     IR spectroscopy (**Figures 4-8 and 4-9; Table 4-4**) reveals the presence of calcite, gypsum, apatite and clear evidence of clayey minerals. The pattern of absorption bands attributed to clays is compatible with a smectitic mineral. XRD shows clearly a broad peak around 11 to 16 Å (**Figure 4-10**) and DTA + TG + EGE display two marked peaks of evolved water (**Figure 4-12**), around 500°C and 650°C, indicating the presence of at least two distinct clay phases. A weak shoulder at around 450°C is also noticed. The calcite content deduced from EGA is 51 wt% (**Figure 4-13**) which is in good agreement with mass loss measurements during purification of the sample (**Table 4-5**) leading to a calcite content of 45.5 wt%.

     A test using FTIR was made on sample K99-1-22C to quantify the calcite and clay contents. This was done by using standard spectra obtained on pure calcite and Wyoming montmorillonite. For calcite, two major absorption bands were used; 1420 cm^{-1} and 872 cm^{-1}. The first band gave 46 wt% and the second 46.6 wt%, to be compared with 45.5 wt% found by gravimetry. For the clay, the absorption band at 1030 cm^{-1} was not used because of the presence of phosphate and other compounds absorbing in this region. The absorption band at 470 cm^{-1} was therefore used with the Wyoming montmorillonite as reference. This gave a clay content of 23.7 wt% to be compared with 21 wt% for the dried residue (**Table 4-5**) after acid treatment and to 24.5 wt% found by combining the leachate analysis and dried residue (**Tables 4-6 and 4-7**).

     Combining these results, an overall composition for sample K99-1-22 is:

Calcite:	around 48.5 wt%
Apatite:	4–5 wt%
Gypsum:	> 17.5 wt%
Clay:	24.5 wt%
Total:	> 95 wt% (without considering moisture – at least 1% as shown by TG).

     Because the clay materials found in this sample appear to be a mixture, it is difficult to derive a structural formula for them. A fragment of sample K99-1-22 was examined under the SEM with EDS analysis (**Figures 4-16, 4-17 and 4-18**); calcite, gypsum and clay were easily recognised. Pure apatite particles were sometimes found (probably a microcrystalline mineral) and small particle of barium sulphate was identified. Calcite is found as automorphic crystals (about 10 µm size) or as remnants of fossils or tests. Gypsum is found less often, but no quantitative conclusion may be driven due to the small size of the sample studied and also due to the limited amount of time devoted to sample examination. The "clayey" material is often found as a coating (around 3 to 5 µm thickness) extending sometimes over large areas (100 x 100 μm^2) or wrapping calcite crystals. This material is composed of tiny submicronic plates with "wavy shaped" edges.

Table 4-6. XRF semi-quantitative analysis of the dried residue for samples K99-1- 22C and K99-1-13C (Na and light elements are not dosed and the normalisation is based on the major oxides).

Component	K99-1-22C 72 hours in HCl (wt%)	K99-1-13C 1 hour in HCl (wt%)
MgO	3.1	13.7
Al_2O_3	20.8	16.3
SiO_2	62.8	53.7
P_2O_5	0.4	0.6
SO_3	0.1	0.4
Cl	<0.1	<0.1
K_2O	<0.1	0.1
CaO	1.7	6.6
TiO_2	1.1	0.8
V_2O_5	<0.1	Not detected
Cr_2O_3	0.4	0.5
Fe_2O_3	8.4	6.5
NiO	<0.1	0.1
ZnO	<0.1	0.2
BaO	0.5	0.3

Table 4-7. Analysis of the leachate for the purification of sample K99-1-22C (1 g of sample in 100 mL dilute HCl solution). Analytical techniques used are atomic absorption, ICP/AES and ion chromatography.

Element	Al	Si	Mg	Fe	Ca	Na	K	SO_4^{--}	PO_4^{--}
(mg/L)	89	85	78	27	2500	49	0,53	88 ± 9	231 ± 23

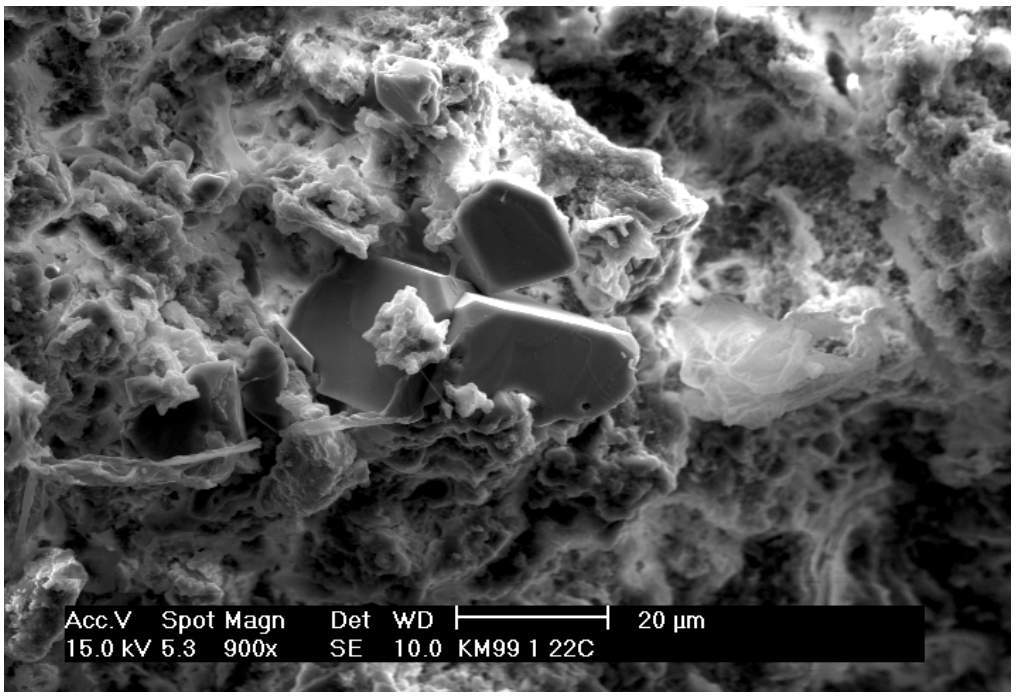

Figure 4-16. *SEM image of sample K99-1-22C displaying calcite crystals and the "clayey" material. The white particle on the right is a Ca phosphate rich mineral.*

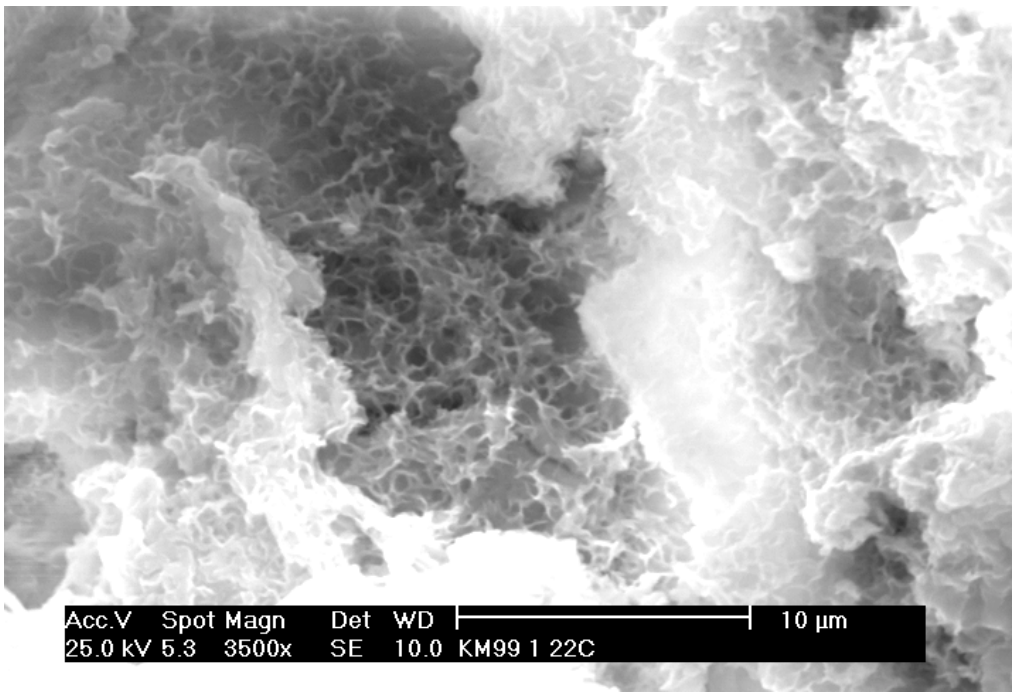

Figure 4-17. *SEM image of the clayey material in sample K99-1-22C. The platelet morphology is clearly visible on this picture.*

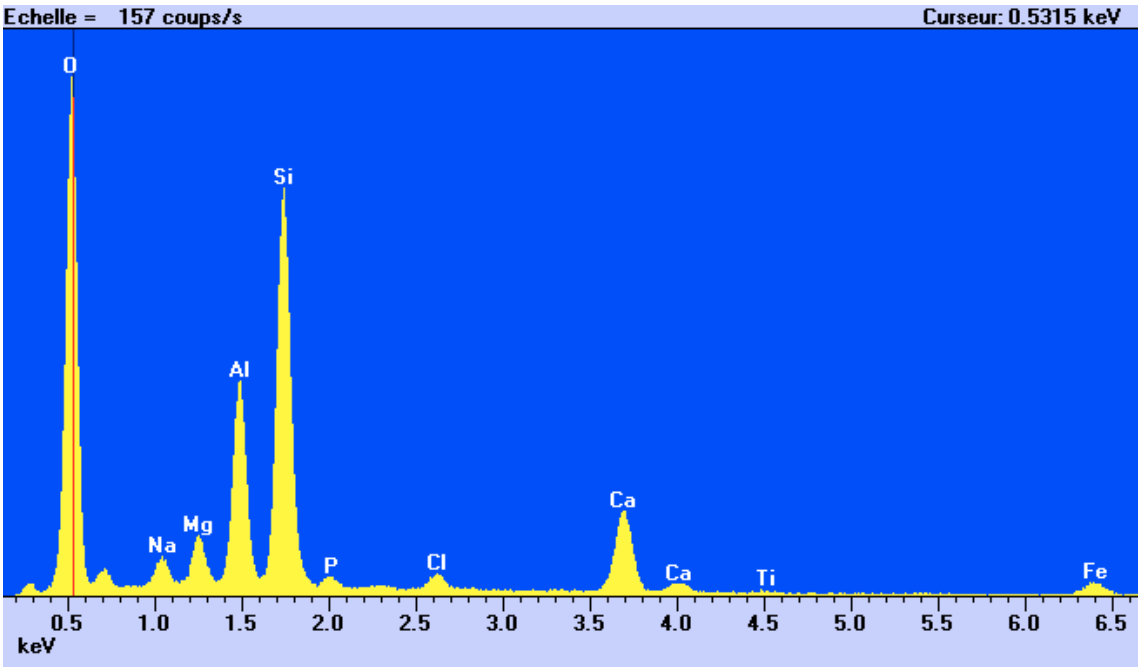

Figure 4-18. *EDX spectrum of the clayey material found on K99-1-22C sample (15 kV).*

The morphology of the clayey fraction could be confirmed at higher magnifications, e.g. the wavy shape of platelet edges (**Figure 4-17**). Morphological considerations also indicate that this clay is not attributed to detritic sedimentation but rather has crystallised in the pore spaces, possibly under diagenetic conditions (per. comm. H. Khoury and T. Milodowski, 1999). Qualitative EDX spectra have been obtained from different spots of the sample to depths of about 2 µm. The calcite seems to be pure and any traces are under instrumental detection limits. Analyses performed on the clayey material (**Figure 4-18**) give variable compositions, suggesting that this clayey fraction is sometimes intimately mixed with calcite or apatite.

Main results derived from a preliminary study of the spectra show:

– Si, Al, Mg, Ca and O are usually the major elements characterising the clayey material.
– Na and Fe are present at significant levels in the clayey material.
– Si/Al ratio seems to be rather stable (based on the heights of peaks).
– P is sometimes detected at significant levels.
– K is not detected.
– Cl and F are detected at low levels.

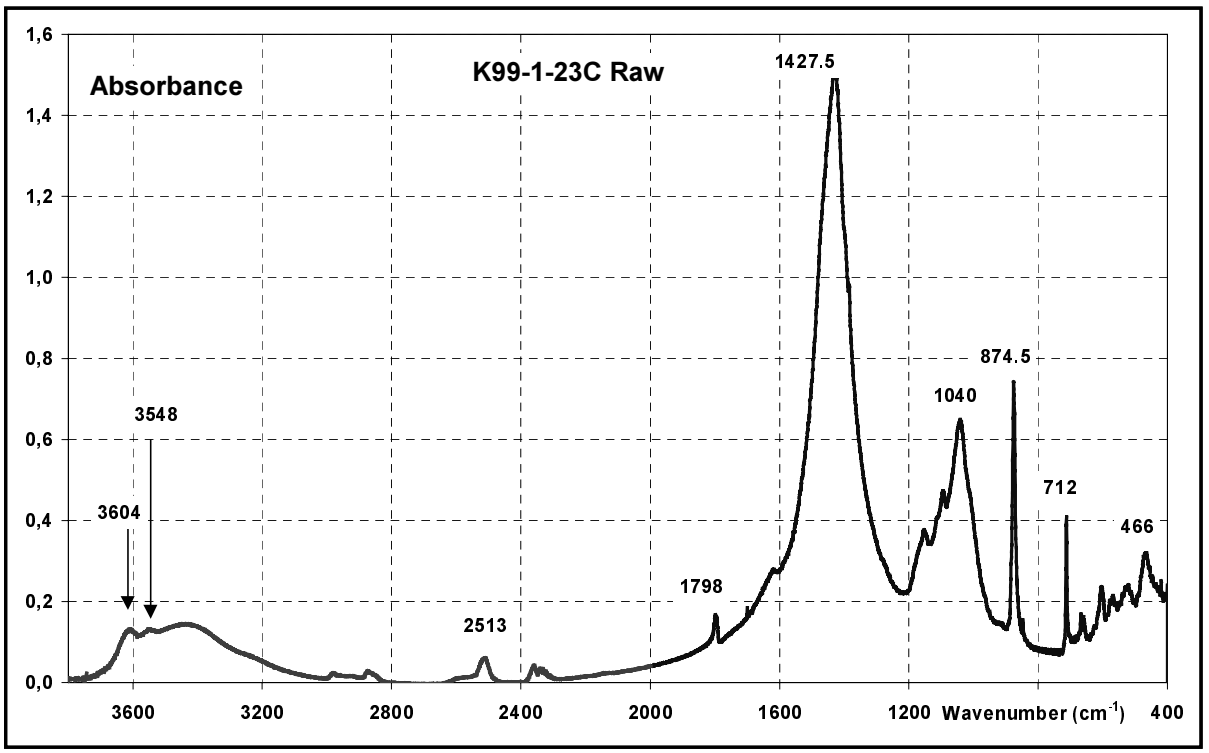

Figure 4-19*. Sample KM99-1-23 C. Infrared spectrum of the initial material (diluted in a KBr pressed pellet) (resolution is 0.5 cm^{-1}).*

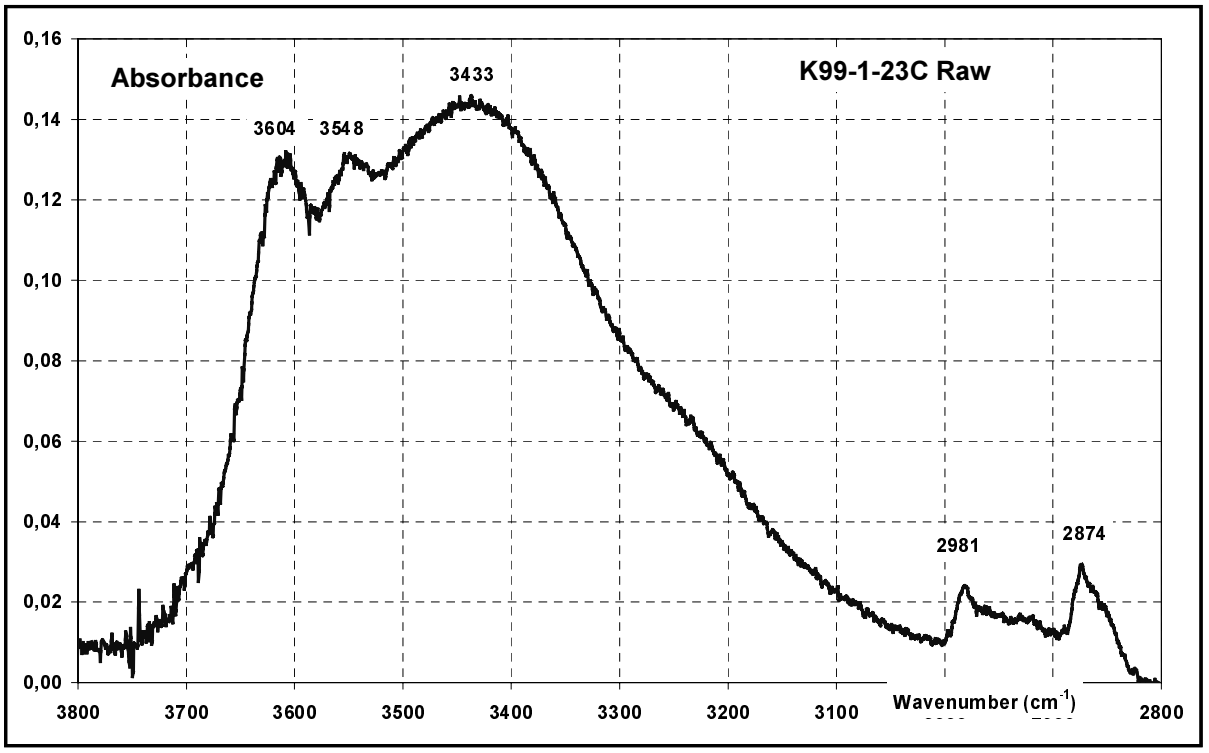

Figure 4-20. *Sample KM99-1-23 C. Infrared spectrum of the initial material (diluted in a KBr pressed pellet). Spectral region of OH stretching (resolution is 1 cm^{-1}).*

- K99-1-23 (raw material ground in a porcelain mortar + purified fraction with HCl 0.15 N)

  IR spectroscopy on the raw material (**Figures 4-19 and 4-20**) and on the purified fraction (**Figures 4-21 and 4-22**) are in good agreement with the results obtained for sample K99-1-22. The IR spectrum of the residue after acid purification of the raw material confirms that the clayey fraction is close to a smectitic clay (or a mixture of smectitic clays).

  Two complementary XRD spectra were obtained from sample K99-1-23C and on the residue of K99-1-23C treated by acetic acid (**Figure 4-23**). Long acquisition times were necessary in order to detect the diffraction pattern of the residue. Calcite (strong), gypsum (medium) and fluorapatite (weak) were detected on the XRD spectrum and a smectitic material (montmorillonite type), fluorapatite and to a lesser extent calcite were found on the acid treated residue. The basal spacing of the clay is about 15.7 A. Some specific features (like the 060 spacing) suggest that this clay is not a purely dioctaedric smectite.

  From the acid treatment of sample K99-1-23 (**Table 4-5**), the calcite content is 51.7 wt% (mean of two measurements); the clay phase content is estimated at 15 wt% (to be compared to 22 wt% for K99-1-22). The SEM images (**Figures 4-24 and 4-25**) show that calcite and the clayey material are very easily detected but that gypsum is less common. Calcite is also found as automorphic crystals (about 10 µm size) or as remnants of fossils or tests, and the clayey material has the same morphology as sample K99-1-22.

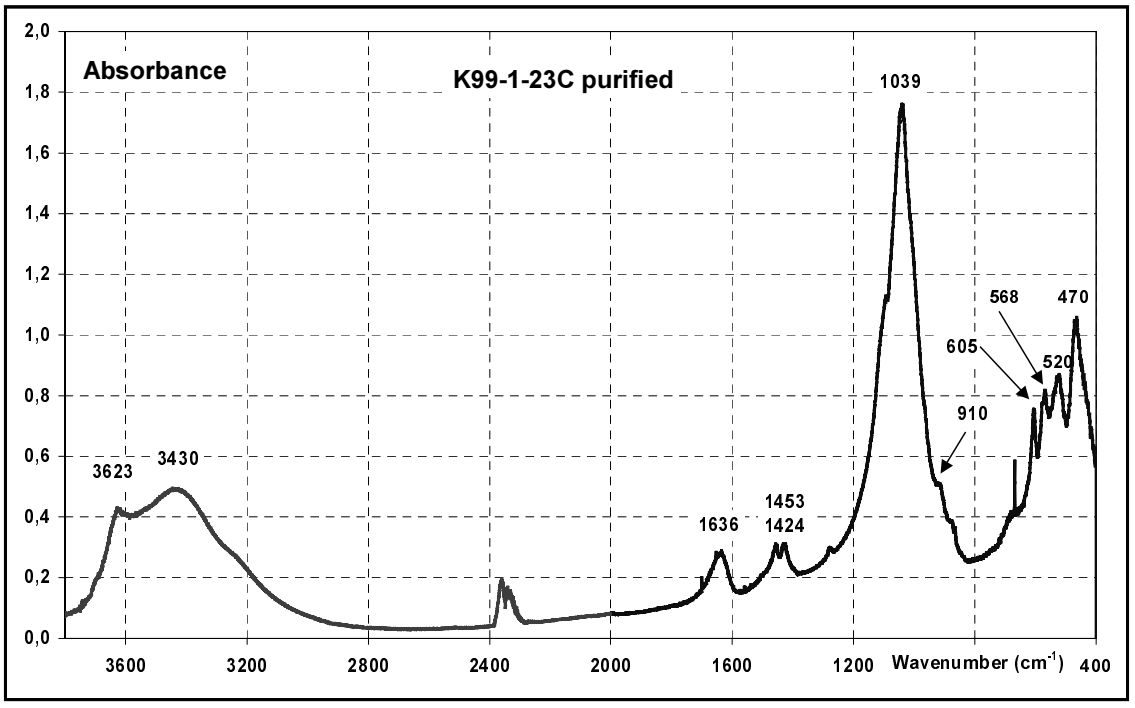

Figure 4-21. *Sample K99-1-23C – Residue after acid treatment. Infrared spectrum (resolution is 1 cm^{-1}).*

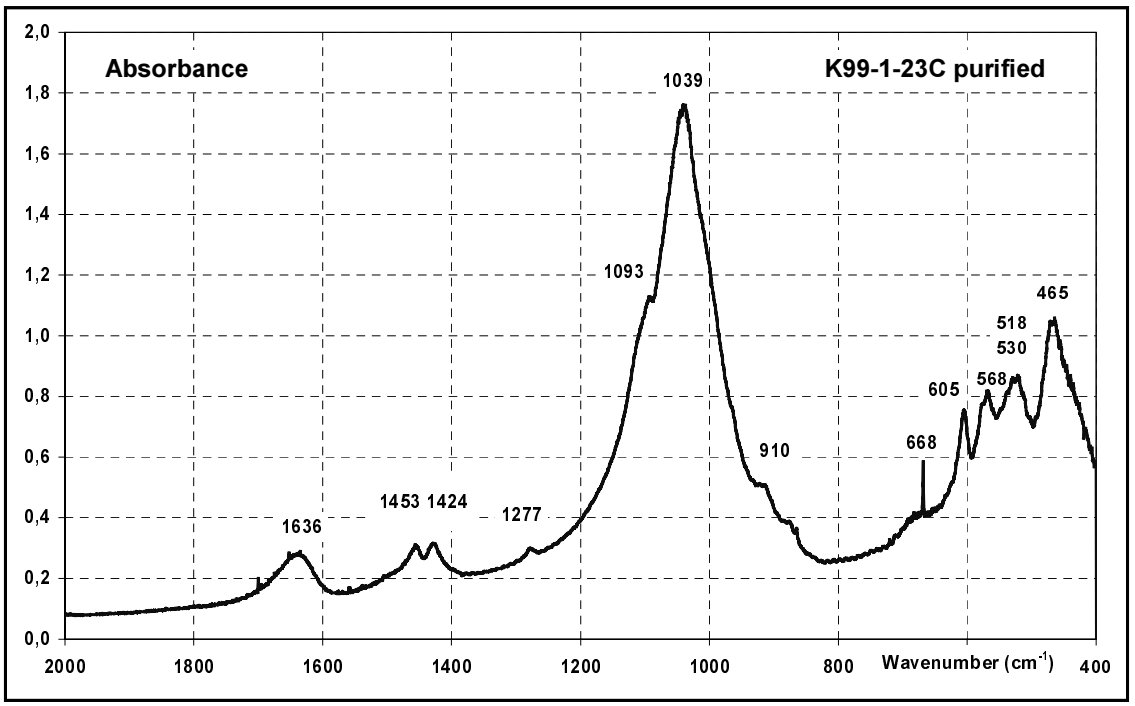

Figure 4-22. *Sample K99-1-23C – Residue after acid treatment. Detail of the IR spectrum (resolution is 1 cm^{-1}).*

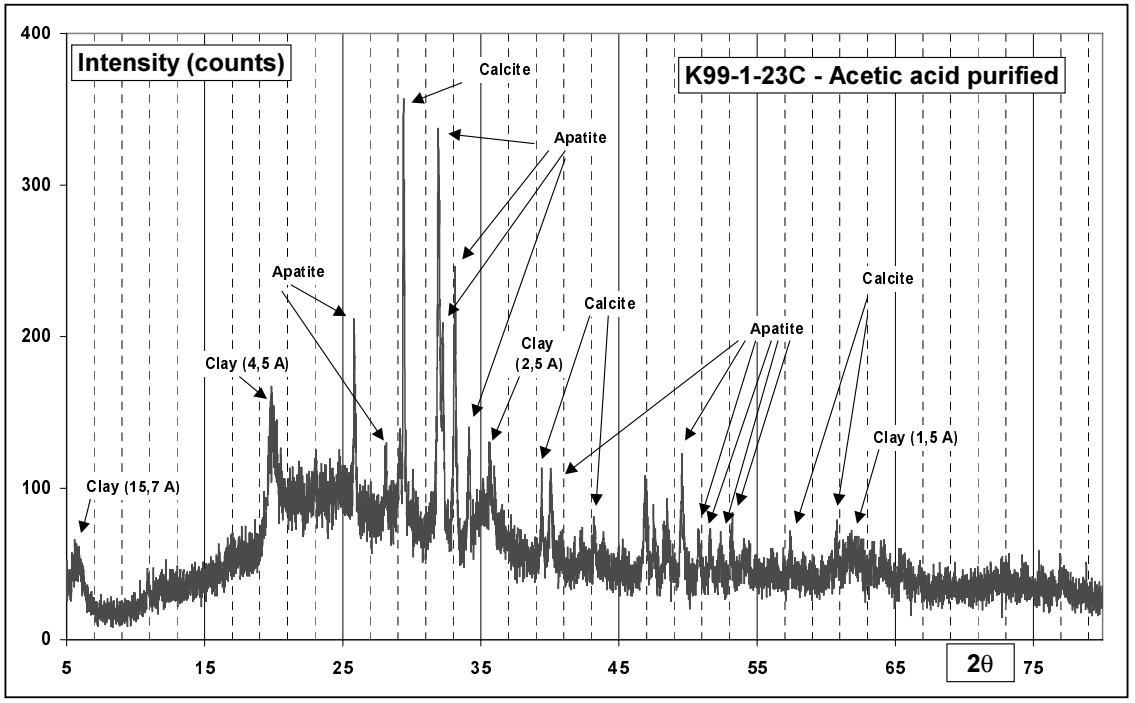

Figure 4-23. *XRD spectrum of the residue of sample K99-1-23C treated by acetic acid. Main diffraction lines of the smectitic clay fractions are indicated as well as diffraction lines of calcite and fluorapatite (Cu cathode).*

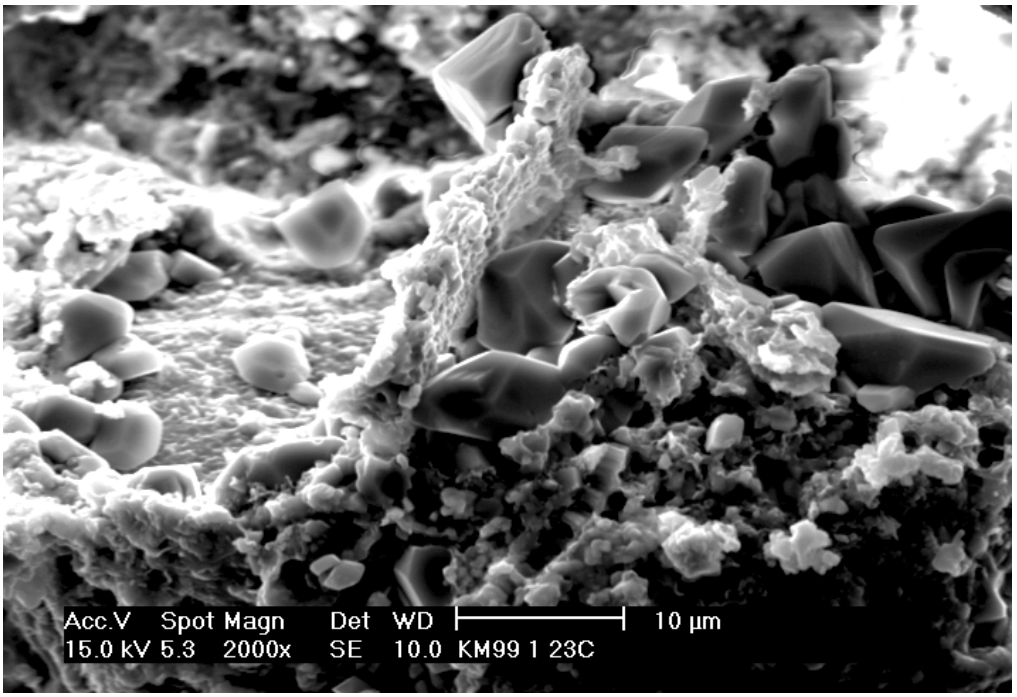

Figure 4-24. *SEM image of sample K99-1-23C. Automorphic crystals of calcite are wrapped in the "clayey" material.*

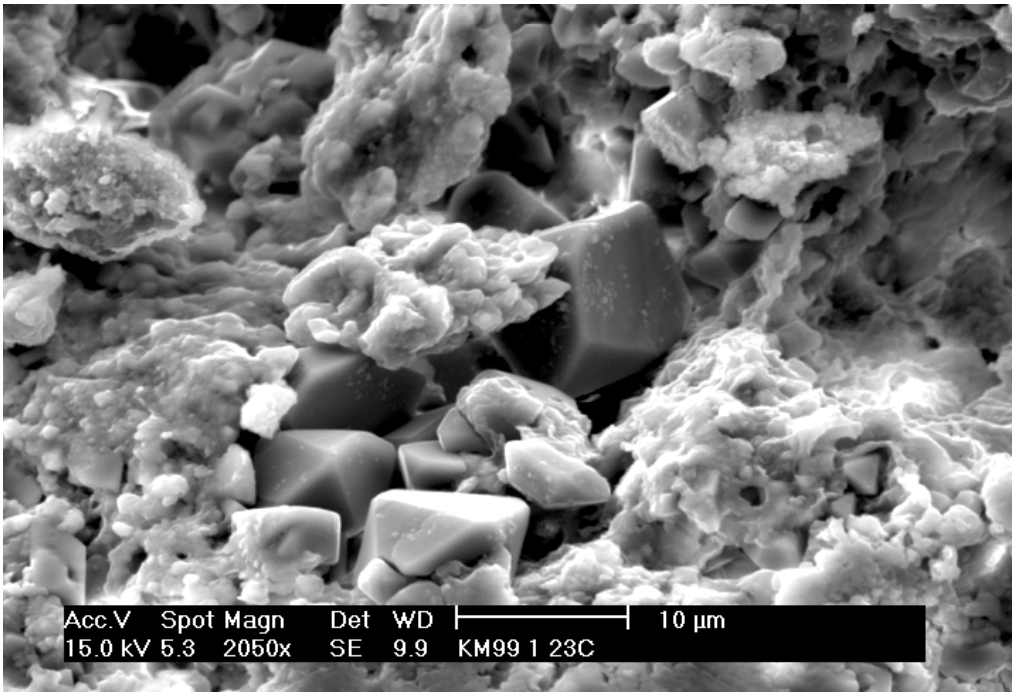

Figure 4-25*. SEM image of sample K99-1-23C. Calcite crystals wrapped in the clayey material.*

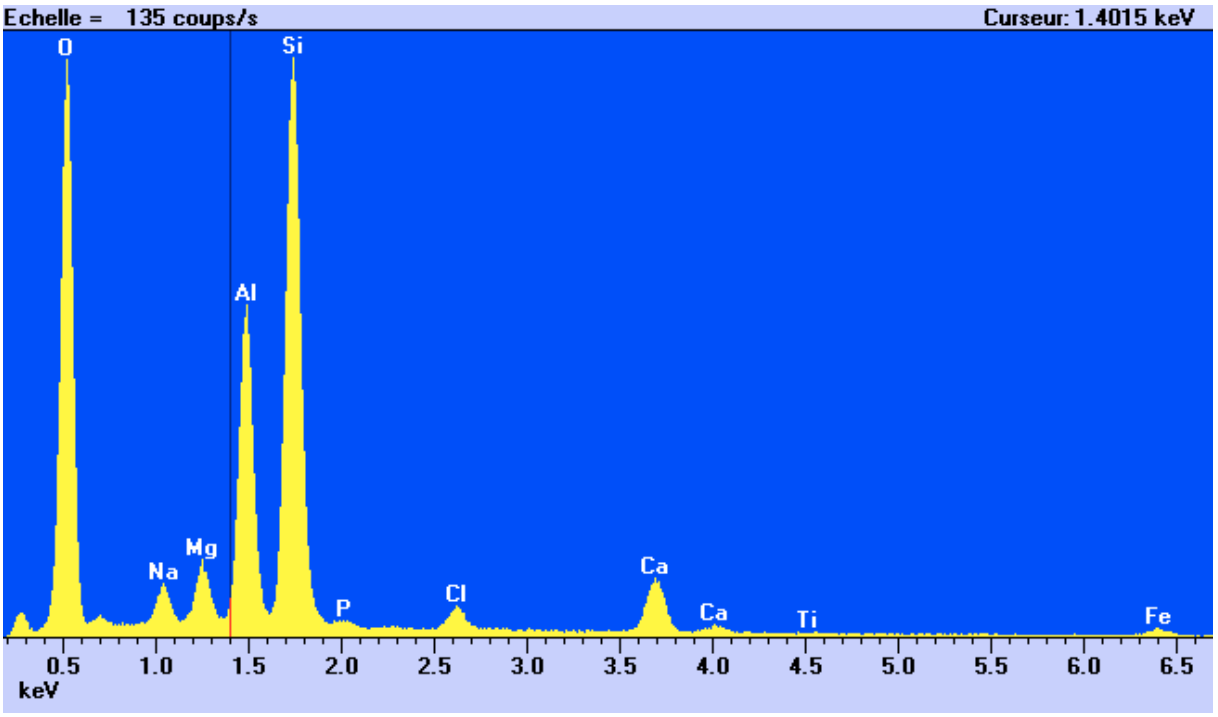

Figure 4-26. *EDX spectrum of a clay particle in sample K99-1-23C (15kV).*

The qualitative chemical analyses obtained on samples K99-1-23 (**Figure 4-26**) and K99-1-22 are in very close agreement suggesting that the clay phases are similar for these two samples.

Conclusions

Analyses performed on a limited number of samples from the two selected profiles have been presented. Due to the exploratory character of these investigations, some bias on sample representativeness is possible. Some of the analyses are still in progress and these conclusions are therefore preliminary. However at the present state of knowledge, the different investigation methods used give consistent and corroborated information which is also in good agreement with investigations performed at the University of Jordan and ERM Poitiers (see Sections 4.3.2 and 4.3.4):

1. Calcite, gypsum and fluorapatite where clearly identified as crystalline mineral phases (the calcite content ranges between 43 and 67 wt%);
2. The three samples studied contain a clay fraction with a concentration ranging up to 22-25 wt %;
3. The gypsum content is greater than 15 wt% in all samples with the following decreasing order of concentration: K99-1-11 > K99-1-14 > K99-1-22 > K99-1-13 > K99-1-12;
4. The clay is most probably a mixture of smectitic minerals; up to three distinct phases for K99-1-11 and two distinct phases for the other samples (consistent with preliminary investigations at the University of Jordan and ERM Poitiers); the crystallinity of the clay is possibly not very high;
5. This clay contains Na, Mg and Ca as exchangeable cations;

6. A phase corresponding probably to a Ca-Na zeolite is found on one sample (lower part of the first profile), in association with calcite in fracture fillings;
7. The clay also probably contains Fe;
8. In one sample, a spatial organisation of minerals (calcite, gypsum) also involving this clay is clearly seen (fracture fillings ?);
9. Organic matter is not clearly evidenced;
10. The purification procedure employed in this preliminary study has probably perturbed the clay (pH too low). Further investigations will be made using a milder procedure.

Fractions of these grounded samples were dissolved in diluted acetic or hydrochloric acid (about 0.15 N). The recorded mass loss due to CO_2 loss makes possible the evaluation of the calcite content (it is supposed that the calcite is pure $CaCO_3$). The purified residue is then filtered and rinsed on 0,45 µm filter, dried in air at 50°C and weighted. For the K99-1-23 C and K99-1-13 C runs, the dissolution runs were performed in about 80 ml acid until mass loss stabilised (about 1 hour with intermittent shaking) and then acid was added and it was verified that the mass loss didn't change. For the run with K99-1-22 C, after the mass loss had become stable, the leachate volume was completed to 100 mL with DI water and left 3 days at 25 °C.

4.3.4 Preliminary studies (SARL Etudes Recherches Matériaux (E.R.M., Poitiers[10])

General

This intermediate report focusses on the Khushaym Matruk site in Central Jordan. The objective is to show the presence of clays in biomicrite and to investigate their evolution during alkaline alteration. To that end, the mineralogical evolution of the clay-bearing rock was studied at the contact of a cemented zone in a fossil area where water no longer flows today.

This report dedicated to the mineralogical analyses of the material and contains the following analytical data:

1. X-ray diffraction patterns (bulk sample powder and oriented samples on both the bulk sample and the < 2µm fraction);
2. Calcimetry data for quantitative analysis of carbonates;
3. Cation exchange capacity and exchangeable cation data on the < 2µm fractions;
4. Decomposition of X-ray diffraction patterns on the < 2µm fractions ((001) peaks);
5. Chemical analysis, optic microscopy and electronic microscopy observations will presented in a final report.

[10] A Cassagnabere and F Rassineux.

Material and analytical methods

1. Material

   Six samples from Central Jordan were collected (Khushaym Matruk site) and referenced as shown in **Table 4-8**.

Table 4-8. Summary of sample references and types of work carried out.

ERM References	ANDRA References	Planned Work
1	K99-1-1	Exhaustive study
2	K99-1-2	Exhaustive study
3	K99-1-3	Exhaustive study
5	K99-1-5	Exhaustive study
7	K99-1-7	Exhaustive study
26	K99-1-26	Thin section

Analytical methods

The analytical methods classically employed have been detailed in a specific report (ERM, 1997) and in ERM's quality assurance manual (AQMODOP.DOC file, 1999). Consequently, their description will not be systematically repeated in this report where a few specific points only will be detailed. For further information, the reader shall refer to the document mentioned above.

Some methods or experiments of a more specific nature, used in the scope of the present study, are presented and described in the same paragraphs as their results and ensuing interpretations.

The 2 µm size fractionation of initial sample was achieved by centrifugation. This operation based on Stokes law was performed using a high-capacity centrifuge at regulated temperature. The principle consists in adjusting rotation speed (acceleration g) and time to obtain the cut point at 2 µm.

Stokes law is expressed by the following formula:

$$V = (2/9)\, g\, r^2\, (\rho - \rho_0) / \eta$$

where V = falling velocity of particles (in cm/s), g = 9.81 m^2/s, ρ = density of particles, ρ_0 = density of the liquid, η = viscosity of the liquid, et r = radius of particles (in cm).

1. Crystallographic nature of minerals determined by X-ray diffraction.

   The acquisition of diffraction patterns was performed using a Siemens D 500 Kristalloflex diffractometer (Cu Kα radiation) equipped with an EDS solid detector (Si(Li) diode) cooled down by Peltier effect. The diffraction patterns were recorded on a microcomputer with a DACO-MP (SOCABIM) numerical system. Two types of diffraction patterns were performed for each sample:

- one randomly oriented powder pattern recorded in the angular range 3-65°2θ (Cu Kα) so as to determine the nature or the mineral components. A scanning speed of 1°2θ / minute was used;
- two oriented-sample diffraction patterns: one air-dried (i.e. recorded at room temperature) and one after ethylene glycol saturation in order to accurately identify the various clay minerals. The advantage claimed for oriented samples is that they increase the intensity of the (00l) peaks of clay minerals, which makes their identification easier and improves the counting statistics for further computer processing. Moreover, these preparations facilitate the implementation of treatments classically used in clay mineralogy. The diffraction patterns obtained from the bulk sample were recorded in the range 2.5 to 15°2θ (with a scanning speed of 0.375°2θ / minute (step size of 0.025°2θ, 4 seconds per step)). The diffraction patterns obtained from the < 2µm fraction were recorded in the range 2.5 to 32°2θ (with a scanning speed of 0.375°2θ / minute (step size of 0.025°2θ, 4 seconds per step). This angular range covers low angles, where the strongest peaks of clay minerals can be found as well as portions of diffraction patterns with peaks of lower intensity, but of great interest sometimes for identification (Brown and Brindley, 1980). Recording in these angular ranges is particularly essential for a proper characterisation of interstratified clay minerals (Reynolds, 1980).

2. ClayXR computing program for automatic identification (Bouchet, 1992).

   Further information (mostly relating to interstratified clay minerals) was obtained by comparing experimental results with theoretical diffraction patterns calculated with the NEWMOD© calculation program (Reynolds, 1985).

3. Chemical analyses carried out at the CRPG, Nancy by ICP-MS.

4. Cation exchange capacity (C.E.C.) of each sample was measured according to a small-amount protocol (100 mg) on the basis of Jackson's method (1964, ammonium acetate) and verified using the magnesium chloride method set forth in paragraph 4.4.

5. Proportions of exchangeable ions (Ca^{2+}, Na^{+}, Mg^{2+} and K^{+}) released during the ammonium-acetate saturation were determined by atomic absorption spectrometry and flame emission.

6. The level of carbonates was measured using a Bernard calcimeter. This method provides a result whose accuracy range is below absolute 5% (ERM, 1997).

Results: Characterisation of the mineral

1. X-RAY diffraction

   – Randomly oriented powder patterns.

   Five randomly oriented powder patterns of samples K99-1-1, K99-1-2, K99-1-3, K99-1-5 and K99-1-7 were performed from raw material samples without any separation in order to determine the main minerals present in quantity over the detection threshold of X-ray diffraction (**see Appendix 8**). **Table 4-9** shows the minerals that were identified on the powder diffraction patterns obtained from the bulk sample (example: **Figure 4-27**).

Table 4-9. Summary of the various mineral species identified from X-ray powder diffraction on the bulk sample.

Samples	Calcite	Gypsum	Clays	Other phases
K99-1-1	XXX	XXX	X	?
K99-1-2	XXX	X	Trace	?
K99-1-3	XXX	X	Trace	Feldspar?, zeolite?
K99-1-5	XXX	–	Trace	Zeolite?, hematite?, anhydrite?
K99-1-7	XXX	Trace	Trace	Zeolite?, Feldspar?

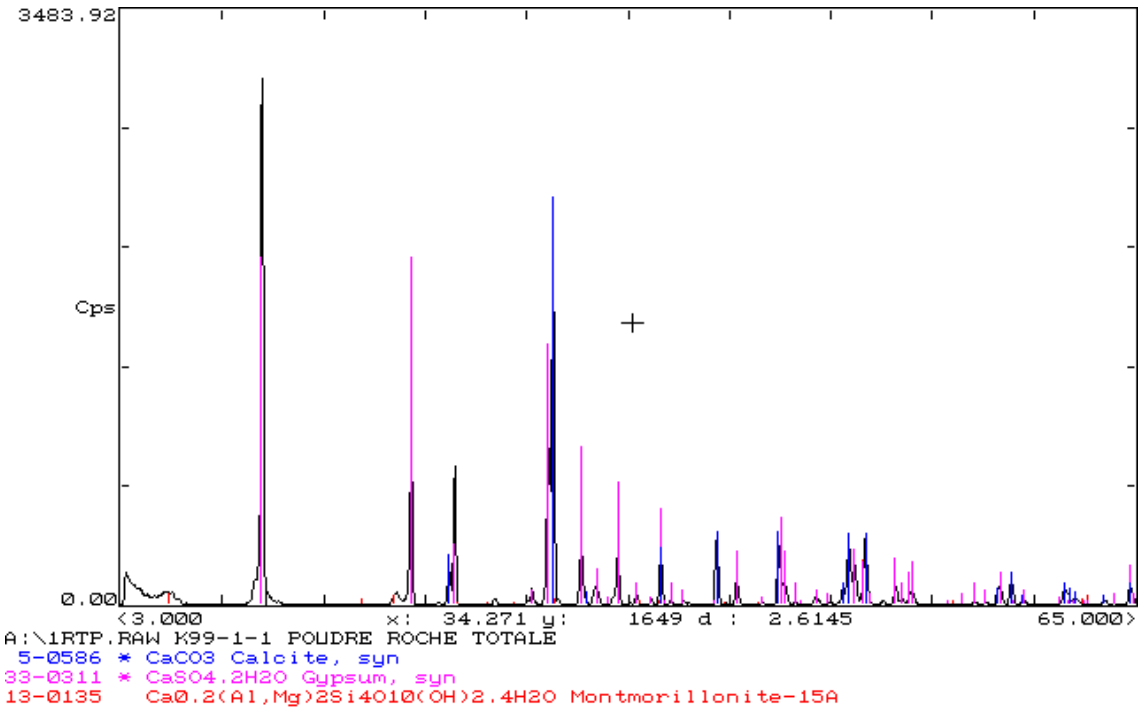

Figure 4-27. *Randomly oriented powder pattern (from 3 to 65 °2θ) of sample K99-1-1.*

Considering the possible superposition of the diffraction peaks of the various constituent minerals of the material, some minerals present in small quantity may not have been identified on these diffraction patterns. Identification of clay minerals, performed from the oriented-sample diffraction patterns, will be detailed below.

– Oriented-sample diffraction patterns.

Figure 4-28 shows all the various X-ray diffraction patterns (oriented samples) recorded on the bulk sample. The clay content of samples is not high enough to be exploitable in X-ray diffraction, given the great amount of calcite. A swelling mineral (smectite-like?) with a peak moving from 15 Å (air-dried sample) to 17.2 Å after ethylene glycol saturation has been observed in all of the 5 samples.

2. Calcimetry.

Very high values were obtained with the Bernard calcimeter: between 37 and 87% (**Table 4-10**). These values indicate the presence of a great quantity of carbonates. Samples K99-1-2 and K99-1-3 show approximately the same levels of carbonates (close to 87%), like samples K99-1-5 and K99-1-7 (close to 70%), whereas sample K99-1-1 only contains 37% of carbonates.

Table 4-10. Calcimetry data expressed as a percentage of carbonates.

Samples	K99-1-1	K99-1-2	K99-1-3	K99-1-5	K99-1-7
Carbonates %	37	86.4	87	68.9	72.5

3. Fine analysis of the clay fraction.

This part of the study is aimed at performing a more accurate identification of the clay material in samples. To that end, the crystallographic and structure of samples were investigated through a number of treatments, specific experiments and measurements. The concentration of the clay fraction was necessary for a number of analyses to be performed without a disturbance from the presence of minor phases. In this respect, the grain sizing of samples was carried out (size fractionation by centrifugation) to concentrate clay minerals.

4. Preparation and separation methodology of samples.

The size fractionation of fractions below 2 microns **(Table 4-11)** was performed by centrifugation (AQMODOP.DOC file, 1999) on 25 grams of samples previously treated with hydrogen peroxide (H_2O_2 at 70°C) for destroying the organic matter and with hydrochloric acid (HCl at pH 5) for destroying carbonates.

5. Oriented-sample diffraction patterns on separated fractions (< 2µM).

The study of oriented samples performed from the < 2 µm fraction showed the systematic presence of swelling clay minerals. But the amounts of these clay minerals were shown to vary greatly from one sample to another (very variable recovery rates: see below under ‘separations’).

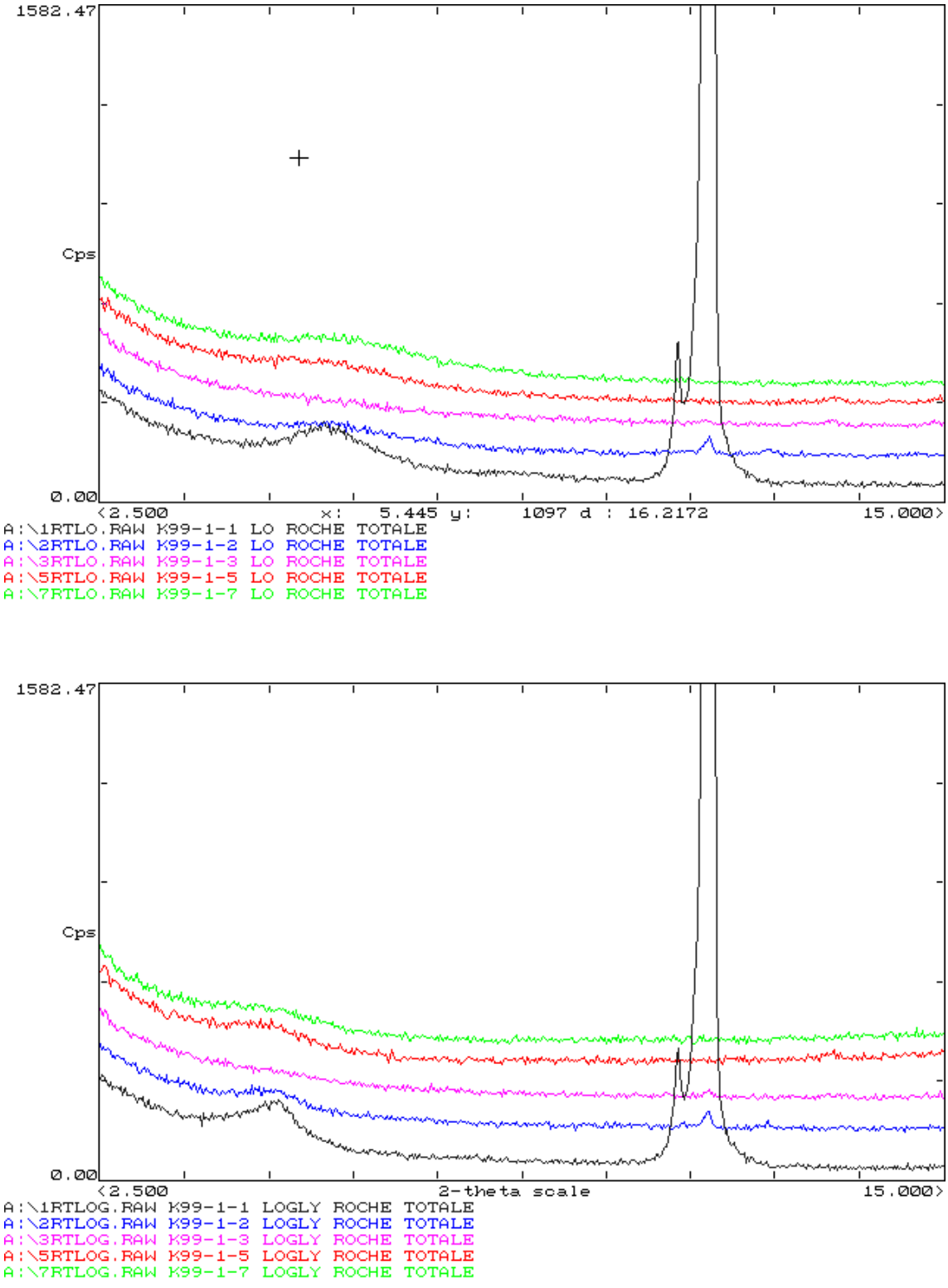

Figure 4-28. *Oriented-sample diffraction patterns of the various studied samples, air-dried (LO, top) and after ethylene glycol saturation (LOGLY, bottom). Angular range 2.5–15°2θ Cu Kα.*

Figure 4-29 displays all the various X-ray diffraction patterns recorded on the < 2 µm fraction. Sample numbers (ANDRA references) are mentioned on the X-ray diffraction patterns provided in this report. The decompositions performed on these diffraction patterns are presented under two forms:

– without vertical zoom (from 2.5 to 22°2θ);

– with a vertical zoom aimed at showing weak peaks (diagram represented from 7 to 22°2θ).

The interpretation of the diffraction pattern obtained from the related rock (K99-1-7) reveals the presence of two major groups of phyllosilicates:

- a swelling clay mineral (perhaps even a mixture of swelling clay minerals): peaks near 17.5, 8.6 and 5.6 Å after ethylene glycol saturation. A background of relative intensity in small angles (near 4 °2θ) may be considered as an indication of interstratification; consequently, this mineral would not be a pure smectite but an interstratified mineral (the nature of layers will be discussed in the paragraph dedicated to the decomposition of diffraction patterns).
- a mineral at 10 Å (mica- or illite-group) characterised by a very weak peak.

The four other diffraction patterns can be grouped together as follows:

– Samples K99-1-1 and K99-1-2.

The diffraction patterns obtained from these two samples show the presence of swelling clay minerals (a priori interstratified) with a slightly higher smectite content than those in the related rock (*(002)* peak near 8.5 Å after ethylene glycol saturation). They represent the most abundant phyllosilicates in both samples. Moreover, sample K99-1-1 shows two very weak peaks:

a) near 10.9 Å after ethylene glycol saturation (peak concealed on the "air-dried" diffraction pattern): illite-group mineral?? (identification to be checked).

b) near 7.28 Å: halloysite ???

Noteworthy amounts of kaolinite were found in sample K99-1-2 (peaks near 7.2 and 3.57 Å).

Samples K99-1-3 and K99-1-5

a) swelling clay minerals characterised by a background of higher intensity in small angles (near 4 °2θ) than that in the related rock. Higher order *(00l)* peaks were found to be very weak.

b) These swelling clay minerals are seemingly mixed layers whose proportion of non-swelling layers is greater than that in mixed layers of the related rock.

A mica- or illite-group mineral (very weak peak near 10 Å) was found in sample K99-1-5.

The peaks with very variable intensities observed near 5.95-6.0 Å and near 2.95–6.00 Å are artefacts related to treatments undergone by samples during separations (for some samples, the rinsing process did not eliminate all of the newly-formed products during treatments: crystallisation of soluble salts).

6. Decomposition of 001 peaks on oriented-sample diffraction patterns.

Figure 4-29 shows the decompositions of the diffraction patterns with two different vertical zooms in order to permit visualisation of sharp peaks on the one hand (first order peaks of swelling clay minerals) and weak peaks on the other hand. As for the latter, the intensity of decomposed peaks is so low that results shall be verified; to that end, the performance of new acquisitions with greater amounts of matter would be essential, for the best recordings possible have been obtained given the material available today.

The decomposition of peaks at 17 Å shows two peaks: a main peak (17.0-17.4 Å) and a peak situated at d >17.5 Å. The latter, situated at d > 20 Å for those samples with a background of high intensity in small angles (samples 3 and 5), is directly connected to the intensity of the background in small angles on the recorded diffraction pattern: it is not an additional mineral but one of both components of the peak at 17 Å of a same randomly interstratified mineral (R=0). The width of the peak at 17 Å is significantly smaller (FWHM = 0.6°2θ) for samples 1 and 2 than for the three other samples (FWHM ≥ 1°2θ).

Positions of the higher order peaks are very close to those of smectites *stricto sensu* (near 8.50 and 5.62 Å) for samples 1 and 2 (FWHM < 1°2θ). The diffraction patterns of samples 3 and 5 are characterised by greater widths (FWHM > 1°2θ), and more or less noteworthy splits and displacements of their positions in comparison with smectite values. The occurrence of a mixture of several interstratified swelling clay minerals was confirmed by the complexity of the analysis of results (particularly the peak displacement direction according to the positions of non-interstratified swelling clay minerals). For lack of supplementary data about these phases (chemistry, randomly oriented powder patterns of separated fractions for determination of their di- or trioctahedral character), a more accurate identification could not be performed. It is only assumed that the constituent layers of the interstratified swelling clay minerals are smectite layers and layers at 10 Å, with no possibility of specifying whether the latter are illite layers or layers of dehydrated smectite (near 10 Å then), or whether these 2 types of layers at 10 Å coexist in a same swelling clay mineral. Indeed, Claret et al. (1999) have shown the impossibility of finely interpreting such diffraction patterns without the performance of several saturation runs intended to homogenise the interlayer composition of smectites.

The decomposition of the diffraction patterns (relating to weak peaks) revealed the following other important points:

- the diffraction patterns of samples 1 and 2 show a peak at d >7.2 Å (FWHM > 0.5°2θ) which seems slightly affected by ethylene glycol saturation. For sample 2, this peak comes with that of kaolinite (d # 7.15 Å, FWHM # 0.27°2θ). Identification of the mineral corresponding to the peak near 7.2 Å remains hypothetical: halloysite at 7 Å or kaolinite-rich kaolinite/smectite mixed layer;

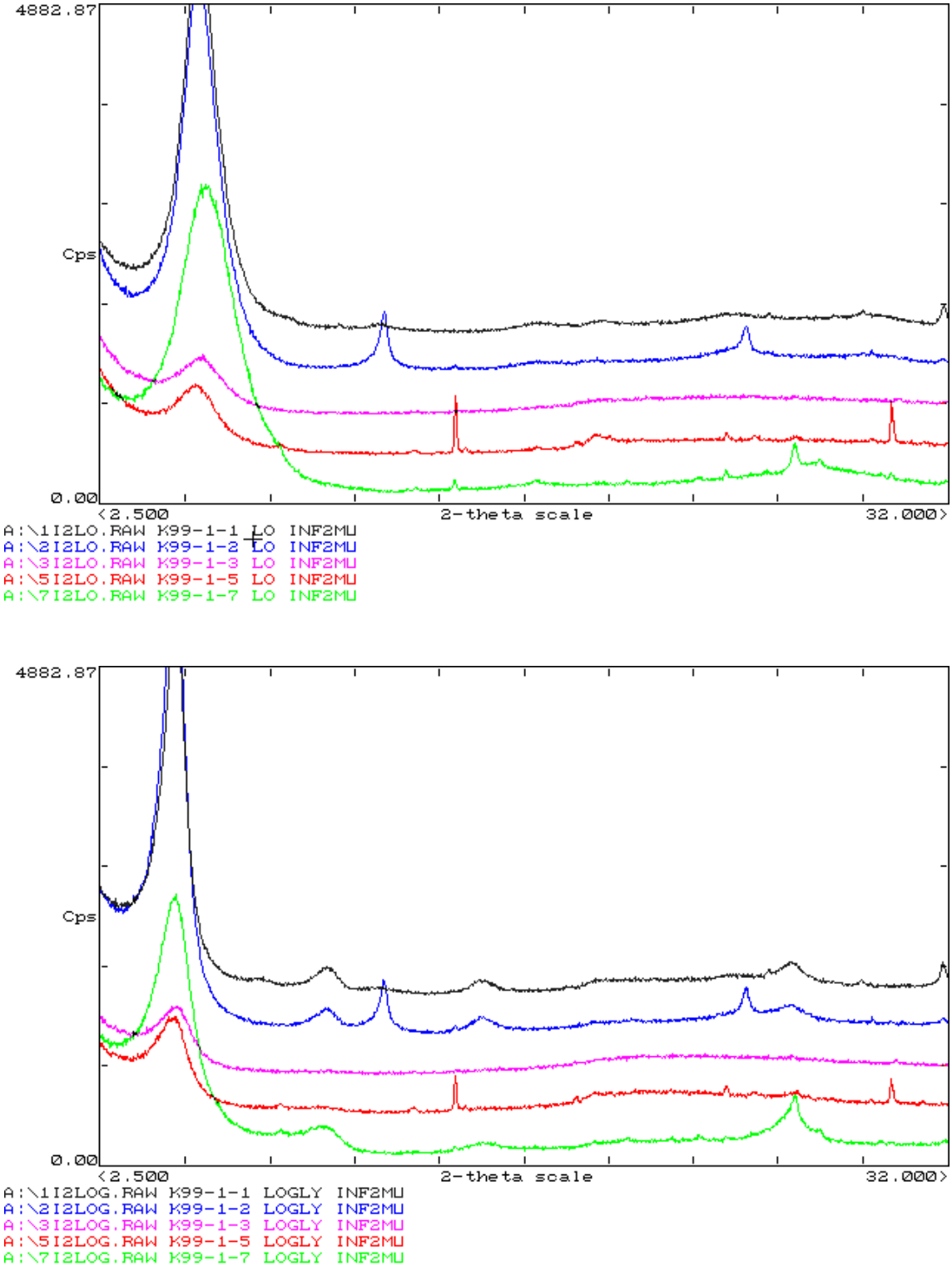

Figure 4-29. *Oriented-sample diffraction patterns (< 2 µm fraction) of the various studied samples, air-dried (LO, top) and after ethylene glycol saturation (LOGLY, bottom). Angular range 2.5-15°2θ Cu Kα.*

- the peak near 10 Å is relatively thin (FWHM <0.3°2θ) as regards the related rock and sample 5. The identified mineral belongs to the mica group (detrital micas?);
- the width of the peak near 10.9 Å of sample 1 seems affected by the ethylene glycol saturation. Such a value is not consistent with the position of a non-interstratified clay mineral; considering the low intensity of the peak, further data are required to perform the mineral identification (whether it is a clay mineral or not).

A few peaks of very low intensity were necessary to obtain a good fit during decomposition. The signification of these thin peaks (near 7.2 or 8.5 Å) will not be discussed here because their true presence remains questionable.

7. Measurements of C.E.C. and exchangeable ions.

The method consists of a sample saturation using magnesium chloride (method developed at the pedology laboratory of Poitiers), then in a displacement by ammonium acetate that replaces magnesium; the latter is determined in solution by atom absorption (Mg is one of the elements whose quantity is determined with the greatest precision (0,05%) using this technique). This method can be used in the presence of calcium carbonates and on small amounts of matter (10 mg). Results are expressed as milliequivalents per hundred grams of material or as charge centimoles per kilogram.

The protocol is as follows:

- Weighing of the 10 mg test portion of <50 µm powder sample (dry at 105°C) in a 1.7 ml polypropylene “Treff” vial.
- Contact for thirty minutes with 1ml of normal magnesium chloride (1/2 mole per litre), with agitation.
- Centrifugation of vial (4000 rev/min for 10 min), elimination of the supernatant liquid.
- The operation (2 and 3) is repeated twice or three times.
- The Mg^{2+}-saturated clay deposit is “rinsed” 5 or 6 times with ethyl alcohol up to disappearance of excess chloride and Mg ions (verification with silver nitrate).
- Displacement of the combined Mg by a normal solution of ammonium acetate (5 x 1 mL).
- The solution to be determined is obtained in a 100 mL flask + 10 mL of La_2O_3 at 5% + 5 x 1 mL of ammonium acetate N extraction solution (operation 6), then adjusted with distilled water.

The results obtained with both methods are presented in **Table 4-12**.

The <2 µm fraction of these samples was found to be nearly calcic homoionic (less than 5 cmoles.kg^{-1} of Mg and less than 1 cmole.kg^{-1} of K). The measurement of exchangeable ions was disturbed by the presence of products soluble in the material. Indeed, some samples display a total amount of determined ions greater than the measured exchange capacity.

Table 4-11. Recovery rates obtained after fractionation (< 2 µm) and estimated in weight percentage.

Samples	K99-1-1	K99-1-2	K99-1-3	K99-1-5	K99-1-7
< 2 µm fraction %	>7	>5	>3	>8	>9

Table 4-12. Less than 2 µm fraction – Measurements of C.E.C. and exchangeable ions (expressed as charge centimoles.kg^{-1} or meq./100g) using the NH_4 and Mg saturation method. The sum of E.B. corresponds to the arithmetical sum of the measured exchangeable bases.

Samples	Ca	Mg	Na	K	Sum of E.B	CEC (Mg)	CEC (NH_4)
K99-1-1	85.86	2.42	0.00	0.00	88.28	82.26	83.30
K99-1-2	91.88	2.46	0.00	0.00	94.35	78.09	80.84
K99-1-3	78.58	4.31	0.00	0.00	82.88	69.18	115.13
K99-1-5	121.72	2.00	0.00	0.00	123.72	94.92	113.70
K99-1-7	86.18	1.15	0.00	0.95	88.27	80.88	82.64

The first series of CEC measurements obtained by NH_4 saturation revealed abnormally high values for samples K99-1-3 and K99-1-5. Consequently, the CEC was measured by Mg saturation for verification.

Both methods yielded high CEC values. Nevertheless, for samples K99-1-3 and K99-1-5, the values recorded using the second method seem more credible than those obtained with the first method. The results on samples K99-1-1, K99-1-2 and K99-1-7 (close to 80 cmoles.kg^{-1}) were confirmed and those obtained on samples K99-1-3 and K99-1-5 were found to be lower (70 and 95 cmoles.kg^{-1} respectively). This is certainly due to the presence of NH_4 released by the material, probably by some organic matter still present despite the H_2O_2 treatment.

The CEC (Mg) of sample K99-1-5 remains very high, especially since the presence of a greater amount of smectite in this sample was not confirmed by the X-ray diffraction analysis. As previously stated, this may be caused by the presence of organic matters or more hypothetically to the presence of other phases (zeolites?).

Comments on results

The randomly oriented diffraction patterns revealed the constant presence of calcite in all of the 5 samples. Gypsum was clearly identified in samples K99-1-1 and in lesser proportions in samples K99-1-2 and K99-1-3. Only sample K99-1-1 showed clay proportions high enough to be identified from the bulk sample. The presence of smectite-like clay in sample K99-1-1 was confirmed by the oriented-sample diffraction patterns on the bulk sample.

Measurements with the Bernard calcimeter revealed high levels of carbonate in every sample varying between 70 and 87%, except sample K99-1-1 with only 37% of carbonates. The fine analysis of the clay fraction (< 2 µm) allowed comparison between samples and the related rock (K99-1-7):

1. The oriented-sample diffraction patterns of sample K99-1-7 show the presence of an interstratified-type swelling clay mineral and a mineral at 10 Å (probably mica-like).
2. The oriented sample diffraction patterns of samples K99-1-1 and K99-1-2 show the presence of pure smectite and interstratified swelling clay minerals with a slightly higher smectite content than the related rock, and a peak above 7,2 Å comparable either to halloysite or to a kaolinite/smectite mixed layer with a very high kaolinite content. The peak at 10,9 Å of sample K99-1-1 is either an illite-group mineral or a mixed layered mineral (determination impossible without further information). The oriented-sample diffraction patterns of sample K99-1-2 show the presence of kaolinite.
3. The oriented-sample diffraction patterns of samples K99-1-3 and K99-1-5 show the presence of interstratified swelling clay minerals with a slightly lower smectite content than the related rock, and a mineral at 10 Å (probably mica-like) for sample K99-1-5 only.
4. The measures of CEC (Mg) and exchangeable bases are consistent with X-ray diffraction data for samples K99-1-1, K99-1-2, K99-1-3 and K99-1-7 but do not confirm the observations performed on sample K99-1-5.

Petrographic analyses

At this early stage in the petrographic studies, only the following microphotographs are presented (**Plates 4-1 to 4-6**) with some brief comments.

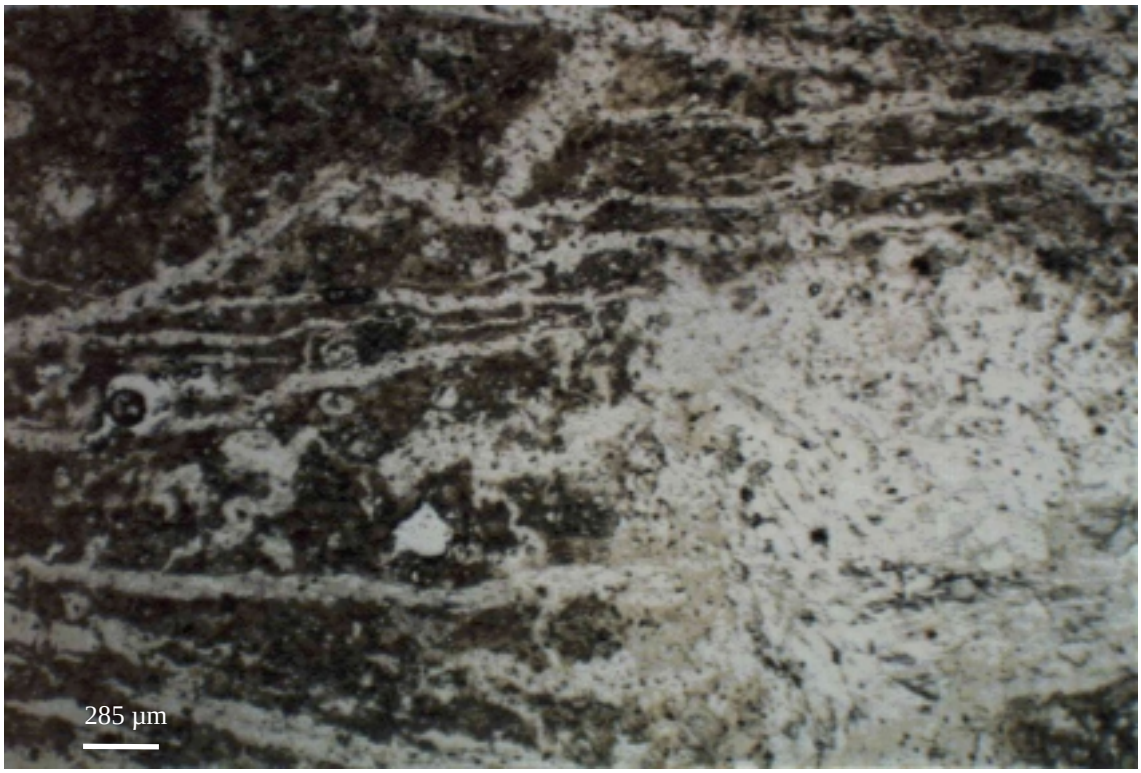

K99-1-1: Plain polarised light

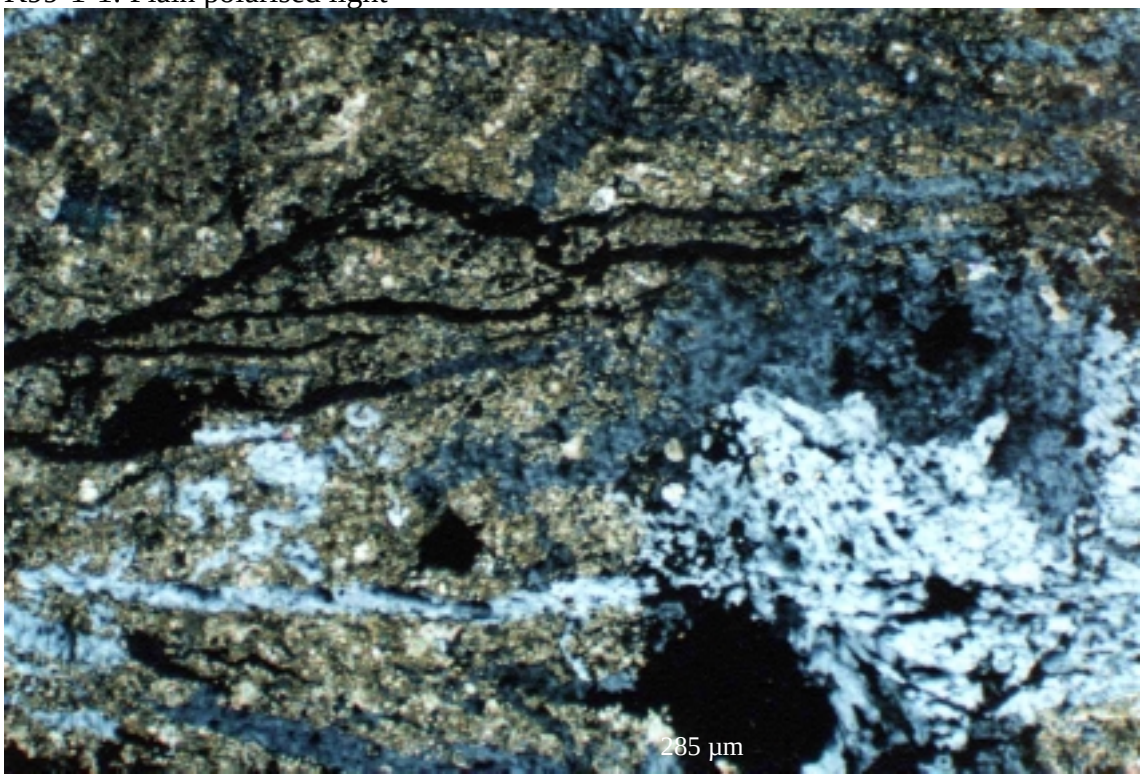

K99-1-1: Cross-polarised light

Plate 4-1. *Microphotographs under optical microscope showing: intensely cracked rock with gypsum fracture filling. The pale foraminiferous micrite shows intensely altered area replaced in most cases by gypsum. The cracked network is interlaced.*

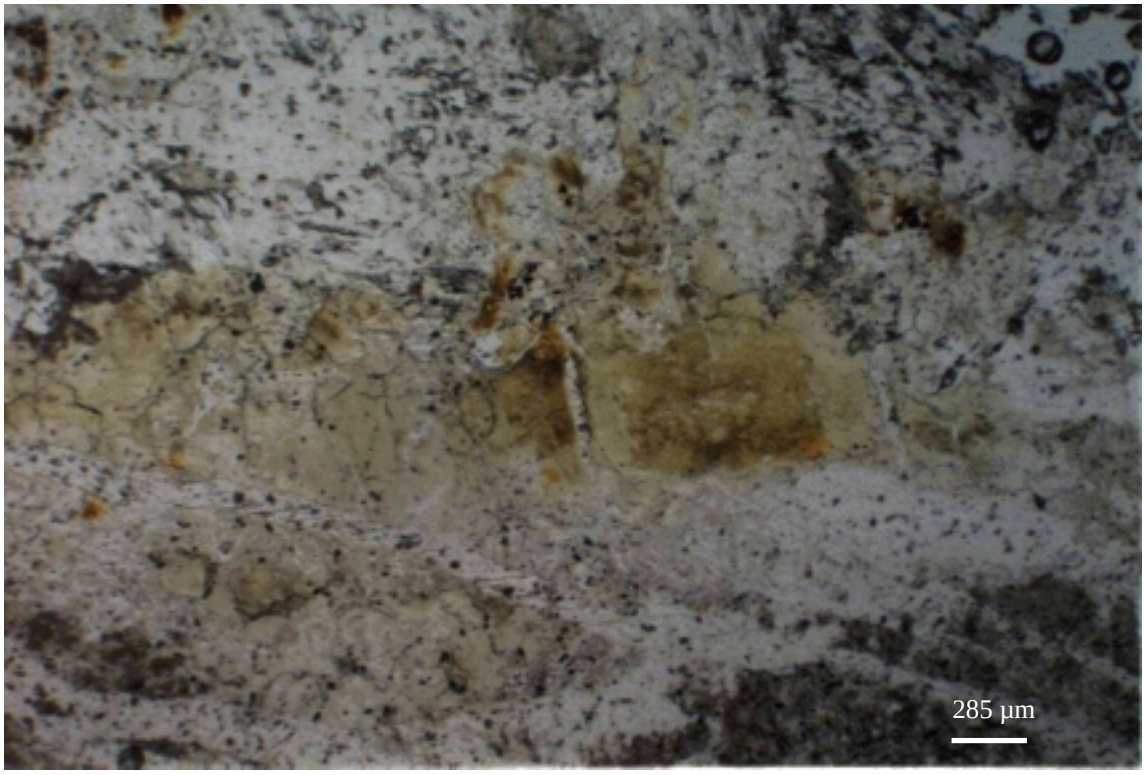

K99-1-1: Plain polarised light

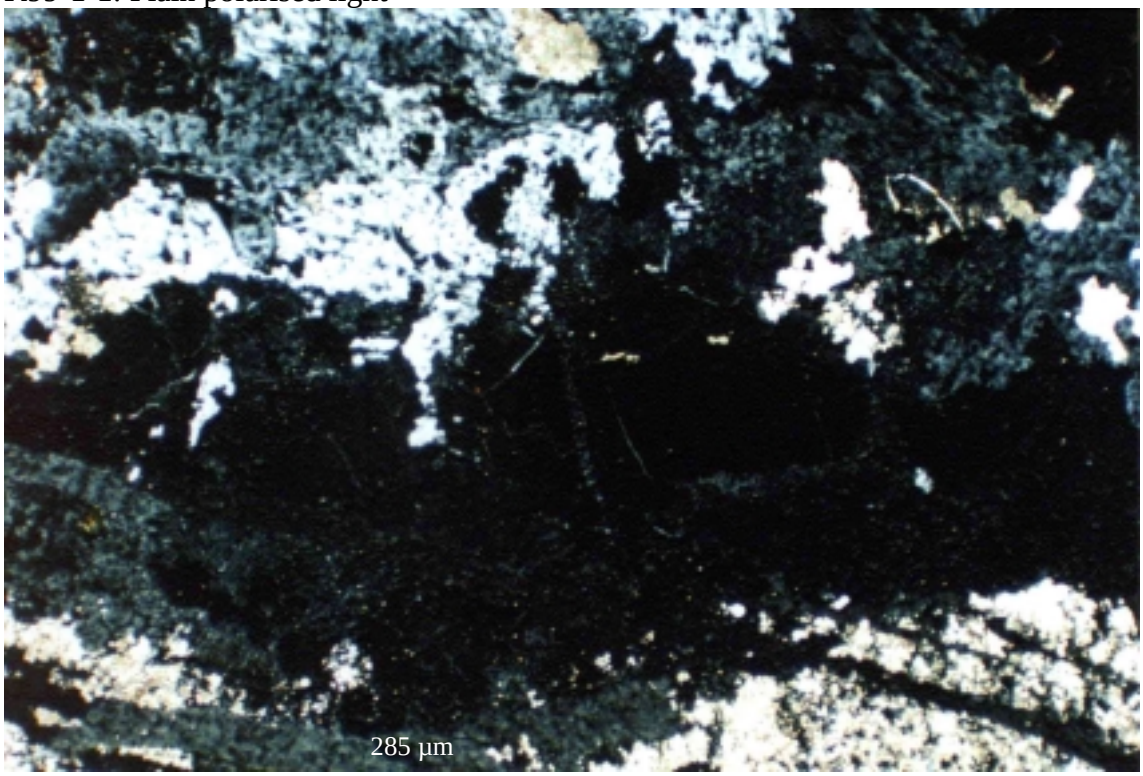

K99-1-1: Cross-polarised light

Plate 4-2. *Microphotographs under optical microscope showing: not yet determined mineral in the gypsum fracture filling area (black in cross-polarised light).*

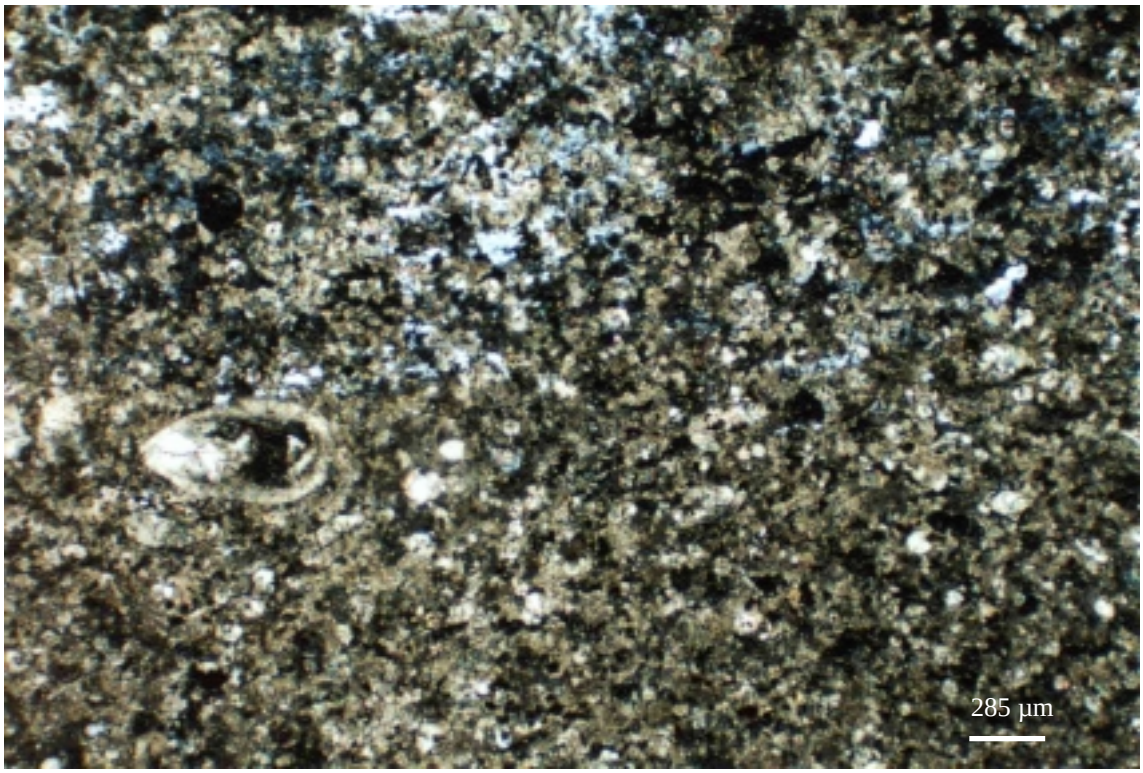

K99-1-2: Cross-polarised light

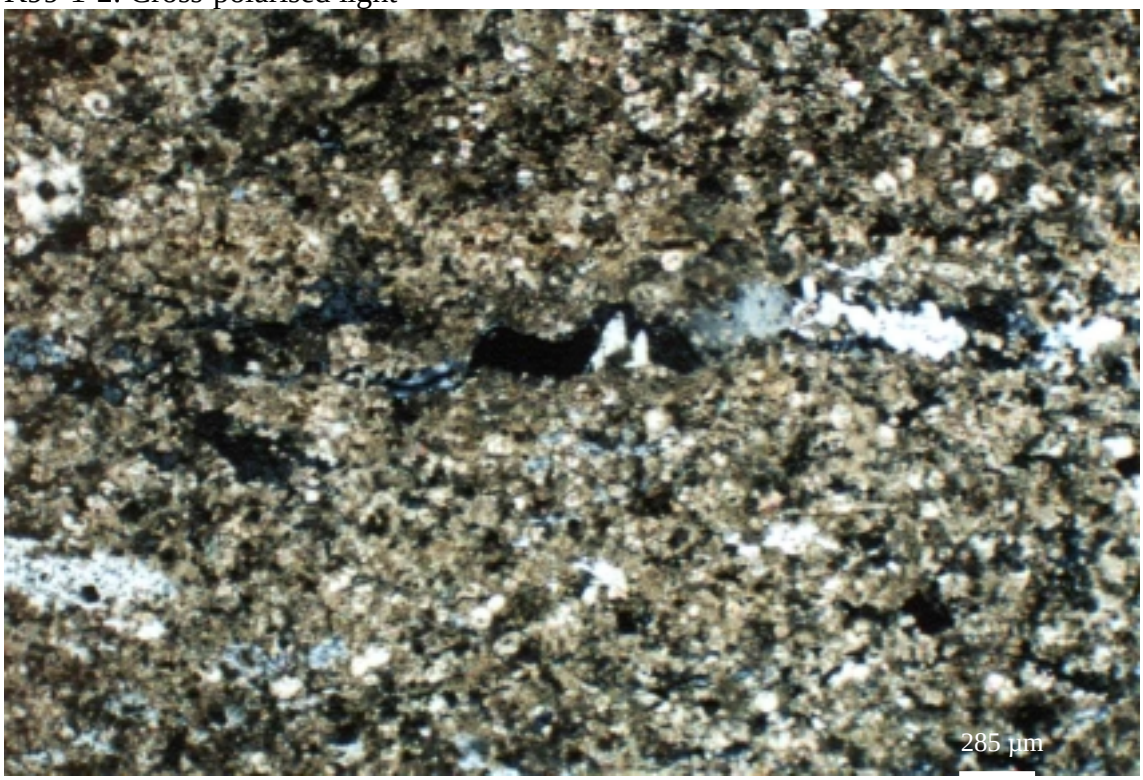

K99-1-2: Cross-polarised light

Plate 4-3. *Microphotographs under optical microscope showing: general aspect of the pale micrite and diffuse gypsum more or less associated with the cracked network.*

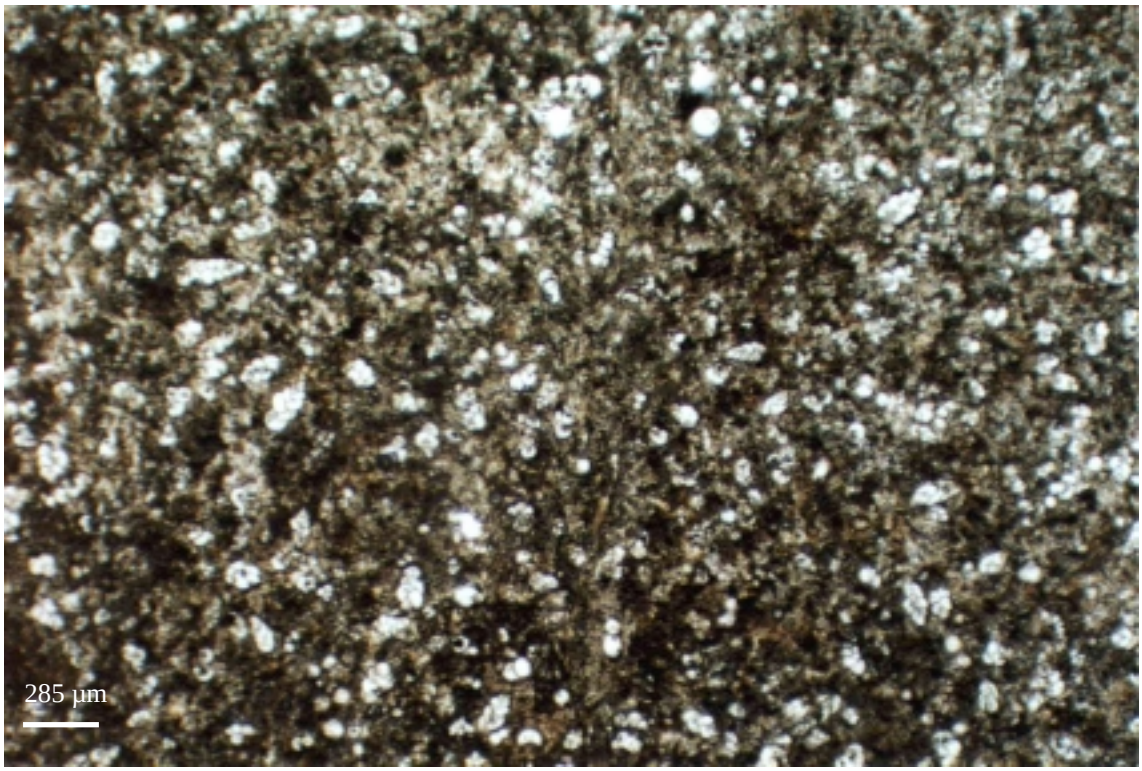

K99-1-3: Plain polarised light

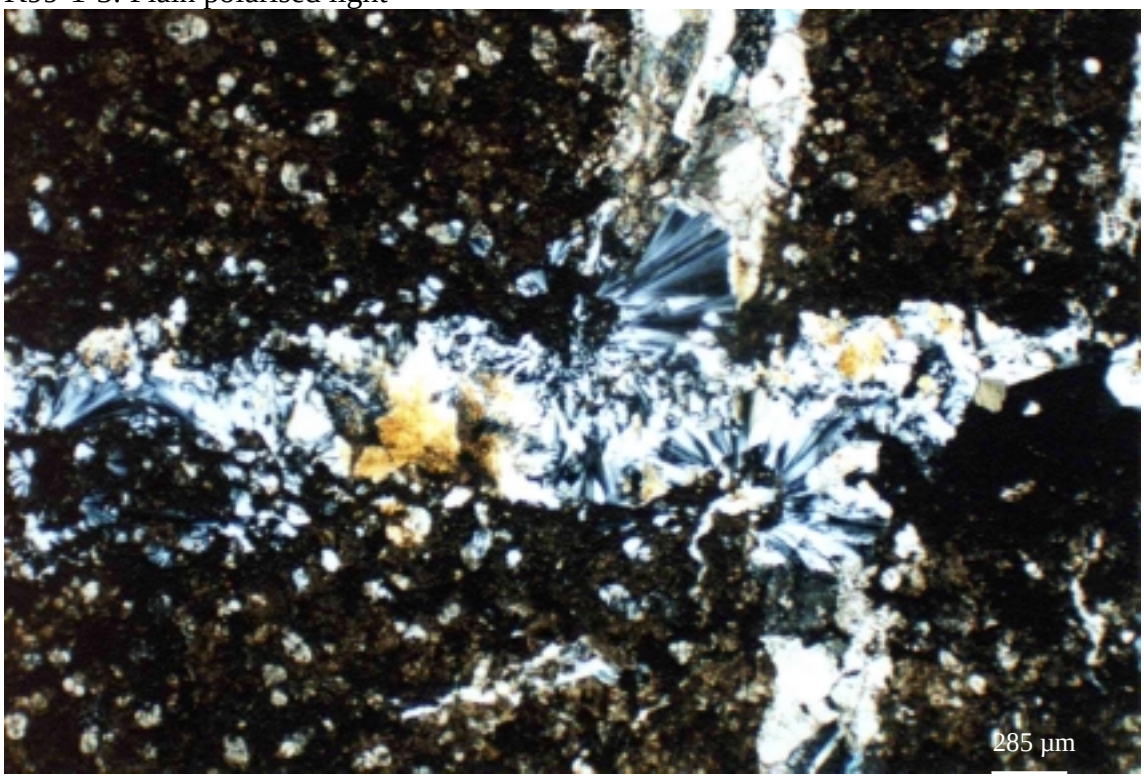

Plate 4-4. *Microphotograph under optical microscope showing: pale foraminiferous micrite, including crystals with bigger size than in sample K99-1-7. Secondary fissures (filled with acicular minerals) cross through "primary" carbonate cracks (K99-1-3: Cross-polarised light).*

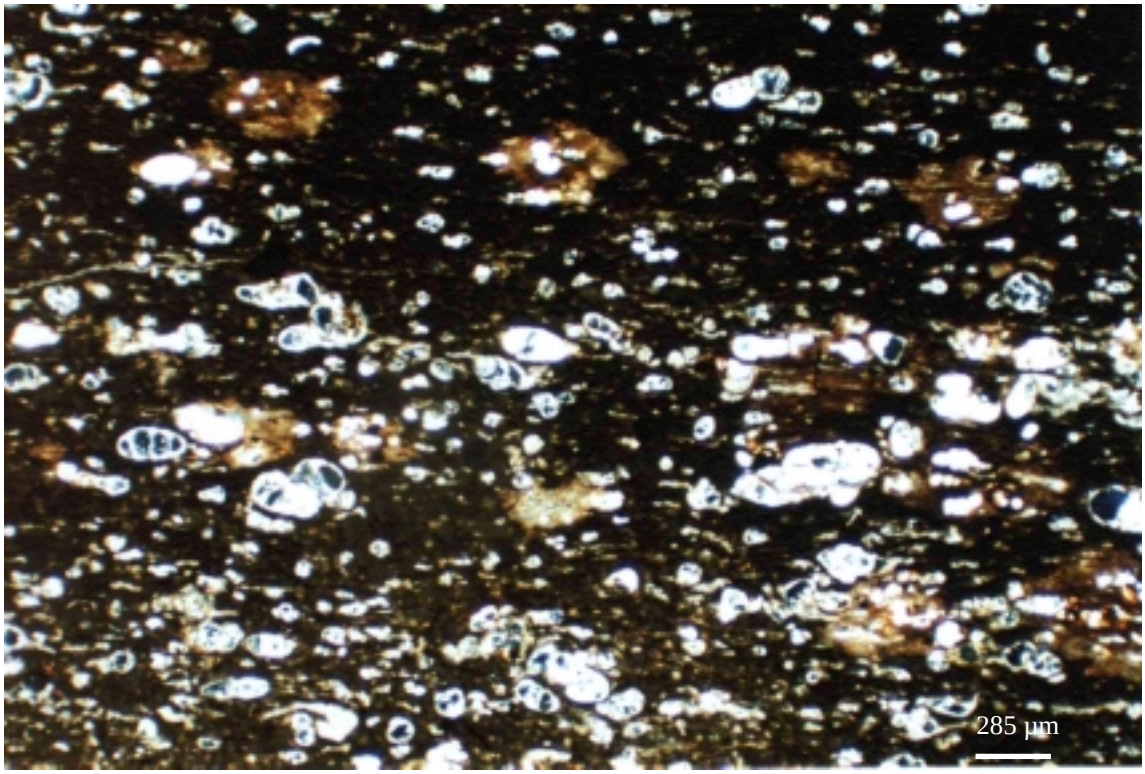

Plate 4-5. *Microphotographs under optical microscope showing: foraminiferal limestone in which cement is an opaque micrite. The cement is darker than in sample K99-1-7; organic matter or iron oxi-hydroxides also present (to be confirmed) (K99-1-5: Cross-polarised light).*

.

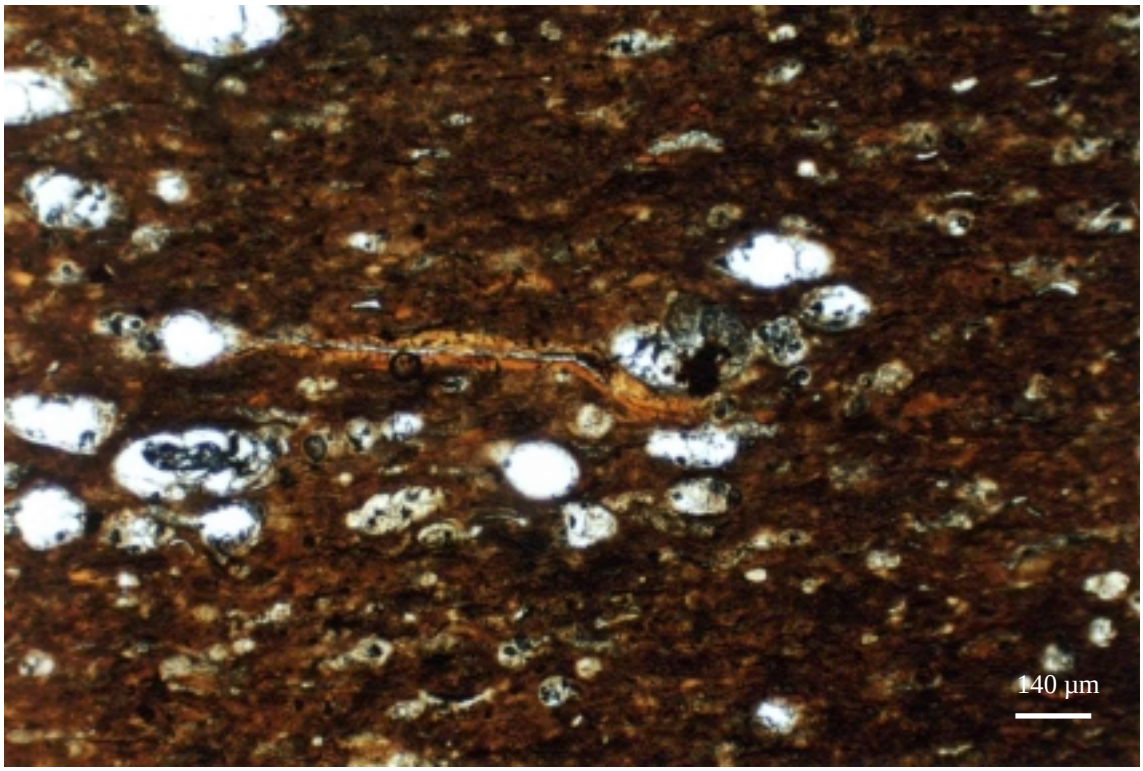

Plate 4-6. *Microphotograph under optical microscope showing: general aspect of the related rock. Foraminiferal micrite shows a very well defined stratification (K99-1-7: Plain polarised light).*

4.3.5 Conclusions

Three profiles have been sampled during the reconnaissance mission to Khushaym Matruk (**Figure 4-30**). Based on the scoping chemical analysis and XRD spectra carried out by the University of Jordan, two complementary studies have been carried out subsequently by the CEA, Cadarache and ERM, Poitiers. These have involved:

- Profile 1: from the contact zone between metamorphosed rock (i.e. cement zone) and unaltered Bituminous Marl, a distance of 5.8m. This has been studied by ERM using classical methods (i.e. XRD and petrographic observations, optical microscopy and MEB)
- Profile 2 (locality 6) and Profile 3 (locality 5): contact zone between altered and unaltered metamorphosed rock by CEA using IRTF, DTA-TG, XRD, SEM-EDX and wet chemical analysis.

These exploratory studies had the general objectives to identify clay phases in the Bituminous Marl, estimate their amounts and evaluate the potential of the site for further investigation on the clay fraction and clay/leachate reaction products. The potential role of vertical/sub-vertical fractures to the circulation of hyperalkaline fluids to depth was also borne in mind, and sampling adjacent to such potential fractures in the unaltered marl was given priority when observed.

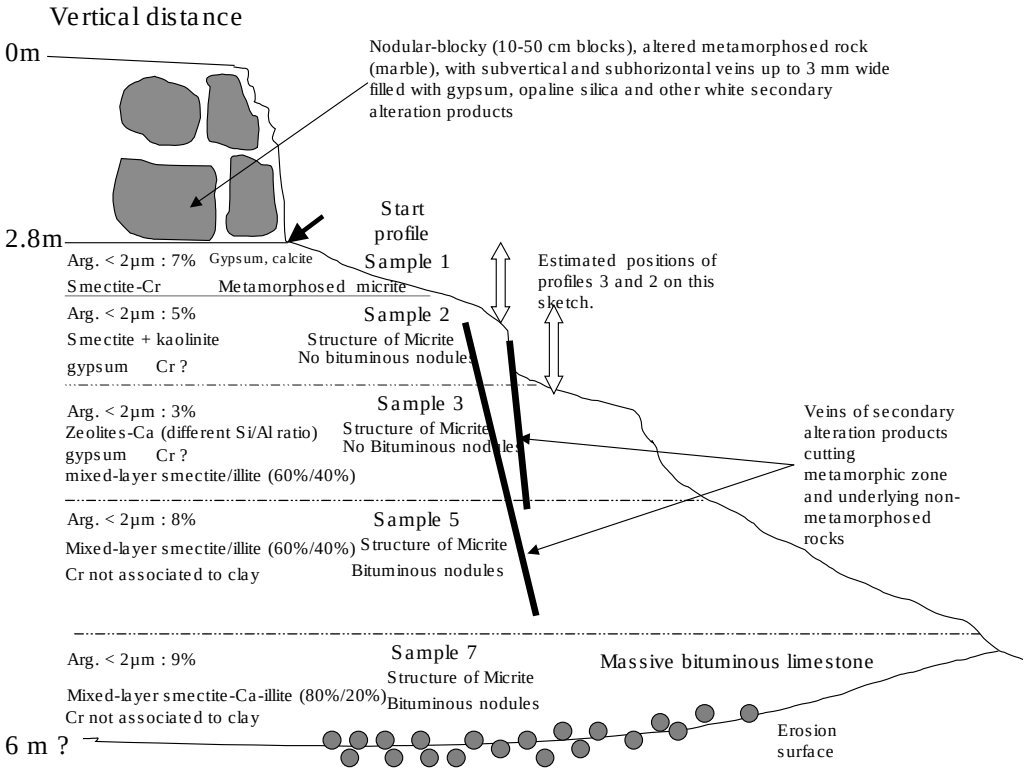

Figure 4-30. *Khushyam Matruk: Location of the studied profiles and samples, and summary of the mineralogy.*

According to some performance assessment (PA) requirements, the Bituminous Marl at Maqarin contains too little clay (~2 wt%) to evaluate its behaviour when in contact with hyperalkaline solutions. Khushaym Matruk, in contrast, seems to be a more promising site with outcropping massive Bituminous Marl containing a clay rich fraction (<2μm) of at least 9 wt% and as much as 24 wt%. Such an amount is adequate to conduct most of the studies necessary to describe and evaluate the behaviour of clay in the presence of an alkaline plume.

Profile 1 was sampled over a few metres from the altered metamorphosed marl down to what was observed as "the unaltered marl". Among the seven samples collected, five were selected to extract the <2μm fraction for identification of the clay minerals (**Figure 4-30**). Selection of samples was made to reflect various parts of the profile, i.e. Sample 7 representing unaltered marl, Samples 3 and 5 crosscut by gypsum veins, Sample 2 significantly altered marl, and Sample 1 representing a greenish (Cr-rich) area corresponding to the "baked" marl during the metamorphism.

In the "unaltered" marl, Sample 7, the amount of clay in the <2μm fraction is about 9 wt%. This value is consistent with previous results from the University of Jordan. The identified clay is mostly a mixed layer illite (10Å)/smectite (17Å) containing 80% smectite. The other four samples were then compared to Sample 7. The results have been summarised in **Figure 4-30**.

With respect to the Profile 2 and 3 studies; although the comparison with Profile 1 can only be qualitative since different samples were investigated, there is good agreement between the nature of the clay phases. In addition, the Profile 2 and 3 samples gave insight into the chemical composition of the clays with respect to the major cations Ca, Mg and Na.

From the overall studies carried out on these five samples, heterogeneity is observed by:

1. The total amount of the <2μm fraction, from 9 wt% in Sample 7 to 3 wt% in Sample 3 and 5 wt% in Sample 5;
2. The type of mixed layer, from an illite/smectite with 80% of smectite in sample 7, to illite/ smectite with 60% of smectite in Samples 5 and 3, and smectite in Samples 2 and 1;
3. The distribution of kaolinite, present only in Sample 2;
4. The distribution of Cr, mostly present as small nodules (1μm) in the host marl where it is clearly associated with clays in Sample 1;
5. The distribution of the bituminous nodules, where they are present in the host marl but disappear at the top of the profile;
6. The structure of the rock, where sedimentary structures are preserved in all samples except Sample 1 which represents a "baked" variety of rock, and
7. The distribution of secondary minerals such as zeolite and gypsum. Zeolite is largely present in Sample 3 as fracture infilling or as a secondary product in the adjacent rock. Gypsum replaces calcite (in Samples 1 and 2); it is not present in the unaltered marl.

Samples from Khushaym Matruk seem to contain enough clay to support further study of clay stability in the presence of hyperalkaline waters. However, since Khushaym Matruk is not presently an active system, proof of fossil alteration by alkaline fluids is required. For example, the evolution of the clay fraction and the occurrence of zeolite may be an indication that the non-metamorphosed rock has been in contact with alkaline solutions. Potentially, the clays present in the profile may have four origins: 1) detritic, 2) diagenetic, 3) metamorphic, and 4) produced during hyperalkaline alteration. Clays in Sample 1 are metamorphic in origin (association with Cr and loss of the sedimentary structure), and clays in Sample 7 are detritic and/or diagenetic. The origin of the clays in the other samples is not yet clear. Samples 2, 3 and 5 present different clay characte-ristics and two origins can be suspected: an alkaline plume effect, or, different host rock type. In this respect the occurrence of zeolite may favour the effect of an alkaline plume.

Considering the overall results, Khushaym Matruk appears a promising site but a detailed sampling campaign needs now to be planned. Continuous sampling of the same host rock, from the unaltered marl to the contact with the cement zone, is required. The feasibility of extracting the <2µm clay fraction has been proved, and some indicators of the effects of alkaline perturbation have been detected.

5 Some general comments

The final day in Jordan was devoted to post-reconnaissance mission discussions involving an appraisal of what was accomplished, and how present and future information should be compiled, documented, and distributed.

It was agreed that all systematically collected samples were to be sent for archivation to ANDRA (Central Jordan) and BGS (Maqarin). Splits from the Central Jordan profiles would be left with the University of Jordan.

Prior to leaving Jordan, a preliminary list of all samples to be archived was documented, indexed by a number, locality and brief description. This list has been subsequently updated by Tony Milodowski (BGS) with material studied in Phases I, II and III, and presently archived at BGS. The new list has been circulated to all reconnaissance participants for comment/modification, and an interim list has been now distributed for general use (**Appendix 9**). Based on future requirements of the various groups, the listed samples will be available on request.

To avoid unnecessary duplication between the various groups, although some will be unavoidable, groups have been encouraged to make use of earlier BGS and University of Jordan experience when planning their respective programmes of study. Close collaboration is the only way the project can meet the level of ambition outlined in the Phase IV proposal.

6 General conclusions

The Reconnaissance Mission and subsequent reporting of field data and laboratory studies has helped considerably in structuring the Phase IV Technical Proposal. On the basis of the mission, taking into consideration scientific, logistical and economic criteria, the following future issues have been clarified:

Maqarin sites

1. Regional field studies will be restricted to clarifying specific structural problems (e.g. the importance of slumping) still left unresolved from this mission and the previous Phase III study.
2. Since there is already sufficient information, no further regional geomorphology studies will be carried out.
3. Structural field studies will concentrate on the Eastern Springs area (i.e. site scale) as part of the hydrostructural modelling task.
4. No surface drilling is envisaged at the Eastern Springs.
5. Main activities will concentrate on Adit A-6. These will include:
   - detailed structural mapping,
   - drilling of additional boreholes,
   - hydrogeological characterisation of the boreholes (e.g. hydraulic conductivity and potentially cross-hole testing),
   - hydrochemical and microbiological characterisation of available groundwater from the boreholes,
   - mineralogy and geochemistry of unaltered marl, cement zone and the transition zone rocks, and
   - geomagnetic studies.
6. The mineralogy, geochemistry and geomagnetic studies will be augmented by outcrop sampling from the Eastern Springs area.
7. In addition to the adit, hydrochemical monitoring will continue at all existing sites (e.g. Railway Cutting, Western Springs, domestic springs in the area etc.) to establish seasonal chemical and isotopic variations and trends in the surface water and groundwater systems.

Central Jordan sites

1. The clay studies warrant further study; this will require excavating strategically located trenches for mapping and sampling.
2. Trenching will be conducted across the cement zone/bituminous-rich marl contact in order to collect a continuous profile to include the cement zone, altered marl and finally the unaltered (‘fresh’) marl at depth.

3. Particular attention will be given to include mineral-infilled vertical/sub-vertical fractures extending from the cement zone to depth into the unaltered marls.
4. Preliminary scoping analysis of sampled material.
5. Detailed analysis of selected samples to:
    - characterise the mineralogy and geochemistry,
    - separate and characterise the clay fraction,
    - determine the origin of the clay fractions,
    - determine the extent and nature of any clay/hyperalkaline water interaction, and
    - observing any evidence of a downward penetrating pH front through the cement zone/marl contact.

7 References

Arkin Y, 1989. Large-scale tensional features along the Dead Sea-Jordan Rift Valley. Tectonophysics, 136, 299–321.

AQMODOP.DOC, 1999. Manuel d'assurance qualité rédigé par le responsable AQ:A. CASSAGNABERE.

Bouchet A, 1992. Mise au point d'un programme de détermination automatique des minéraux argileux. Coll. de Rayons X Siemens, Paris, Comptes Rendus, 2, 52–61.

Brown G, Brindley G W, 1980. X-ray diffraction procedures for clay mineral identification. In : Crystal structures of clay minerals and their X-ray identification. G W Brindley and G Brown (Eds.), Miner. Soc., London, 305–360.

Claret F, Lanson B, Drits V A, Griffault L, 1999. Présentation aux journées scientifiques de l'ANDRA à Nancy.

E R M, 1997. Techniques et protocoles analytiques utilisés par la société E R M Document ERM 97 022 FR 060.

J**ackson M L,** 1964. Soil chemical analysis. Prentice Hall Inc., New Jersey, USA. (3rd Edition).

Kemmerly P R, 1982. Spatial analysis of a karst depression population: Clues to genesis. Bull. Geol. Soc. Am., 93, 1078–1086.

Khoury H, Salameh E, Mazurek M, Alexander W R, 1998. Geology and hydrogeology of the Maqarin area. In: J A T Smellie (Ed.), Maqarin natural analogue study: Phase III. SKB TR-98-04, Swedish Nuclear Fuel and Waste Management Co, p. 39–70.

Kronfeld J, Vogel C, Rosenthal E, Weistein-Evron M, 1988. Age and paleoclimatic implications of the Bet Shean travertines. Quat. Res., 30, 298–303.

Linklater C M (Ed.), 1998. A natural analogue study of cement-buffered, hyperalkaline groundwaters and their interaction with a repository host rock: Phase II, Nirex Report, S/98/003, Nirex, Harwell, U.K.

Mouterde S J, 1953. La flore du Djebel Druze. Dar el-Machreq, Beymouth.

Reynolds R C, 1980. Interstratified clay minerals. In : Crystal structure of clay minerals and their X-ray identification. G W Brindley and G Brown (Eds.), Miner. Soc., London, 249–303.

Reynolds R C, 1985. Description of program NEWMOD© for the calculation of the one-dimensional X-ray diffraction patterns of mixed-layered clays. Users Manual; R C Reynolds (Ed.), 8 Brook Road, Hanover, New Hampshire, 03755.

Stiller M, Kaufman A, 1985. Paleoclimatic trends revealed by the isotopic composition of carbonates in Lake Kinneret. Zeit. T. Gletsch. Glazialgeol., 21, 79–87.

Willcox G, 1999. Charcoal analysis and Holocene vegetation history in southern Syria.

Appendix 1

Reconnaissance mission to Jordan
(April 28th to May 7th, 1999)

Reconnaissance mission to Jordan (April 28th to May 7th, 1999)

1 Background

Based on the meeting held at BGS, Nottingham on January 25th/26th, it was decided to initiate a reconnaissance mission to the Eastern Springs area of Maqarin and to Central Jordan. This was estimated to 10 days and was carried out from April 28th to May 7th. The following programme was identified and agreed upon.

2 Tasks to be accomplished

In addition to familiarising the group with the general features and geology of the sites, several major tasks to be accomplished have been identified.

2.1 Eastern Springs, Maqarin

As well as the specific tasks outlined below, rock samples (outcrop and potentially existing drillcore material) will be collected when possible to enable some studies to start up immediately following the mission. These will include matrix diffusion studies on selected high pH water/rock reaction profiles.

2.1.1 TASK 1: Background information

Prior to travelling to Jordan, the existence and availability of relevant background information/data concerning the sites is required. This will include satellite imagery, number of open boreholes from earlier drilling campaigns, availability of specialised equipment, adequate logistic back-up for the mission etc.

2.1.2 TASK 2: Structural evaluation

A site-scale structural evaluation of the Eastern Springs area is required; outcrop is limited and such studies will be confined mostly to road/rail cuttings, Adit A-6 and wadi slopes. These studies will focus on establishing the structural geometry of the site, and sampling strategic fracture filling phases for future mineralogical, geochemical and isotope (e.g. age-dating) studies.

2.1.3 TASK 3: Geomorphological evaluation

Earlier geomorphological studies were successful in helping to understand the recent geological evolution of northwest Jordan and the Maqarin region in particular. Additional study is required, and the purpose of this task will be to conduct regional-/site-scale evaluations of tectonic and geomorphological features that may further constrain geological events related to the formation of the cement zones and subsequent hyperalkaline groundwater evolution.

2.1.4 TASK 4: Geophysical measurements

Site-scale surface resistivity surveys are planned at the Eastern Springs area to help locate potential borehole sites for future hydrogeological, hydrochemical and tracer experiment studies. It was hoped that some downhole resistivity measurements may help to supplement the surface surveys, but apparently all the existing boreholes are either sealed or have collapsed. Resistivity equipment is available in Jordan.

2.1.5 TASK 5: Adit A-6 activities

It is hoped to conduct preliminary core drilling in Adit A-6 (i.e. at the M1 sampling location) using the Nagra Hilti portable machine to intercept the contact between the cement zone and Bituminous Marl. To this end the reconnaissance mission will assess the feasibility of drilling and sampling in the adit. This will include also a safety evaluation of drilling in the adit, for example, shoring-up requirements for the walls and roof in the vicinity of the proposed drilling. In addition, an available source of water for drilling and a generator for operating the drill and supplying lighting etc. are required. It may be that some preliminary drilling can be attempted during the mission.

If successful, the borehole(s) will be used subsequently to sample core from the cement zone, the contact between the cement and the marl, and to sample groundwaters (± colloids) from isolated, packed-off borehole sections.

2.2 Central Jordan

Because of Phase I-III project priorities at the Maqarin site, the amount of time spent in Central Jordan has been restricted. It is hoped that this mission will provide the opportunity of finally assessing the full potential of the fossil hyperalkaline reaction zones (e.g. late-stage hyperalkaline plume evolution; long-term hydration studies etc.), and also to locate clay-rich horizons to study the stability of clay in the presence of hyperalkaline groundwaters, as an analogue of bentonite stability.

The Daba-Siwaqa area in Central Jordan needs to be revisited and sampled, and the Suweileh area 15 km northwest of Amman needs to be fully evaluated with respect to clay/hyperalkaline stability. These, and other possibilities will be assessed by Dr. Hani Khoury prior to the mission; if shown to be promising, sampling will be carried out.

Appendix 2

Collage of photographs viewing the topography of the Eastern Springs area from the east

Appendix 3

Satellite imagery of the Yarmouk River Valley, Jordan, with geomorphological interpretation

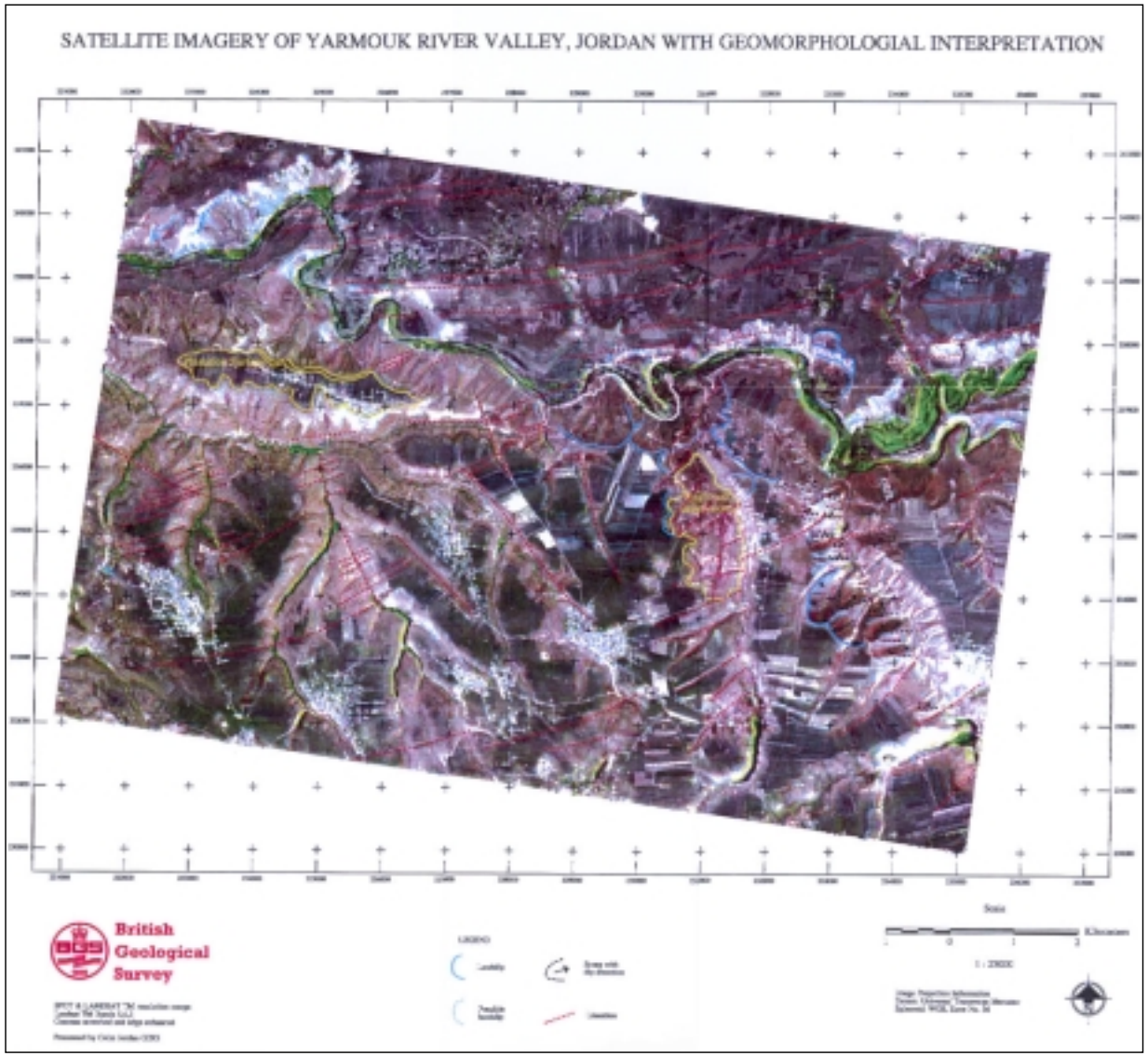
SATELLITE IMAGERY OF YARMOUK RIVER VALLEY, JORDAN WITH GEOMORPHOLOGIAL INTERPRETATION
British
Geological
Survey

Appendix 4

Eastern Springs area: Tabulated results of the fracture mapping (orientation, frequency, vein-fill etc.)

Wadi Shallala (West Side)

Fracture Number	Strike	Dip	Dip azimuth	Half-length (m)	Intersection character	Vein -fill	Distance from start (m)	Separation	Comments	Formation	Bedding strike	Bedding dip	Bedding dip azimuth
1		85		>8	T	U	0.00	0.10		B3	36	10	126
2		85		>8	T	U	0.10	0.30			28	22	118
3		90		>8	T	U	0.40	0.60					
4	002	88	092	>8	T	U	1.00	0.30					
5		90		>8	T	U	1.30	0.25					
6		90		>8	T	U	1.55	0.25					
7		88	078	>8	T	U	1.80	0.80					
8		88	078	>8	T	U	2.60	2.00					
9		90		>8	T	U	4.60	0.20					
10		90		>8	T	S	4.80	1.70	Micritic sediment fill				
11		88	083	>8	T	S	6.50	0.30	Micritic sediment fill				
12		90		>8	T	S	6.80	2.20	Micritic sediment fill				
13		87	078	>8	T	S	9.00	0.10	Micritic sediment fill				
14		87	086	2.00	I	C	9.10	0.20					
15		88	84	4.00	I	C	9.30	1.40					
16		88	268	>8	T	U	10.70	0.30					
17		88	268	4.00	I	G	11.00	0.20	1 mm normal slip, polished and slickensided surface pre-dates powdery gypsum fill				
18		88	259	>8	T	G/S	11.20	0.20	White powdery gypsum fill Developed on top, and along dilated Margins of micritic sediment fill				
19		90		0.50	I	G	11.40	0.02					
20		90		0.50	I	G	11.42	0.06					
21		90		>1	R	U	11.48	0.10					
22		88	086	>8	T	G	11.58	1.92					
23		86	256	0.50	I	G	13.50	0.90					
24		84	254	1.20	I	G	14.40	0.02					
25		89	078	0.20	I/R	U	14.42	0.03					
26		84	255	0.90	I	U	14.45	0.75					
27		90		>8	T	G/S	15.20	0.07	White powdery gypsum fill . Developed on top, and along dilated margins of micritic sediment fill				
28		90		>0.5	I	S/C	15.27	0.16	Sediment fill resting on early calcite. Coating				

Wadi Shallala (West Side) (contd.)

Fracture Number	Strike	Dip	Dip azimuth	Half-length (m)	Intersection character	Vein -fill	Distance from start (m)	Separation	Comments	Formation	Bedding strike	Bedding dip	Bedding dip azimuth
29		88	262	>4	I/O	G	15.43	0.57					
30		88	262	>8	T	G	16.00	0.50					
31		88	262	>8	T	C	16.50	0.50					
32		88	266	>8	T	G/S	17.00	0.90	Polished and slickensided calcite Coating indicating normal down Thrown movement to the east, associated with a 10–15 cm wide fracture zone with euhedral nailhead calcite coatings				
33		88	086	>8	T	G/C	17.90	0.00					
34	070	88	340	>0.5	R/O	G/S	17.90	1.05	Polished and slickensided calcite Surface indicating reversed movement, down throwing to north. 2 generations of calcite: (a) early calcite fill deformed by slicken development; (b) later euhedral nailhead calcite lining voids between asperities. 3 mm aperture				
35	354	90		>8	T	G/C	18.95	0.02					
36	354	90		0.40	R	G/C	18.97	0.13					
37	352	90		1.60	R/I	G/C	19.10	0.15					
38	352	88	082	>8	T	G	19.25	0.05	Curvilinear				
39	352	90		>0.5	O/R	S/G	19.30	1.20					
40	000	88	270	>8	T	G/S	20.50	0.30	Fracture zone with 15–20 cm wide jigsaw breccia containing <1 to 6 cm decalcified marl blocks, with micritic gypsum and infiltrated sediment matrix fill				
41	000	88	270	>8	T	U	20.80	2.00					
42	002	90		0.20	R	U	22.80	0.50					
43	002	90		>8	T	U	23.30	0.60					
44	352	90		>8	T	U	23.90	0.70					
45	354	90		>8	T	G/S	24.60	0.10					
46	350	88	260	1.20	I	U	24.70	0.20					
47	344	90		0.30	I	U	24.90	0.40					

Wadi Shallala (West Side) (contd.)

Fracture Number	Strike	Dip	Dip azimuth	Half-length (m)	Intersection character	Vein -fill	Distance from start (m)	Separation	Comments	Formation	Bedding strike	Bedding dip	Bedding dip azimuth
48	038	23	128	>2	B	U	25.30	0.00	Dilated bedding plane				
49	353	90		>8	T	C/G/S	25.30	1.20					
	350	74	260	N/D	N/D	U	26.50	0.10					
	350	74	260	N/D	N/D	U	26.60	2.10					
	352	82	262	>8	T	C	28.70	0.90	Late euhedral nailhead calcite coating rests on earlier slickensided calcite surface				
	348	80	258	>8	T	C	29.60	0.80	Late euhedral nailhead calcite coating rests on earlier slickensided calcite surface				
	324	70	234	0.50	R	U	30.40	0.00	Curvilinear				
	038	48	128	2.00	I/R	G	30.40	2.70	Sub-parallel to bedding				
	346	86	256	>2	R/T	C	33.10	0.20					
	354	90		>8	T	G/C	33.30	0.80					
	354	88	264	0.20	R	FE/	34.10	0.50	Iron stained surfaces				
	348	82	258	>8	T	FE/G	34.60	0.50	White powdery gypsum fill developed on top, and post-dates Fe oxide film				
	344	82	254	>8	T	FE/G	35.10	0.40	White powdery gypsum fill developed on top, and post-dates Fe oxide film. Fe oxide staining of wallrock to depth of 4 mm				
	342	82	252	>8	T	C/FE/G	35.50	0.10	Calcite pre-dates iron oxide, which in turn is post-dated by white powdery gypsum				
	344	82	254	>8	T	C/FE	35.60	0.15					
	340	84	250	>8	T	C/FE	35.75	0.01					

Wadi Shallala (West Side) (contd.)

Fracture Number	Strike	Dip	Dip azimuth	Half-length (m)	Intersection character	Vein -fill	Distance from start (m)	Separation	Comments	Formation	Bedding strike	Bedding dip	Bedding dip azimuth
	345	90		0.20	I	C/FE	35.76	0.03					
	348	90		0.80	I	G	35.79	1.36					
	348	90		0.15	I	G	37.15	0.05					
	348	90		>8	T	G	37.20	0.25	Fault showing 40 cm . Displacement, illustrated by displacement of concretion. Downthrows to west				
	354	90		1.60	I	U	37.45	0.43					
	349	82	259	>8	T	G	37.88	0.22					
	349	84	259	0.70	I	U	38.10	0.90					
	064	68	154	>2	O/R	S/G	39.00						

Bin	Frequency
0–0.24	30
0.25–0.49	11
0.5–0.74	9
0.75–0.99	8
1.0–1.24	2
1.25–1.49	2
1.5–1.74	1
1.75–2.0	3
>2.0	4
Total	**70**

Summary Statistics (Fracture spacing)	
Mean	0.557142
Standard Error	0.075156
Median	0.3
Mode	0.5
Standard Deviation	0.628804
Sample Variance	0.395394
Kurtosis	2.003852
Skewness	1.600764
Range	2.7
Minimum	0
Maximum	2.7
Sum	39
Count	70

Maqarin Railway Cutting

Dominant fracture set 010/90

Fracture Number	Strike	Dip	Dip azimuth	Half-length (m)	Intersection character	Vein -fill	Distance from start (m)	Separation	Comments	Formation	Bedding strike	Bedding dip	Bedding dip azimuth
1	18	80	108							B3	92	2	2
2	340	83	250			Calcite	15		Multi-generation crack seal				
3	342	88	252				10		Multi-generation crack seal				
4	342	90	252				14		Multi-generation crack seal				
5	10	86	100										
6	264	74	354						3 cm downthrow north				
7	290	30							Listric shear surface				
8	270	70	360										
9	12	90				Gypsum							
10	12	46	102										
11	4	90		1.5	Bedding	Gypsum	0	3.2	Beginning of scan line (east)				
12	296	46	26	T-G			3.2	2					
13	12	86	102	0.6		Gypsum	5.2	2.1					
14	12	90		T-G			7.3	4.3					
15	10	90		T-G			11.6	6.1	Down east (?) drag-fold				
16	6	90		2	Fracture	Gypsum	17.7	0.5					
17	8	90		2	Fracture	Gypsum	18.2	2					
18	9	90					20.2	1.9					
19	8	84	98				22.1	1.3					
20	12	90					23.4	3.8					
21	10	54				Gypsum	27.2	9					
22	4	90				Gypsum	36.2	0.08					
23	10	90				Gypsum	36.28	0.92					
24	12	90		1	Bedding		37.2	2					
25	12	90		T-G			39.2	2.2					
26	14	90					41.4	0.1					
27	14	90					41.5	0.1					
28	14	90					41.6	2.6					
29	290	60	200	1	Fracture		44.2	0.4					
30	8	84	98			Gypsum	44.6	2.6					
31	10	88	100				47.2	5					
32	12	90					52.2	1.55	10 cm wide fracture zone (2 cm space)				
33	348	62	78				53.75	5.15					
34	12	90					58.9	0.6					
35	10	60	100			Calcite	59.5	0.05					
36	10	90				Calcite	59.55	0.45					
37	10	90				Gypsum	60	2					

Maqarin Railway Cutting (contd.)

Dominant fracture set 010/90

Fracture Number	Strike	Dip	Dip azimuth	Half-length (m)	Intersection character	Vein -fill	Distance from start (m)	Separation	Comments	Formation	Bedding strike	Bedding dip	Bedding dip azimuth
38	10	90				Gypsum	62	6					
39	10	62	100				68	4.6					
40	10	90					72.6	1.3					
41	10	90					73.9	7.5					
42	12	90					81.4	4.8					
43	8	90					86.2	3.95					
44	10	90					90.15	8.2					
45	16	90					98.35	0.2					
46	8	90					98.55	8.95					
47	10	90					107.5	5					
48	10	90					112.5		End scanline (west)				
49	354	90							En-echelon				

Bin	Frequency
0–0.99	10
1–1.99	4
2–2.99	8
3–3.99	3
4–4.99	3
5–5.99	3
6–6.99	2
7–7.99	1
>8	3
Total	**37**

Summary Statistics (Fracture spacing)	
Mean	3.040540541
Standard Error	0.429126312
Median	2.1
Mode	2
Standard Deviation	2.610273449
Sample Variance	6.813527477
Kurtosis	-0.148791048
Skewness	0.844199718
Range	8.95
Minimum	0.05
Maximum	9
Sum	112.5
Count	37

River Bridge Terrace

Dominant fracture set 315/90

Fracture Number	Strike	Dip	Dip azimuth	Half-length (m)	Intersection character	Vein -fill	Distance from start (m)	Separation	Comments	Formation	Bedding strike	Bedding dip	Bedding dip azimuth
1	314	70	224					ca 10 cm		B3	Horizontal		
2	320	68	230					ca 10 cm		B3	Horizontal		
3	318	74	228					ca 10 cm		B3	Horizontal		
4	306	78	216					ca 10 cm		B3	Horizontal		
5	316	78	226					ca 10 cm		B3	Horizontal		
6	308	78	218					ca 10 cm		B3	Horizontal		
7	308	78	218					ca 10 cm		B3	Horizontal		
8	14	88	284					ca 10 cm		B3	Horizontal		
9	332	86	62					ca 10 cm		B3	Horizontal		
10	310	90						ca 10 cm		B3	Horizontal		
11	28	90						ca 10 cm		B3	Horizontal		
12	20	90						ca 10 cm		Alluvium	Horizontal		
13	22	90						ca 10 cm		Alluvium	Horizontal		
14	20	90						ca 10 cm		Alluvium	Horizontal		

Sentry Post Cutting (Maqarin Bridge)

Dominant fracture set 320/74

Fracture Number	Strike	Dip	Dip azimuth	Half-length (m)	Intersection character	Vein -fill	Distance from start (m)	Separation	Comments	Formation	Bedding strike	Bedding dip	Bedding dip azimuth
1	82	72	172				0	0	Start of scan line: Fracture zone	B3			
2	314	74	44	1.5	Fracture		0.1	0.10		B3			
3	310	74	40	1.5	Fracture		0.46	0.36		B3			
4	318	70	48	2.4	Fracture	Calcite	0.91	0.45		B3			
5	235	70	325	2.2	Intact		1.69	0.78		B3			
6	30	70	300				2.33	0.64		B3			
7	350	82	80	0.22	Fracture		2.39	0.06		B3			
8	176	73	266	0.15	Fracture	Calcite	3.59	1.20		B3			
9	353	74	263	1.5	Fracture	Calcite	3.71	0.12		B3			
10	220	70	310	2.3	Fracture		4.13	0.42		B3			
11	308	68	38			Calcite	4.23	0.10		B3			
12	310	70	40			Calcite	4.29	0.06		B3			
13	308	72	38			Calcite	4.33	0.04		B3			
14	312	70	42			Calcite	4.43	0.10		B3			
15	0	88	270	1.2	Fracture	Calcite	4.51	0.08		B3			
16	320	82	50	0.2	Fracture		4.6	0.09		B3			
17	320	82	50	0.05	Fracture		4.65	0.05		B3			
18	320	82	50	0.08	Fracture		4.78	0.13		B3			
19	24	84	114	1.2	Fracture	Calcite	5.41	0.63		B3			
20	312	76	222				5.88	0.47		B3			
21	304	58	54	2	Fracture	Calcite	6.9	1.02		B3			
22	290	60	20				7.4	0.50	End Scan line. Major shear	B3			
23	149	68	239			Calcite			Crack-seal multi-generation	B3			
24	346	72	76		Fracture				This is cut by latter calcite vein (#23)	B3			
25	340	90	70			Calcite			Crack-seal multi-generation	B3			
26	300	72	30			Calcite			Crack-seal multi-generation	B3			
27	320	62	50			Calcite			Crack-seal multi-generation	B3			
28	326	78	56			Calcite				B3			
29	334	72	64			Calcite				B3			
30	310	78	40			Calcite				B3			
31	294	82	200			Calcite				B3			
32	114	60	204			Calcite				B3			
33	146	62	236			Calcite				B3			
34	284	90				Calcite			Slickenfibres indicate dextral	B3			
35	330	84	244			Calcite			Slickenfibres indicate dextral	B3			
36	330	82	240			Calcite				B3			

Sentry Post Cutting (Maqarin Bridge) (contd.]

Dominant fracture set 320/74

Fracture Number	Strike	Dip	Dip azimuth	Half-length (m)	Intersection character	Vein -fill	Distance from start (m)	Separation	Comments	Formation	Bedding strike	Bedding dip	Bedding dip azimuth
37	300	80	30			Calcite				B3			
38	320	78	230			Calcite				B3			
39	332	78	62			Calcite				B3			
40	22	60	322			Calcite				B3			
41	332	80	62			Calcite				B3			
42	330	82	240			Calcite				B3			
43	328	82	238							B3			
44	328	80	238							B3			
45	332	80	242			Calcite				B3			
46	330	80	240			Calcite				B3			
47	326	82	236			Calcite				B3			
48	330	78	240			Calcite				B3			
49	334	80	244			Calcite				B3			
50	324	88	234			Calcite				B3			
51	328	78	238			Calcite				B3			
52	330	84	240							B3			
53	328	78	238			Calcite				B3			
54	326	82	236			Calcite				B3			
55	332	82	242			Calcite				B3			
56	332	82	242			Calcite				B3			

Bin	Frequency
0–0.09	6
0.1–0.19	5
0.2–0.29	0
0.3–0.39	1
0.4–0.49	3
0.5–0.59	1
0.6–0.69	2
0.7–0.79	1
0.8–0.89	0
0.9–0.99	0
>1	2
Total	**21**

Summary Statistics (Fracture spacing)	
Mean	0.352380952
Standard Error	0.074867835
Median	0.13
Mode	0.1
Standard Deviation	0.343087522
Sample Variance	0.117709048
Kurtosis	0.498975822
Skewness	1.119165026
Range	1.16
Minimum	0.04
Maximum	1.2
Sum	7.4
Count	21

Appendix 5

Ground surface resistivity measurements at the Eastern Springs site

Ground surface resistivity measurements at the Eastern Springs site

1 Resistivity surveying

1.1 General background

The electrical resistivity varies between different geological materials, dependent mainly on variations in water content and dissolved ions in the water. Resistivity investigations can thus be used to identify zones with different electrical properties, which can then be referred to different geological strata. Resistivity is also called specific resistance, which is the inverse of conductivity or specific conductance.

The most common minerals forming soils and rocks have very high resistivity in a dry condition, and the resistivity of soils and rocks is therefore normally a function of the amount and quality of water in pore spaces and fractures. The degree of connection between the cavities is also important. Consequently, the resisitivity of a type of soil or rock may vary widely. However, the variation may be more limited within a confined geological area, and variations in resistivity within a certain soil or rock type will reflect variations in physical properties. For example, the lowest resistivities encountered for sandstones and limestones mean that the pore spaces in the rock are saturated with water, wheras the highest values represent strongly consolidated sedimentary rock or dry rock above the groundwater surface. Sand, gravel and sedimentary rock may also have very low resistivities, provided the pore spaces are saturated with saline water. Fresh crystalline rock is highly resistive, apart from certain ore minerals, but weathering commonly produces highly conductive clay-rich saprolite. The variations in characteristics within one type of geological material makes it necessary to calibrate resistivity data against geological documentation resulting, for example, from surface mapping, test pits or drilling.

The amount of water in a material depends on the porosity, which may be divided into primary and secondary porosity. Primary porosity consists of pore spaces between the mineral particles, and occurs in soils and sedimentary rocks. Secondary porosity consists of fractures and weathered zones, and this is the most important porosity in crystalline rock such as granite and gneiss. Secondary porosity may also be important in certain sedimentary rocks, such as limestone. Even if the porosity is rather low, the electrical conduction taking place through water filled pore spaces may reduce the resistivity of the material drastically. The degree of water saturation will of course affect the resistivity, and the resitivity above the groundwater level will be higher than below if the material is the same. Consequently, the method can be used for finding the depth to groundwater in materials where a distinct groundwater table exists. However, if the content of fine grained material is significant, the water content above the groundwater surface, held by hygroscopic and capillary forces, may be large enough to dominate the electrical behaviour of the material.

The resistivity of the pore water is determined by the concentration of ions in solution, the type of ions and the temperature.

The presence of clay minerals strongly affects the resistivity of sediments and weathered rock. The clay minerals may be regarded as electrically conductive particles which can absorb and release ions and water molecules on its surface through an ion exchange process.

1.2 Measurement

Measurement of the resistivity of the ground is carried out by transmitting a controlled current (I) between two electrodes pushed into the ground, while measuring the potential (U) between two other electrodes. Direct current (DC) or an alternating current (AC) of very low frequency is used, and the method is often called DC-resistivity. The resistance ® is calculated using Ohm's law:

$$R = \frac{U}{I}$$

The material parameter resisitivity (ρ), which is the inverse of electrical conductivity (σ), is related to the resistance via a geometrical factor. It is common, but not necessary, to place the potential electrodes symmetrically spaced on the line between the current electrodes. The resistivity of ground can be calculated using:

$$\rho = K \frac{U}{I}$$

where the geometrical factor is:

$$K = 2\pi \left[\frac{1}{r_{11}} - \frac{1}{r_{12}} - \frac{1}{r_{21}} - \frac{1}{r_{22}} \right]^{-1}$$

for a generalized array.

In homogeneous ground the apparent resistivity will equal the true resistivity, but will normally be a combination of all contributing strata. Thus, the geometrically corrected quantity is called apparent resistivity (ρ_a). There are different collinear electrode configurations in use: Wenner Schlumberger, dipole-dipole and pole-pole. In our case Schlumberger array was applied.

The interpretation of results was carried out using special software provided with the equipment (see below).

1.3 Equipment used

ABEM Terrameter SAS 4000 with the following specifications:

Current : 0.2 – 1000 mA
Voltage : 400 – 800 V
4 input channels, galvanic isolated
Accuracy $\Delta V/I$ better than 1%.

Appendix 6

Drilling equipment and packer systems

Drilling equipment and packer systems

1 Drilling equipment

1.1 Inventory

1.1.1 Equipment and supplies presently at the University of Jordan, Amman

1. Hilti core drilling apparatus complete with standard drill rig, model DCM-2, 1¼" UNC.
2. 1 extension rod, ca. 30 cm.
3. Hand pump for drilling fluid.
4. Diamond drill bit, ca 120 mm O.D., barrel length ca. 30 cm.
5. Custom base plate (supplied by Mr. Toni Baer).
6. 4 x 1 m core barrel extension, 65 mm O.D. (Hilti, custom article).
7. 1 x 0.5 m core barrel extension, 60 mm O.D. (Hilti, custom article).
8. 2 diamond drill bits, 67 mm O.D. (Hilti, custom article).
9. 1 head piece for drill bits, 60 mm O.D., 1¼" UNC attachment (Hilti, custom article)
10. Generator for Hilti.
11. Anchoring bolts for custom base plate (Hilti, HSA-KA M12x180 and M12x120).
12. Miscellaneous tools (including large pipe wrench).
13. Extension cords and miscellaneous material for illumination.

1.1.2 Equipment and supplies presently at the University of Bern, Switzerland

1. 3 x 1 m core barrel extension, 60 mm O.D. (Hilti).
2. 1 x 0.5 m core barrel extension, 60 mm O.D. (Hilti).
3. Anchoring bolts for custom base plate (Hilti, HSA-KA M12x180 and M12x120).

1.1.3 Supplier for Hilti equipment:

Hilti (Switzerland) AG
Soodstrasse 61
CH-8134 Adliswil, Switzerland
www.hilti.com

1.1.4 Supplier for custom base plate

Toni Baer
Gerstenegg
CH-3864 Guttannen, Switzerland

1.2 Installations on site

Preparing drill sites included installation of a protective shelter with square timber and corrugated sheet metal. The custom base plate is bolted to a flat section of solid tunnel wall with 4 rock anchors that self-wedge on pull. The Hilti standard base and rig is mounted to the single large bolt of the custom base plate. This allows to orient drilling direction as desired and would also allow for drilling closely spaced holes from the same base plate mount.

The Hilti core drilling apparatus and illumination of the adit were powered from the same generator located a small distance from the tunnel entry.

2 Packer system

2.1 Inventory and specifications

2.1.1 Equipment and supplies presently at the University of Jordan, Amman

1. 1 single hydraulic packer system (CSP 54/120/1000).
2. 1 double hydraulic packer system (CSP 54/120/1000).
3. Extension rods, 2-m pieces, 1-m pieces, 0.5-m pieces (¾" NW threading).
4. 3 large shut-off valves for extension rods (¾" NW threading).
5. 4 valves with small pressure gauges for hydraulic packers (0-40 bar).
6. 4 valves with large pressure gauges for sampling / testing fluid lines (0-25 bar).
7. Pre-assembled feed through lines for double packer.
8. Lots of polyamid fluid line (red, blue, yellow) 6 mm O.D., 4 mm I.D.
9. 4 reinforced packer lines with fittings (black), 20 m each, 8.1 mm O.D., 4 mm I.D.
10. Fittings, plugs, line cutter, wrenches, teflon tape, etc.
11. Hand pump for hydraulic packers (and simple hydro testing) with pressure gauge mounted on aluminum fluid reservoir (60 bar max.)

2.1.2 Equipment and supplies presently at the University of Bern, Switzerland

1 single hydraulic packer with two lines to the test interval (CSP 54/120/1000):

1. 4 2-m extension rods, 1 1-m extension rod (¾" NW threading).
2. polyamid fluid line (red, yellow) and packer line (black) 6 mm O.D., 4 mm I.D.

All hydraulic packers are 1 m in inflatable length, and individual packer assemblies are about 2 m in overall length. The lower interval of the double packer system is pre-assembled to 2 m length, but can be modified. The double packer can be used as two single packers. The packers are designed for about 40 bar (600 psi) operation pressure (max. 65 bar, 975 psi). Valve assemblies for test lines and packer lines are pre-fit with snap-on connectors to fit the hand pump.

2.1.3 Additional equipment

All equipment supplied by:

COMDRILL Drilling Equipment GmbH
Im Kresigraben 29
D-74257 Untereisesheim

2.2 Installation instructions

2.2.1 Connecting polyamid tubing (6 mm O.D., 4 mm I.D.)

There are 3 parts required: nut, ferrule, supporting sleeve.

The supporting sleeve is very important to support the inner diameter of the tubes – otherwise the ferrule can not clamp down properly.

2.2.2 Completed assembly

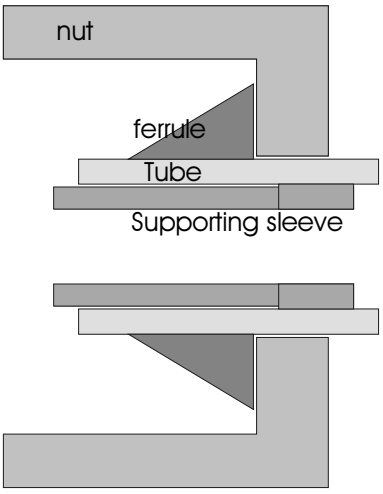

2.2.3 Instructions for a single packer

1. Determine the length of packed-off interval; add position marks to the assembly.
2. Attach packer line (black) to packer – do not tighten yet.
3. Attach valve assembly with pressure gauge (small) to packer line (tighten).
4. Fill packer with pump holding inlet high, without inflating packer ! (use clean spring water).
5. Loosen packer line at packer to bleed air.
6. Retighten and refill water without inflating.
7. Repeat air bleeding.
8. Refill if necessary and tighten connection.
9. Shut off valve (this completes pre-filling of the packer)
10. Attach vent line (yellow) and sampling line (red) to lower end of packer (tighten carefully).
11. Attach fitting to hold plug to vent line, leave open for now.
12. Attach valve with pressure gauge (large) and snap-on connector to sampling line.

13. Attach extension of vent line to upper end of packer; use heavy duty wire to support vent line to extend to the deep end of the drill hole.
14. Prepare extension rods.
15. Use Teflon sealing tape on all threads (extensions, large shut off valve); keep threads clean.
16. Attach large shut off valve to extension rod.
17. Set packer; adding extension rods as you push in the packer.
18. Inflate packer; pressure test for leaks; 40 bar pressure is sufficient.

2.2.4 Instruction for a double packer system

The double packer system contains a special extension in form of a steel bar construction to be mounted between packers. Its length is preset for a 2-m packed-off interval but can be adjusted by removing some portions (requiring a pair of large wrenches or a vise). The spacer is attached to the packers by a cone-in-cone fitting with a large nut.

The lines (vent, sampling, packer) from the upper packer/interval need to be fed through the lower interval. Three tube lengths are prepared for the full length of the interval spacer (small tubing role, fittings already attached, black is used for packer line). Make sure not to mix up lines by testing air flow. The upper packer is furnished with a vent making simultaneous saturation of both packers easy (fresh spring water). The central rod of the upper packer is sealed. The lower packed-off interval is open to the extension rods and requires one of the large shut-off valves, like in the case for a single packer system.

Both, the lower and the upper packer can be used as a single packer. If the upper packer is used as a single packer, one needs to make a transition from the interval spacer to the extension rod (by taking off a small piece from the spacer assembly). In a short hole, the interval spacer itself might be long enough as an extension. There is no large shut off valve required in this case.

2.3 Single interval pressure tests

Simple single interval pressure tests can be performed by monitoring pressure decay after a pressure pulse. A small pulse can be generated by pre-pumping with the hand pump against a closed valve to 60 bar max., followed by quick opening of the valve (using the sampling line). One requires a stop watch, a prepared table for making rapid notes on time-stamped pressure readings, and a second person to call out the time. The initial decay is quite fast and important for evaluating the hydraulic properties.

A pressure recovery test can be done to establish the in situ pressure. This may need weeks in the biomicrite. Ideally, one would require a gauge fit for low pressures (<2 bar, or <5 bar), rather than the standard models supplied with the equipment (0-25 bar).

Appendix 7

Fracture mapping data from Adit A-6

Adit interval	Discon-tinuity	Horizon-tal distance (m)	Strike	Dip azimuth	Dip	Trace length (m)	Intersection or termination characteristics	Deformation	Displace-ment (m)	Aperture (mm)	Mineral fill	Comments
0-50 m	1	0.00		090	80	>1.00	O	NONE	NONE	1	ET, G	Fibrous ettringite and gypsum fill cross-cutting adit-longitudinal calcite vein (Disc. No. 2)
0-50 m	2	1.20	120	030	42	1.20	I/R	NONE	NONE	1-3	C, T, ET	Cross-fibre ettringite reactivating tufa-filled fracture developed by re-opening of old calcite veinlet
0-50 m	3	0.70	120	030	40	>0.70	I/O	NONE	NONE	1-2	C, T, ET	Cross-fibre ettringite reactivating tufa-filled fracture developed by re-opening of old calcite veinlet
0-50 m	4	0.70	130	040	70	>0.15	R/O	NONE	NONE	1	T, ET	Cross-fibre ettringite reactivating tufa-filled fracture
0-50 m	5	1.30	120	030	40	0.15	R	NONE	NONE	1	T, ET	Cross-fibre ettringite reactivating tufa-filled fracture
0-50 m	6	1.48	175	085	82	3.47	R/O	NONE	NONE	<0.5	NONE	Cross-cuts Disc Nos. 9, 10, 11
0-50 m	7	2.20	135	045	45	0.70	O/I	NONE	NONE	<0.5	T	Terminated by Disc. No. 8
0-50 m	8	2.20	006	276	82	3.55	R	NONE	NONE	<1	T, ?ET, ?G	Cross-cuts Disc Nos. 7, 9, 10, 11
0-50 m	9	3.00	135	045	60	>1	O	FAULT BRECCIA, TENSION GASHES	U/K	3-4	T, ?ET	Complex vein/breccia developed between Disc. Nos. 9 and 10, with tufa-like vein fill developed along both margins of incipent fault breccia in marl, which is cut by sinusoidal tension gashes filled by probable ettringite. Normal movement

(Contd.)

Adit interval	Discon-tinuity	Horizon-tal distance (m)	Strike	Dip azimuth	Dip	Trace length (m)	Intersection or termination characteristics	Deformation	Displace-ment (m)	Aperture (mm)	Mineral fill	Comments
0- 50 m	10	3.10	135	045	60	>1	O	FAULT BRECCIA, TENSION GASHES	U/K	2-5	T, ?ET	Complex vein/breccia developed between Disc. Nos. 9 and 10, with tufa-like vein fill developed along both margins of incipent fault breccia in marl, which is cut by sinusoidal tension gashes filled by probable ettringite. Normal movement
0- 50 m	11	2.90	098	188	70	0.40	R	NONE	NONE	<0.5	NONE	Cut by Disc. Nos. 6 , 8
0- 50 m	13	5.80	125	035	40	1.80	R	NONE	NONE	0.5	?ET	
0- 50 m	14	6.00	095	005	60	>0.4	R/O	NONE	NONE	<0.5	NONE	
0- 50 m	15	6.55	050	320	25	>0.35	R/O	NONE	NONE	1	C	Grey, microcrystalline vein calcite
0- 50 m	16	6.20	134	044	88	>0.4	R/O	NONE	NONE	1-2	?ET, T	Disc. Nos 16, 17, 20 intersect at c. 6.2 m
0- 50 m	17	6.20	008	098	80	>0.4	I/O	NONE	NONE	1-2	?ET, T	Disc. Nos 16, 17, 20 intersect at c. 6.2 m
0- 50 m	19	6.60	005	095	80	>1.9	R/O	NONE	NONE	1-2	?ET, T	
0- 50 m	20	6.20	052	322	25	>2	O	NONE	NONE	<0.5	NONE	Bedding plane joint
0- 50 m	21	7.50	005	095	82	5.30	R	NONE	NONE	<0.5	NONE	
0- 50 m	22	7.90	075	345	22	>3	O	NONE	NONE	<0.5	NONE	Bedding plane joint
0- 50 m	23	9.40	065	335	30	>3	O	NONE	NONE	<0.5	NONE	Bedding plane joint
0- 50 m	24	10.20	138		90	1.90	R/I	NONE	NONE	2-4	?ET, ?G, C,	Terminates Disc. No. 25
0- 50 m	24A	10.20	164	074	70	>1	O/I	NONE	NONE	4-6	?ET, ?G, C,	Terminates against Disc. No. 24

(Contd.)

Adit interval	Discon-tinuity	Horizon-tal distance (m)	Strike	Dip azimuth	Dip	Trace length (m)	Intersection or termination characteristics	Deformation	Displace-ment (m)	Aperture (mm)	Mineral fill	Comments
	25	11.70	129	039	60	1.00	I/R	NONE	NONE	1	?ET, ?G	Cut by Disc. No. 24
0- 50 m	26	11.80	129	039	60	>1	I/O	NONE	NONE	1	?ET, ?G	Terminates at tip of Disc. No. 27
0- 50 m	27	11.80	162	252	84	1.40	I/R	NONE	NONE	0.5	C	Grey, microsparry calcite fill
0- 50 m	28	12.00	162	252	80	1.10	R	NONE	NONE	0.5	C	Grey, microsparry calcite fill
0- 50 m	29	15.90	165		90	1.00	R/I	NONE	NONE	0.5	C	Grey, microsparry calcite fill. Intersects and terminates against Disc. No. 31
0- 50 m	30	15.30	126	036	30	>1	I/O	NONE	NONE	<0.5	NONE	Terminates against Disc. No. 31
0- 50 m	31	15.30	184	274	26	>1	R/O	NONE	NONE	<0.5	NONE	Intersects Disc. Nos. 29, 30
0- 50 m	32	15.90	074	344	28	>3	O	NONE	NONE	<0.5	NONE	Bedding plane joint
0- 50 m	33	16.40	074	344	28	>3	O	NONE	NONE	<0.5	NONE	Bedding plane joint
0- 50 m	34	17.40	070	340	26	>3	O	NONE	NONE	<0.5	NONE	Bedding plane joint
0- 50 m	35	17.60	070	340	26	>3	O	NONE	NONE	<0.5	NONE	Bedding plane joint
0- 50 m	36	19.65	060	330	27	2.55	R	NONE	NONE	<0.5	NONE	Bedding plane joint
0- 50 m	37	23.48	135	045	60	>0.6	O/I	SLICKENSIDED	U/K	1	C, ?ET	Microsparry calcite deformed by subhorizontal slickensides, with later (undeformed) fibrous or powdery ettringite (or gypsum) resting on slickensided surfaces. Sinistral strike-slip movement
0- 50 m	38	24.80	164	254	88	3.02	I/R	NONE	NONE	<0.5	C	Grey, microsparry calcite fill. Terminates against Disc. No. 37
0- 50 m	39	25.00	130	040	35	2.00	R	NONE	NONE	<0.5	?ET	

(Contd.)

Adit interval	Discon-tinuity	Horizon-tal distance (m)	Strike	Dip azimuth	Dip	Trace length (m)	Intersection or termination characteristics	Deformation	Displace-ment (m)	Aperture (mm)	Mineral fill	Comments
0- 50 m	40	25.40	135	045	20	0.20	R/|	NONE	NONE	<0.5	NONE	Terminates against Disc. No. 39
0- 50 m	41	25.50	048	318	24	1.00	R/I	NONE	NONE	<0.5	NONE	Bedding plane joint. Terminates against Disc. No. 39
0- 50 m	42	26.35	075	345	24	>3.45	O	NONE	NONE	<0.5	NONE	Bedding plane joint
0- 50 m	43	26.00	130	040	22	0.60	R/I	NONE	NONE	1	?ET, ?G	Intersects Disc. No. 42
0- 50 m	44	26.30	130	040	22	0.40	R/I	NONE	NONE	1	?ET, ?G	Intersects Disc. Nos. 42, 45
0- 50 m	45	28.50	158	068	80	>5.7	I/O	NONE	NONE	1	T, C, ?ET	Conducts high pH water (pH>12) from 30.8 m onwards, after intersection with Disc. No. 49.
0- 50 m	46	28.40	145	055	40	>2	I/O	NONE	NONE	1	?CSH, ?ET	Terminates against Disc. No. 45. Hard, white silicate mineralisa-tion, possibly CSH
0- 50 m	47	27.50	145	055	40	>2	I/O	NONE	NONE	1	?CSH, ?ET	Terminates against Disc. No. 45. Hard, White silicate mineralisa-tion, possibly CSH
0- 50 m	48	29.70	140	050	60	>1	I/O	NONE	NONE	<0.5	NONE	Terminates against Disc. No. 45
0- 50 m	49	30.80	135	045	40	>1	I/O	NONE	NONE	<0.5	T	First point of high pH ground-water inflow in Adit 6. Flow starts at intersection between Disc. Nos. 45 and 49. pH>12. Termi-nates against Disc. No. 45
0- 50 m	50	31.00	145	055	88	0.70	R	NONE	NONE	<0.5	T	Drips high pH water (pH>12)
0- 50 m	51	33.00	140	050	50	>2	O	NONE	NONE	1	C	Drips high pH water (pH>12), possibly partly bedding plane fracture.

(Contd.)

Adit interval	Discon-tinuity	Horizon-tal distance (m)	Strike	Dip azimuth	Dip	Trace length (m)	Intersection or termination characteristics	Deformation	Displace-ment (m)	Aperture (mm)	Mineral fill	Comments
0- 50 m	52	33.00	158	068	52	>2	O	NONE	NONE	<0.5	NONE	
0- 50 m	53	45.00	153	063	66	2.20	R	NONE	NONE	2- 10	J, ET, TH, G, C, T	M2 high pH groundwater discharge site. Active flowing feature, with complex jennite, ettringite-thaumasite, calcite, gypsum mineralisation.
0- 50 m	54	45.55	360	090	85	2.30	R	NONE	NONE	0.5	?CSH, T	Micro-colloform possible CSH.
0- 50 m	55	47.00	153	063	66	1.00	I/R	NONE	U/K	N/D	?J, ?ET, T	Terminates against Disc. No. 54.
0- 50 m	56	48.30	164	074	50	1.00	I	BRECCIA,	U/K	N/D	?J, ?ET, T	Similar mineralisation to Disc. No. 53. Terminates against Disc. Nos. 54, 55. Tension gashes, filled with jennite-ettringite-thaumasite-like mineralisation, in marl indicate reversed movement
100- 113 m	3	101.50	168		90	1.65	R	NONE	NONE	1	C	Grey, microcrystalline calcite
100- 113 m	4	102.50	098	008	88	>1	R/O	NONE	NONE	N/D	NONE	Curvilinear fracture
100- 113 m	5	102.65	098		90	>1	R/O	NONE	NONE	N/D	NONE	
100- 113 m	6	102.90	110		90	>1	R/O	NONE	NONE	N/D	NONE	
100- 113 m	7	103.10	040	130	88	>2	R/O	NONE	NONE	N/D	NONE	
100- 113 m	8	103.80	172		90	0.20	R	NONE	NONE	1	?ET, ?C	Early grey microcrystalline calcite vein reactivated by later ettringite zone begins in adit roof at 104 m. interface dips gently to south

(Contd.)

Adit interval	Discon-tinuity	Horizon-tal distance (m)	Strike	Dip azimuth	Dip	Trace length (m)	Intersection or termination characteristics	Deformation	Displace-ment (m)	Aperture (mm)	Mineral fill	Comments
100- 113 m	9	104.60	016	286	72	0.80	R	NONE	NONE	1	C	Early grey microcrystalline calcite vein. Interface between unaltered marl and metamorphic transition
100- 113 m	10	104.90	178		90	2.20	R	NONE	NONE	1	C	Early grey microcrystalline calcite vein
100- 113 m	12A	106.40	162		90	N/D	R/O	NONE	NONE	4- 5	C, ?ET	Early grey microcrystalline calcite vein with ettringite or CSH along reactivated margins of vein. Swarm of 4 close-spaced veins
100- 113 m	12B	106.46	162		90	N/D	R/O	NONE	NONE	4- 5	C, ?ET	Early grey microcrystalline calcite vein with ettringite or CSH along reactivated margins of vein. Swarm of 4 close-spaced veins
100- 113 m	12C	106.52	162		90	N/D	R/O	NONE	NONE	4- 5	C, ?ET	Early grey microcrystalline calcite vein with ettringite or CSH along reactivated margins of vein. Swarm of 4 close-spaced veins
100- 113 m	12D	106.58	162		90	N/D	R/O	NONE	NONE	4- 5	C, ?ET	Early grey microcrystalline calcite vein with ettringite or CSH along reactivated margins of vein. Swarm of 4 close-spaced veins
100- 113 m	13	108.20	160	070	80	2.00	R	NONE	NONE	N/D	C, ?ET	Early grey microcrystalline calcite vein with ettringite or CSH along reactivated margins of vein
100- 113 m	15	109.10	160		90	>2.2	R/O	NONE	NONE	N/D	C, ?ET	Early grey microcrystalline calcite vein with ettringite or CSH along reactivated margins of vein. Intersects Disc. No. 16

(Contd.)

Adit interval	Discon-tinuity	Horizon-tal distance (m)	Strike	Dip azimuth	Dip	Trace length (m)	Intersection or termination characteristics	Deformation	Displace-ment (m)	Aperture (mm)	Mineral fill	Comments
100- 113 m	16	109.10	160		90	1.70	I/R	NONE	NONE	N/D	C, ?ET	Intersects Disc. No. 15 as part of a close-spaced, enchelon swarm of veins, many of which do not intersect the adit central line. Beyond 112.5 this vein is over-printed by metamorphic alteration and dies out
100- 113 m	17	108.10	172		90	3.20	R	NONE	NONE	N/D	C, ?ET	Early grey microcrystalline calcite vein with ettringite or CSH along reactivated margins of vein
100- 113 m	18	111.00	174		90	0.90	I/R	NONE	NONE	1	C, ?ET	Early grey microcrystalline calcite vein with ettringite or CSH along reactivated margins of vein
100- 113 m	20	110.00	051		90	>1	R/O	NONE	NONE	1	?ET	
100- 113 m	21	110.20	066	336	64	>1	R/O	NONE	NONE	1	?ET	
100- 113 m	22	110.05	090		90	>1	R/O	NONE	NONE	1	?ET	
100- 113 m	23	110.70	052	322	64	>1	R/O	NONE	NONE	1	?ET	

Appendix 8

Randomly oriented powder patterns of the various samples

Randomly oriented powder patterns of the various samples

The X-ray diffraction patterns corresponding to the following samples:

– K99-1-1
– K99-1-2
– K99-1-3
– K99-1-5
– K99-1-7

are presented below:

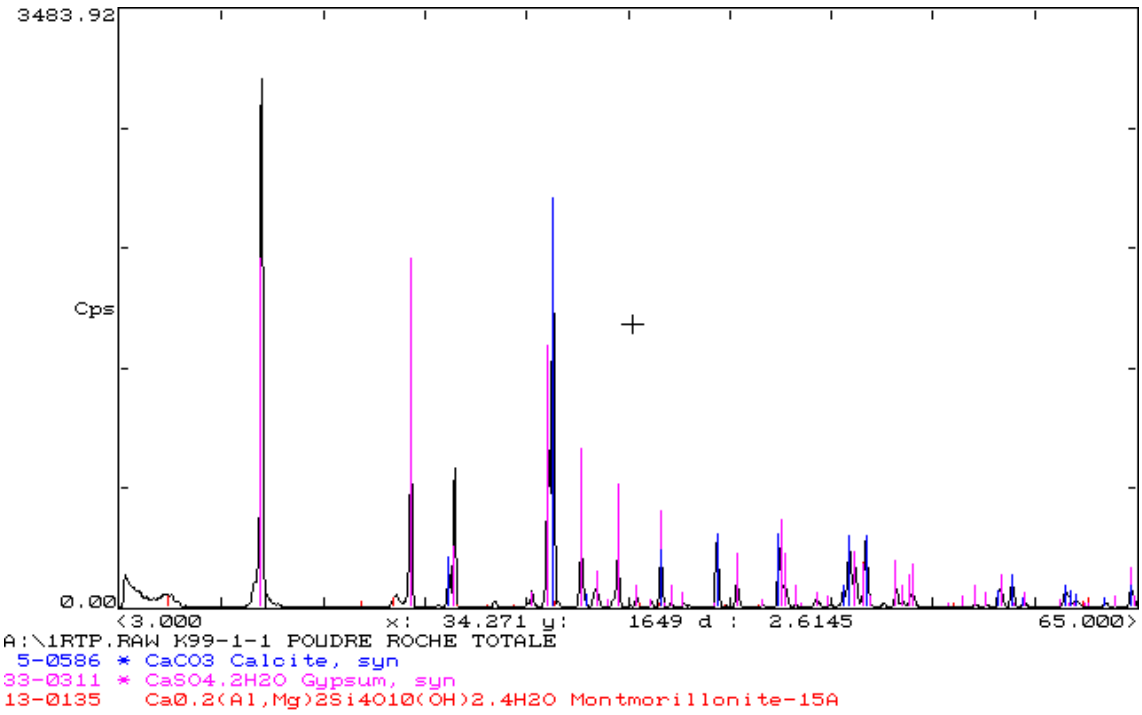

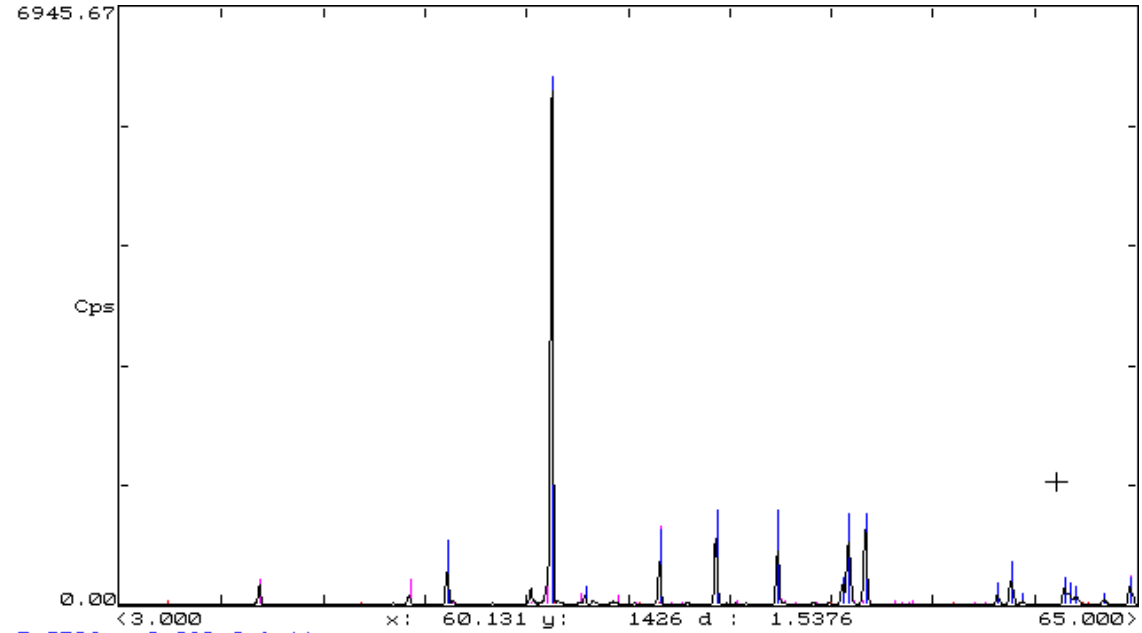
6945.67
Cps
0.00
<3.000
x: 60.131 y: 1426 d : 1.5376
65.000>
5-0586 * CaCO3 Calcite, syn
33-0311 * CaSO4.2H2O Gypsum, syn
13-0135 Ca0.2(Al,Mg)2Si4O10(OH)2.4H2O Montmorillonite-15A
A:\2RTP.RAW K99-1-2 POUDRE ROCHE TOTALE

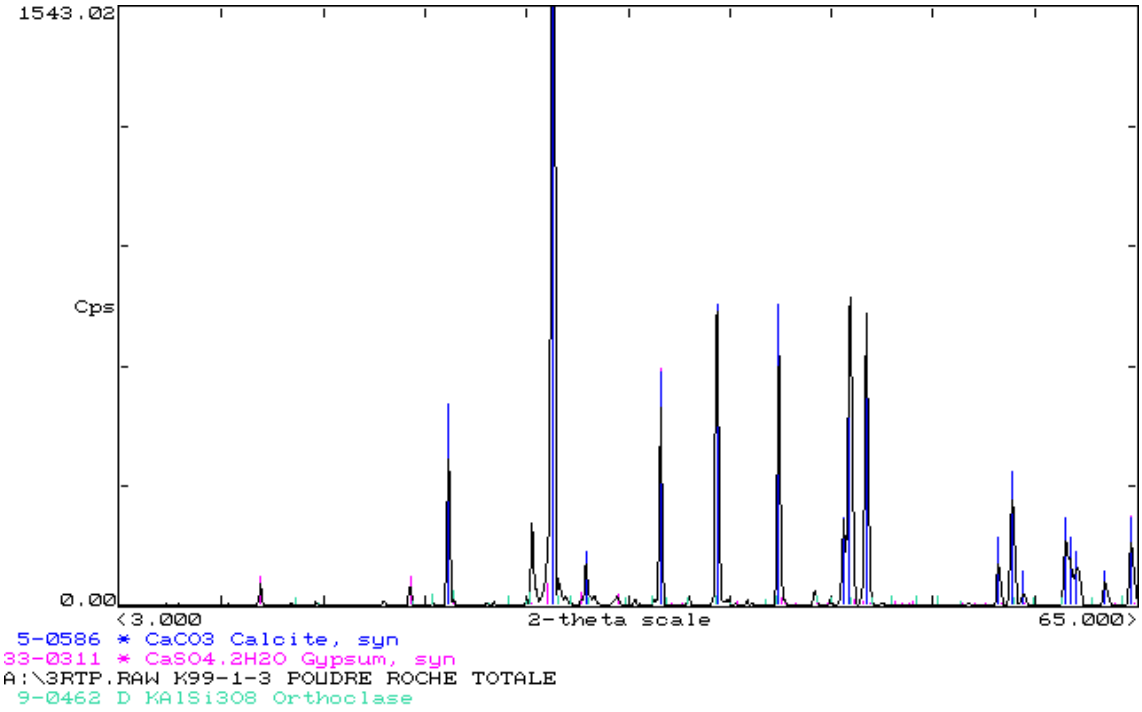
1543.02
Cps
0.00
<3.000
2-theta scale
65.000>
5-0586 * CaCO3 Calcite, syn
33-0311 * CaSO4.2H2O Gypsum, syn
A:\3RTP.RAW K99-1-3 POUDRE ROCHE TOTALE
9-0462 D KAlSi3O8 Orthoclase

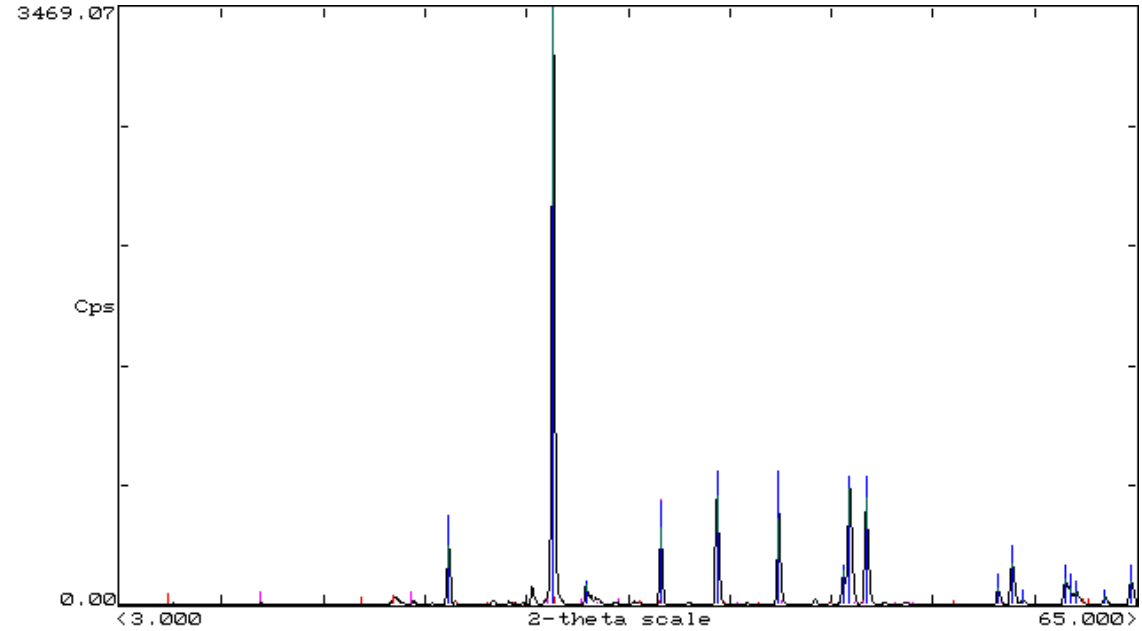
3469.07
Cps
0.00
<3.000
2-theta scale
65.000>
5-0586 * CaCO3 Calcite, syn
33-0311 * CaSO4.2H2O Gypsum, syn
A:\7RTP.RAW K99-1-7 POUDRE ROCHE TOTALE
13-0135 Ca0.2(Al,Mg)2Si4O10(OH)2.4H2O Montmorillonite-15A

Appendix 9

Maqarin Project: Sample archive list

Site	Sample No.	Sub-sample code	Description	Archive (A) / Supsamples (B,C etc.)			
				BGS	CEA	ANDRA	U. JORDAN
KHUSHAYM MATRUK	K99-1-1		Top of Profile 1 (0 m distance) within metamorphic zone [altered by hydration].			A	B
KHUSHAYM MATRUK	K99-1-2		Base of metamorphic zone, 6.5 m along Profile 1.			A	B
KHUSHAYM MATRUK	K99-1-3		Partly metamorphosed rock within rubbly clastic limestone horizon, 10.8 m along Profile 1.			A	B
KHUSHAYM MATRUK	K99-1-4		Partly metamorphosed rock within rubbly clastic limestone bed, 10.8 m along Profile 1.			A	B
KHUSHAYM MATRUK	K99-1-5		Shaley bituminous limestone/marl, 14.6 m along Profile 1.			A	B
KHUSHAYM MATRUK	K99-1-6		Shaley bituminous limestone/marl, 20.3 m along Profile 1.			A	B
KHUSHAYM MATRUK	K99-1-7		Base of shaley bituminous limestone/marl bed, 30.3 m along Profile 1.			A	B
KHUSHAYM MATRUK	K99-1-8		Profile 2 – Horizon A – Travertine.		C	A	B
KHUSHAYM MATRUK	K99-1-9		Profile 2 – Horizon B – Green-stained horizon – upper green horizon described as “Green 1”.		C	A	B
KHUSHAYM MATRUK	K99-1-10		Profile 2 – Horizon C – Boundary between upper green horizon (“Green 1”) and lower green horizon ("Green 2").		C	A	B
KHUSHAYM MATRUK	K99-1-11		Profile 2 – Horizon D – Boundary between “Green 2” and underlying grey-green horizon.		C	A	B
KHUSHAYM MATRUK	K99-1-12		Profile 2 – Horizon E – Grey green horizon.		C	A	B
KHUSHAYM MATRUK	K99-1-13		Profile 2 – Horizon F – Red horizon beneath Horizon E.		C	A	B
KHUSHAYM MATRUK	K99-1-14		Profile 2 – Horizon G – Grey horizon beneath Horizon F.		C	A	B

(Contd.)

Site	Sample No.	Sub-sample code	Description	Archive (A) / Supsamples (B,C etc.)			
				BGS	CEA	ANDRA	U. JORDAN
KHUSHAYM MATRUK	K99-1-15		Spot 2 – metamorphic zone outcrop halfway to top of hill, red "cement zone". N3116500, E3614933.		C	A	
KHUSHAYM MATRUK	K99-1-16		Spot 3 – vertical fracture fillings in Bituminous Marl. N3116367, E3614897.			A	
KHUSHAYM MATRUK	K99-1-17		Spot 4 – Bituminous Marl with calcite-filled fractures. N3116464, E3614842.			A	
KHUSHAYM MATRUK	K99-1-18		Spot 4 – baked marl with large vertical calcite-filled veins, N3116464, E3614842.			A	
KHUSHAYM MATRUK	K99-1-19		Spot 5a – Veins cutting Bituminous Marl, location as at Profile 2, base of Profile.			A	
KHUSHAYM MATRUK	K99-1-20		Spot 5b – Contact between grey and white marl, sharp contact, Profile 2 site.			A	
KHUSHAYM MATRUK	K99-1-21		Spot 5c – 2 pieces: one sample is Bituminous Marl (grey); second sample is an infill of a large horizontal fracture (grey and white fracture infill).			A	
KHUSHAYM MATRUK	K99-1-22		Spot 6a – N3116569, E3614776 – Soft red to grey-green marl lying under green altered marl, beneath travertine layer.		C	A	B
KHUSHAYM MATRUK	K99-1-23		Spot 6b – 50 cm beneath Spot 6a – grey marl with vertical fractures.		C	A	B
KHUSHAYM MATRUK	K99-1-24		Spot 6c – sample from interface between travertine and green altered marl.			A	B

(Contd.)

Site	Sample No.	Sub-sample code	Description	Archive (A) / Supsamples (B,C etc.)			
				BGS	CEA	ANDRA	U. JORDAN
KHUSHAYM MATRUK	K99-1-25		Spot 7 – 100 m south of Spot 6c – sample from interface between travertine and green altered marl.			A	B
KHUSHAYM MATRUK	K99-1-26		Metamorphic zone rock with fractures from top of hill.			A	
KHUSHAYM MATRUK	K99-1-27		Metamorphic zone rock from top of hill.			A	
KHUSHAYM MATRUK	K99-1-28		Spot 5 – green altered marl layer.		C	A	
EL HAMMAM QUARRY	H99-1-1a		Green banded marble from Daba Marble Zone.	A			
EL HAMMAM QUARRY	H99-1-1b		Green banded marble from Daba Marble Zone.	A			
EL HAMMAM QUARRY	H99-1-1c		Green marble and green alteration products from Daba Marble Zone.		A		
EL HAMMAM QUARRY	H99-1-1d		Green marble and green alteration products from Daba Marble Zone.			A	
EL HAMMAM QUARRY	H99-1-2		Black marble from Daba Marble Zone.	A			
EL HAMMAM QUARRY	H99-1-3		Green-red banded marble from Daba Marble Zone.	A			
EL HAMMAM QUARRY	H99-1-4		Red and black marble from Daba Marble Zone.	A			
EL HAMMAM QUARRY	H99-1-5		Pink marble from Daba Marble Zone.	A			
EL HAMMAM QUARRY	H99-1-6		Marble with alteration/hydration products.	A			
EL HAMMAM QUARRY	H99-1-7		Black marble with alteration/hydration products.	A			
EL HAMMAM QUARRY	H99-1-8		Black marble with veins.	A			

(Contd.)

Site	Sample No.	Sub-sample code	Description	Archive (A) / Supsamples (B,C etc.)			
				BGS	CEA	ANDRA	U. JORDAN
EL HAMMAM QUARRY	H99-1-9		Red marble with green alteration products and white secondary minerals filling veins.	A			
SWEILEH, AMMAN	S99-1-1		Coarse sparry calcite mineralisation, with banded growth fabric infilling karst.			A	
SWEILEH, AMMAN	S99-1-2		Coarse sparry calcite mineralisation, with banded growth fabric Infilling karst – later generations of calcite, resting on top of S99-1-1.			A	
SWEILEH, AMMAN	S99-1-3		Soft clayey layer from road cut exposure of bituminous phosphorite/limestone.			A	
SWEILEH, AMMAN	S99-1-4		Fracture fillings with grey to greenish alteration coatings.			A	
SWEILEH, AMMAN	S99-1-5		Green alteration products from altered horizons in road cut exposure of bituminous phosphorite/limestone.			A	
WEILEH, AMMAN	S99-1-6		Green alteration products from altered horizons in road cut exposure of bituminous phosphorite/limestone.			A	
SWEILEH, AMMAN	S99-1-7		Soft clayey horizon in road cut exposure of bituminous phosphorite /limestone.			A	
SWEILEH, AMMAN	S99-1-8		As S99-1-4.			A	
SWEILEH, AMMAN	S99-1-9		Green alteration of marl/limestone in road cut exposure of bituminous phosphorite/limestone.			A	
SWEILEH, AMMAN	S99-1-10		Apatite-rich country rock, possibly slightly metamorphosed.			A	

(Contd.)

Site	Sample No.	Sub-sample code	Description	Archive (A) / Supsamples (B,C etc.)			
				BGS	CEA	ANDRA	U. JORDAN
MAQARIN	M99-1-1		Basalt from between base of basalt exposure and west-end of road sentry post on Jordanian side of Yarmouk [collected by U Mäder].	A			
MAQARIN	M99-1-2		Basalt from the base of the basalt pile on Jordanian side of Yarmouk [collected by U Mäder].	A			
MAQARIN	M99-1-3		Basalt from the base of the basalt pile on Jordanian side of Yarmouk [collected by U Mäder].	A			
MAQARIN	M99-1-4		Wadi Shallala road cutting profile [ex-M99-1-1WS]. Carbonate (micritic)-gypsum joint filling in Massive Limestone Zone 1 [refer to Wadi Shallala fracture logging profile].	A			
MAQARIN	M99-1-5		Wadi Shallala road cutting profile [ex-M99-1-2WS]. Calcite-micrite-gypsum joint filling in fractures at junction between Massive Limestone Zone 2 and Highly Fractured Limestone Zone 1 [refer to Wadi Shallala fracture logging profile].	A			
MAQARIN	M99-1-6		Wadi Shallala road cutting profile [ex-M99-1-3WS]. Wallrock limestone to M-99-1-5.	A			
MAQARIN	M99-1-7		Wadi Shallala road cutting profile [ex-M99-1-4WS]. Micritic-gypsiferous and tufa-like joint filling in fractures from margin of healed jigsaw breccia, in Highly Fractured Limestone Zone 2, at junction with Massive Limestone Zone 2 [refer to Wadi Shallala fracture logging profile].	A			

(Contd.)

Site	Sample No.	Sub-sample code	Description	Archive (A) / Supsamples (B,C etc.)			
				BGS	CEA	ANDRA	U. JORDAN
MAQARIN	M99-1-8		Wadi Shallala road cutting profile [ex-M99-1-6WS]. Calcite coating on joints (pre-tufa/micrite fill) forming disk-like concentrations of calcite on fracture surface in Massive Limestone Zone 3 [refer to Wadi Shallala fracture logging profile].	A			
MAQARIN	M99-1-9		Wadi Shallala road cutting profile [ex-M99-1-7WS]. Limestone wallrock to M99-1-8.	A			
MAQARIN	M99-1-10		Wadi Shallala road cutting profile [ex-M99-1-8WS]. Calcite vein filling or joint coating with later micritic or gypsiferous material filling joint opened by parting of the interface along the wallrock and early calcite vein, in Massive Limestone Zone 3 [refer to Wadi Shallala fracture logging profile].	A			
MAQARIN	M99-1-11		Wadi Shallala road cutting profile. Wallrock and fissure surface to M99-1-10 [ex-M99-1-9WS].	A			
MAQARIN	M99-1-12		Wadi Shallala road cutting profile [ex-M99-1-10WS]. Micritic or gypsiferous joint fill within bedding parallel fissures developed in the top of the section 2 m beneath the present soil base at the west end of the profile [refer to Wadi Shallala fracture logging profile]. This type of fissure fill increases in intensity of development towards the soil base and decreases in intensity below 3 m depth.	A			

(Contd.)

Site	Sample No.	Sub-sample code	Description	Archive (A) / Supsamples (B,C etc.)			
				BGS	CEA	ANDRA	U. JORDAN
MAQARIN	M99-1-13		Wadi Shallala road cutting profile [ex-M99-1-10WS]. Micritic or gypsiferous joint fill within bedding parallel fissures developed in the top of the section 1 m beneath the present soil base at the west end of the profile [refer to Wadi Shallala fracture logging profile]. This type of fissure fill increases in intensity of development towards the soil base and decreases in intensity below 3 m depth.	A			
MAQARIN	M99-1-14		Wadi Shallala road cutting profile [ex-M99-1-12WS]. Micritic or gypsiferous joint fill within vertical fissures at the west end of the profile [refer to Wadi Shallala fracture logging profile]. This type of fissure fill is similar to the fill observed in bedding parallel fractures in samples M99-1-12 and M99-1-13.	A			
MAQARIN	M99-1-15		Palaeosoil, baked by basalt, sampled from above Maqarin Railway Station.	A			
MAQARIN	M99-1-16		Calcite vein filling from NNE-SSW, vertically inclined joint set, located east of Maqarin bridge sentry post.	A			
MAQARIN	M99-1-17		Bituminous Marl, sampled from Maqarin railway cutting.	A			
MAQARIN	M99-1-18		White fracture fillings from top 3 m of new road cutting immediately to east of Maqarin railway cutting.	A			
MAQARIN	M99-1-19		Shard of chert with weathering rind from Maqarin railway cutting.	A			
MAQARIN	M99-1-20		Altered and hydrated rock from metamorphic zone rocks within landslipped block exposed along road sides of Wadi Sijin [ex-M99-1-4SJ]. Brecciated altered metamorphic rock irregularly veined by white secondary alteration products.	A			

(Contd.)

Site	Sample No.	Sub-sample code	Description	Archive (A) / Supsamples (B,C etc.)			
				BGS	CEA	ANDRA	U. JORDAN
MAQARIN	M99-1-21		Altered and hydrated rock from metamorphic zone exposed in landslipped block along road sides of Wadi Sijin [ex-M99-1-4SJ] cut by white veins and pods of secondary possible ettringite or thaumasite alteration products.	A			
MAQARIN	M99-1-22		Pods and veins of spherulitic to gel-like or massive white secondary mineral in altered metamorphic rock exposed in landslipped block exposed along road sides of Wadi Sijin [ex-M99-1-3SJ].	A			
MAQARIN	M99-1-23		Altered metamorphic rock from landslipped block exposed along road sides of Wadi Sijin [ex-M99-1-1SJ], with pods and veins of secondary white to pale green colloform to radial-fibrous mineral that may possibly be apophyllite or CSH mineral.	A			
MAQARIN	M99-1-24		Complex calcite vein showing banded or poly-episodic mineralisation fabric in coarse calcite. From dominant N-S trending vein set at bottom of access track to Adit A-6 [ex-M99-1-9AD].	A			
MAQARIN	M99-1-25		Hydrated and altered metamorphic zone rocks, showing polygonal fracture pattern, with reddened altered fracture wallrocks and white secondary vein fill. Adit A-6, 113.2 m [ex-M99-1-6AD].	A			
MAQARIN	M99-1-26		Large and complex calcite vein showing banded or poly-episodic mineralisation fabric in coarse calcite. From dominant N-S trending vein set exposed in road cutting approximately 200 m west of Adit A-6, and approximately 50 m west of Adit A-4 [ex-M99-1-8AD.	A			

(Contd.)

Site	Sample No.	Sub-sample code	Description	Archive (A) / Supsamples (B,C etc.)			
				BGS	CEA	ANDRA	U. JORDAN
MAQARIN	M99-1-27		White vein fill (possibly ettringite +/- calcite) from N080/50N orientation vein, Adit A-6, 55 m [ex-M99-1-7AD].	A			
MAQARIN	M99-1-28		Calcite vein filling from N158/90 orientation vein (dominant vein set), within metamorphic zone, Adit A-6, 113 m (east wall). The calcite vein is recrystallised and begins to be overprinted by the metamorphism at this point [ex-M99-1-5AD].	A			
MAQARIN	M99-1-29		Calcite vein filling from same N158/90 orientation vein as M99-1-28 (dominant vein set), within metamorphic zone, Adit A-6, 112 m (east wall). The calcite vein is partly recrystallised and shows reddening along the vein margins at this point. [ex-M99-1-4AD].	A			
MAQARIN	M99-1-30		Tobermorite veins in Bituminous Marl, in close-spaced bedding parallel veins, Adit A-6, 100 m [ex-M99-1-3AD].	A			
MAQARIN	M99-1-31		Tobermorite veins in Bituminous Marl, in close-spaced bedding parallel veins, Adit A-6, 99 m [ex-M99-1-2AD].	A			
MAQARIN	M99-1-32		Tobermorite veins in Bituminous Marl, in close-spaced veins sub-parallel to bedding, Adit A-6, 94.1 m [ex-M99-1-1AD].	A			
MAQARIN	M99-1-33a	**A**	Profile of 8 samples collected by L Trottignon, Adit A-6 along 30 cm interval in roof of adit at 130 distance: A = 0–3 cm, hydrated metamorphic rock.	A			
MAQARIN	M99-1-33a	**B**	B = 3–7 cm, hydrated metamorphic rock.	A			
MAQARIN	M99-1-33a	**C**	C = 7–8 cm, reddened altered metamorphic rock.	A			

(Contd.)

Site	Sample No.	Sub-sample code	Description	Archive (A) / Supsamples (B,C etc.)			
				BGS	CEA	ANDRA	U. JORDAN
MAQARIN	M99-1-33a	**D**	D = 8–13 cm, white altered metamorphic rock.	A			
MAQARIN	M99-1-33a	**E1**	E1 = red + yellow altered metamorphic rock (distance not noted).	A			
MAQARIN	M99-1-33a	**E2**	E2 = pink + purple altered metamorphic rock (distance not noted).	A			
MAQARIN	M99-1-33a	**F**	F = 17–22 cm, white altered metamorphic rock.	A			
MAQARIN	M99-1-33a	**G**	G = 22–27 cm, pink-beige altered metamorphic rock.	A			
MAQARIN	M99-1-33b	**TZ –3**	Profile of 11 samples (designated “TZ”) collected by L Trottignon, Adit A-6 west wall through Transition Zone between Metamorphic Zone and Bituminous Marl between 100–113 m: TZ1 [NOTE: bags received by BGS were poorly labelled] TZ -3 = 50 m, Bituminous Marl	A	B		
MAQARIN	M99-1-33b	**TZ -2**	104 m, Adit A-6, Bituminous Marl, black and wet, with fungi growth	A			
MAQARIN	M99-1-33b	**TZ -1**	109 m, Adit A-6, Bituminous Marl, slightly baked (????) cut by a large N-S fracture in roof of adit.	A			
MAQARIN	M99-1-33b	**TZ 1**	110.5 m, Adit A-6, dark grey baked marl/clay biomicrite with veinlets	A	B		
MAQARIN	M99-1-33b	**TZ 2**	111.5 m, Adit A-6, brownish to reddish-grey baked marl/clay biomicrite with veinlets and green secondary coatings.	A			

(Contd.)

Site	Sample No.	Sub-sample code	Description	Archive (A) / Supsamples (B,C etc.)			
				BGS	CEA	ANDRA	U. JORDAN
MAQARIN	M99-1-33b	**TZ 3a**	113 m, Adit A-6, light brown to grey, soft strongly baked rock.	A	B		
MAQARIN	M99-1-33b	**TZ 3b**	113.3 m, Adit A-6, reddish, baked rock with green alteration products in fine fractures.	A			
MAQARIN	M99-1-33b	**TZ 4a**	113.5 m, Adit A-6, strongly altered metamorphic rock with red and white alteration products/colouration.	A			
MAQARIN	M99-1-33b	**TZ 4b**	114 m, Adit A-6, Unaltered primary metamorphic rock with alteration rim adjacent to fracture filled by secondary hydration/alteration products.	A			
MAQARIN	M99-1-33b	**TZ 5**	115 m, Adit A-6, pale yellow to white, altered and hydrated metamorphic rock, with red-stained microfractures.	A	B		
MAQARIN	M99-1-33b	**TZ 6**	118 m, Adit A-6, hydrated and altered metamorphic rock associated with M1 (Phase II and Phase III) water seepage site.	A			
MAQARIN	M99-1-34		Transition zone between non-metamorphosed Bituminous Marl and Metamorphic Zone, Adit A-6, taken from roof of adit.	A			
MAQARIN	M99-1-35		Altered metamorphic zone (Hydrated Cement Zone), Adit A-6, 130 m distance, 1.5 m above adit floor.	A			
MAQARIN	M99-1-36		Metamorphosed chert from hydrated metamorphic zone interval, Adit A-6, 130 m distance, 1.4 m above adit floor.	A			
MAQARIN	M99-1-37		Pink metamorphic zone rock (partly altered) from dry section of adit wall in Adit A-6, 130 m distance.	A			

(Contd.)

Site	Sample No.	Sub-sample code	Description	Archive (A) / Supsamples (B,C etc.)			
				BGS	CEA	ANDRA	U. JORDAN
MAQARIN	M99-1-38		Metamorphic rock with hydration/alteration rim (Cement Zone), Adit A-6, c.120 m distance.	A			
MAQARIN	M99-1-39		Vertical fracture within altered metamorphic rock with hydration/alteration products (Cement Zone), Adit A-6, c. 130 m distance.	A			
MAQARIN	M99-1-40		Altered metamorphic rock cut by a network of horizontal fractures (Cement Zone), Adit A-6, 130 m distance.	A			
MAQARIN	M99-1-41		Altered and hydrated metamorphic zone rocks (Cement Zone), Adit A-6, 140 m distance.	A			
MAQARIN	M99-1-42		Altered and hydrated metamorphic zone rocks (Cement Zone), Adit A-6, 120 m distance.	A			
MAQARIN	M99-1-43		Altered and hydrated metamorphic zone rocks (Cement Zone), Adit A-6, 130 m distance, 0.5 m above adit floor (west wall).	A			
MAQARIN	M99-1-44		Altered and hydrated metamorphic zone rocks (Cement Zone), Adit A-6, 130 m distance, 0.7 m above adit floor (west wall).	A			
MAQARIN	M99-1-45		Altered and hydrated metamorphic zone rocks (Cement Zone), Adit A-6, 130 m distance, 0.5 m above adit floor (east wall).	A			
MAQARIN	M99-1-46		Pink, altered and hydrated metamorphic zone rocks (Cement Zone), Adit A-6, 130 m distance, 0.8 m above adit floor (east wall).	A			

(Contd.)

Site	Sample No.	Sub-sample code	Description	Archive (A) / Supsamples (B,C etc.)			
				BGS	CEA	ANDRA	U. JORDAN
MAQARIN	M00-1-1		Creamy tobermorite vein fill material, hosted in Bituminous Marl, Adit A-6, 100 m distance		A		
MAQARIN	M00-1-2		Unaltered Bituminous Marl, Adit A-6, 50 m distance		A		
MAQARIN	M00-1-3		Basalt from outcrop directly above Adit A-6		A		
MAQARIN	M00-1-4		Basalt from outcrop approximately 20 m above and to west of Adit A-6		A		
MAQARIN	DD-M-99-1		Drill core from M2 seepage site, Adit A-6, 0–95 cm depth	A			
MAQARIN	DD-M-99-1		Drill core from M2 seepage site, Adit A-6, 95–175 cm depth	A			
MAQARIN	DD-M-99-1		Drill core from M2 seepage site, Adit A-6, 175–268 cm depth	A			
MAQARIN	DD-M-99-1		Drill core from M2 seepage site, Adit A-6, 268–350 cm depth	A			
MAQARIN	DD-M-99-1		Drill core from M2 seepage site, Adit A-6, 350–437 cm depth	A			
MAQARIN	DD-M-99-2		Drill core from Metamorphic Zone seepage site, Adit A-6, 0–75 cm depth	A			
MAQARIN	DD-M-99-2		Drill core from Metamorphic Zone seepage site, Adit A-6, 75–160 cm depth	A			
MAQARIN	DD-M-99-2		Drill core from Metamorphic Zone seepage site, Adit A-6, 160–210 cm depth	A			